8-2018

# Advancing Methods to Quantify Actual Evapotranspiration in Stony Soil Ecosystems

Kshitij Parajuli
*Utah State University*

# ADVANCING METHODS TO QUANTIFY ACTUAL EVAPOTRANSPIRATION IN STONY SOIL ECOSYSTEMS

by

Kshitij Parajuli

A dissertation submitted in partial fulfillment
of the requirements for the degree

of

DOCTOR OF PHILOSOPHY

in

Civil and Environmental Engineering

Approved:

| | |
|---|---|
| _____ | _____ |
| David G. Tarboton, Sc.D.<br>Major Professor | Scott B. Jones, Ph.D.<br>Major Professor |
| _____ | _____ |
| Lawrence E. Hipps, Ph.D.<br>Committee Member | L. Niel Allen, Ph.D.<br>Committee Member |
| _____ | _____ |
| Alfonso Torres-Rua, Ph.D.<br>Committee Member | Richard S. Inouye, Ph.D.<br>School of Graduate Studies |

UTAH STATE UNIVERSITY
Logan, Utah

2018

# ABSTRACT

Advancing methods to quantify actual evapotranspiration in

stony soil ecosystems

by

Kshitij Parajuli, Doctor of Philosophy

Utah State University, 2018

Major Professors: David G. Tarboton, Scott B. Jones
Department: Civil and Environmental Engineering

Quantification of evapotranspiration (ET) is crucial for understanding water balance and efficient water resource planning. However, there is limited understanding and scarce quantification of actual ET ($ET_A$) in natural ecosystems as compared to agricultural settings. The major focus of this study was to improve $ET_A$ estimation in montane (e.g., stony soil) ecosystems, where heterogeneity can be substantial due to diverse vegetation and non-uniform, often stony soils. Three major research objectives were addressed in Chapters 2 through 4 with each objective presented in a separate paper format. Chapter 1 provides an introduction to the topics with Chapter 5 providing a summary, conclusions and recommendations. The influence of stone content on bulk soil hydraulic properties was examined in chapter 2 by determining the water retention curve (WRC) of soil, stone and stone-soil mixtures with varied volumetric stone content. An averaging scheme to describe the WRC of stony soil was proposed based on the individual WRC of the background soil and stone inclusions, showing good agreement with experimental data.

Chapter 3 evaluates $ET_A$ estimation from stony soils in montane ecosystems by accounting for the water retention properties of stones in the soil using our algorithm developed in chapter 2 within a numerical model (HYDRUS-1D). Model results suggested significant overestimation of simulated $ET_A$ when effects of stone content were neglected in comparison to $ET_A$ measured by eddy covariance. The $ET_A$ was simulated for stony soils assuming highly and negligibly porous stones which lead to reductions in simulated $ET_A$ of up to 10% and 30%, respectively, when compared with the 'no stones' condition. These results revealed the important role played by soil stones in modulating the water balance by affecting $ET_A$ in montane ecosystems.

In chapter 4, performance of the Noah-Multiphysics (Noah-MP) land surface model in simulating soil moisture and evapotranspiration under various soil parameterizations was investigated. Noah-MP results were compared with simulations from the HYDRUS-1D numerical model, which provides more detailed representation of soil hydraulics. The Noah-MP model with parameterization including stone content and detailed soil properties was able to provide the best Noah-MP prediction of evapotranspiration. We conclude that improvement in representation of soil properties including stone content information, can substantially advance the ability of numerical and land surface models to more accurately simulate soil water flow and boundary fluxes.

(154 pages)

# PUBLIC ABSTRACT

Advancing methods to quantify actual evapotranspiration in stony soil ecosystems

Kshitij Parajuli

Water is undeniably among the most important natural resources and the most critical in semi-arid regions like the Intermountain West of the United States. Such regions are characterized by low precipitation, the majority of which is transferred to the atmosphere from the soil and vegetation as evapotranspiration (ET). Quantification of ET is thus crucial for understanding the balance of water within the region, which is important for efficiently planning the available water resources. This study was motivated towards advancing the estimation of actual ET ($ET_A$) in mountain ecosystems, where the variation in different types of vegetation and non-uniformity of soil including considerable stone content creates challenges for estimating water use as ET. With the aim of addressing the effect of stone content in controlling soil moisture and ET, this study examined the influence of stone content on bulk soil hydraulic properties. An averaging model referred to as a binary mixing model was used to describe the way in which water is held and released in stony soil. This approach was based on the individual hydraulic behavior of the background soil and of the stones within the soil. The effect of soil stone content on $ET_A$ was evaluated by accounting for the water retention properties of stones in the soil using a numerical simulation model (HYDRUS-1D). The results revealed overestimation of simulated $ET_A$ when effects of stone content were not accounted for in comparison to $ET_A$

measured by the state-of-the-art “eddy covariance” measurement method for $ET_A$. An even larger-scale model was evaluated, named the Noah-Multiphysics (Noah-MP) land surface model. The land surface model was run using different arrangements of complexity to determine the importance of stone content information on simulation results. The version of the model with information about stone content along with detailed soil properties was able to provide the best Noah-MP prediction of ET. The study suggests that improvement in representation of soil properties including stone content information, can substantially advance the ability of numerical and land surface models to more accurately simulate soil water flow and $ET_A$.

# DEDICATION

I would like dedicate this work to my loving wife Medha and daughter Samaira.

# AKNOWLEDGMENTS

I would like to extend my sincere gratitude to my major professors, Dr. David G. Tarboton, and Dr. Scott B. Jones and committee members Dr. Lawrence E. Hipps, Dr. L. Niel Allen, and Dr. Alfonso Torres Rua. Thank you for your time and expertise during this period. Special mention and deepest appreciation goes to my immediate advisor Dr. Jones for his guidance throughout my PhD. I thank him for his patience, suggestion and encouragements during the work and his availability whenever I needed advice. I deeply appreciate his perseverance in pushing me to achieve the best out of myself. Without his encouragement and persistent support, this dissertation would not have been possible. I am equally grateful to Dr. Tarboton for constantly providing me with his feedback and letting me rethink on my ideas.

I am also appreciative of Dr. Morteza Sadeghi and Dr. Lin Zhao from the department of Plants, Soils and Climate at USU, Dr. Gerald Flerchinger and Dr. Mark Seyfried at the USDA-ARS in Boise, Idaho for their assistance and guidance while working through the chapters in this dissertation.

I owe a very special gratitude to Bill Mace, who has helped me in the lab, field and beyond. I thank the people with whom I shared the office space, with special thanks to, Dr. Wenyi Sheng, Dr. Rong Zhou, Dr. Jon Meyer, Sebastian Los, Brant Cook, Ben Rider, Chihiro Naruke, Boniface Fosu, Yen-Heng Lin, Matthew Miksch and Ryan Hodges. I would also like to thank Rhitika Poudel and other friends from Nepalese student's community for being there.

I would like to thank innovative Urban Transitions and Aridregion Hydro-sustainability (iUTAH) project for providing continuous funding and USU Research and Graduate Studies for providing Dissertation Fellowship as well as several travel awards.

Finally, but by no means least, thanks go to my loving parents and grandparents for encouraging me to attend graduate school and for believing in my ability to get to where I am today. Deepest appreciation goes to my wonderful wife Medha and my adored daughter, Samaira, for their patience, love and support they provided throughout the time until the completion of this dissertation. I dedicate this dissertation to my wife, daughter and my parents. This would not be possible without them.

Kshitij Parajuli

CONTENTS

# LIST OF TABLES

# LIST OF FIGURES

Figure Page

Figure Page

# CHAPTER 1

# INTRODUCTION

Water is undeniably among the most important natural resources and the most critical in semi-arid regions like the Intermountain West of the United States. Rapid population growth and urbanization has increased water demands leading to water shortages and drought conditions are on the rise. Moreover, effects of land use and climate change are expected to aggravate the situation by direct impact on water balance components leading to spatiotemporal variations in water availability (Bernstein et al., 2007; Parajuli et al., 2014; Shrestha et al., 2014; Wang and Gillies, 2012). Predicting the effects of land use and climate change on water resources necessitates a detailed understanding of the interactions between soil, vegetation, and the atmosphere (Gayler et al., 2014; Mu et al., 2007). Large volumes of water are transferred to the atmosphere from the soil and vegetation as evapotranspiration (ET). A major unknown variable associated with eco-hydrological systems, ET may constitute up to 95% of the water balance in arid regions, thus accurate quantification of ET is critical to land surface modelling, ecosystem and environmental assessment and water resources management (Kool et al., 2014; Wilcox et al., 2003; Wang et al., 2015). Broad application of eddy covariance method as a standard technique for measuring actual ET ($ET_A$) has been tested in various spatial scales at different land surface conditions (Liu et al., 2013; Nagler et al., 2005; Williams et al., 2004; Wilson et al., 2001). In order to measure the exchanges of carbon dioxide, water vapor, and energy between the land surface and the atmosphere, a number of eddy covariance towers are installed around the world in efforts such as FLUXNET (a global network of

micrometeorological towers). However, several complications exist with application of eddy covariance associated with its expensive installation, computationally challenging high frequency data and requirement of sophisticated micrometeorology expertise. Very few of those eddy covariance towers are installed in high elevation montane ecosystems, limiting the understanding of $ET_A$ in these settings.

Efforts to monitor ET in natural settings are associated with challenges of spatial heterogeneity in soil, and variably distributed vegetation in addition to several other biophysical processes. Various hydrological and land surface models are routinely applied to estimate ET in natural landscapes, however the capability of those models in simulating the spatial soil moisture dynamics which is a governing factor for $ET_A$ is limited due to inadequate soil information and lack of robust methods to account for complicating factors such as stone content in stone-dominant soils. This study focuses on application of numerical models and land surface models to quantify $ET_A$ with potential improvements by accounting for heterogeneity in soil due to stone content in montane ecosystems.

### 1.1. Research objectives

The goal of this research was to quantify and account for the effect of stone content in montane soil ecosystems and evaluate its influence in estimation of $ET_A$ using one-dimensional numerical- and land surface-models.

The specific objectives were to:

i. Examine the impact of stone content on soil hydraulic properties and explore ways to incorporate stone content into the soil water retention curve and applied models.

ii. Evaluate the influence of stone content on soil water properties and actual evapotranspiration using numerical model HYDRUS-1D

iii. Assess potential improvements in actual evapotranspiration simulated by a land surface model (i.e., Noah-MP) when incorporating detailed subsurface properties including the influence of soil-stone content.

## 1.2. Background

### *1.2.1. Effects of stone content on soil water retention*

Soil evaporation is driven by the atmospheric demand during initial stages of drying, but as drying continues, $ET_A$ becomes more restricted by available soil moisture. Soil moisture dynamics are a function of the soil hydraulic properties, which are governed by the soil particle size distribution and constituent composition (Jones and Or, 1998; Sakaki and Smits, 2015). Stone fragments embedded in soil alter the bulk hydraulic properties as a result of their particle-size and distribution. Non-arable soils in natural settings commonly have significant stone content as a result of their formation process and shallow depth to bedrock (Novak and Surda, 2010; Poesen and Lavee, 1994). Soils containing over 35% stone fragments (i.e., particles larger than 2 mm) by volume are referred to as stony-soils (Jahn et al., 2006; Tetegan et al., 2011; Hlavacikova et al., 2016).

The porosity and the density of different rock/stone types vary widely and typically have lower water retention capacity and hydraulic conductivity, depending on their parent rock properties (Flint and Childs, 1984; Ma and Shao, 2008; Ma et al., 2010). Rocks such as, fine sandstone, dolomite and granite may exhibit porosities as low as 3%, which can significantly decrease the stony-soil water storage (Manger, 1963; Parajuli et al., 2017). In

this situation, the soil water reservoir is altered reducing the water available for plant root extraction and thus diminishing the rate of $ET_A$ (Cousin et al., 2003; Tetegan et al. 2011). On the other hand, some stones are capable of holding substantial amount of water and contributing to root water uptake depending upon their water retention function (Coile, 1953; Flint and Childs, 1984; Ugolini et al., 1998). For example, there are rocks such as pumice and coarse sandstones which exhibit porosities nearly 80% and 35% respectively, that may considerably increase the water holding capacity of the soil (Blonquist et al., 2006) and may augment the water flow through the soil (Coile, 1953; Cousin et al., 2003; Ma et al., 2010). Such stones were shown to contribute an average of 15% to the total available water for plants over the range of 1.6% to 52.1% as presented in Flint and Childs (1984).

Two different approaches are common while dealing with stony soils. One approach assumes the stones as non-porous system, in which, stones were assumed to be non-porous inclusions hence any amount of water held by the stones were not accounted for, leading to reduced water estimation per unit volume as pointed out by Cousin et al. (2003) and Ugolini et al. (1998). Plant available water in the soil in such case may be underestimated by up to 34% as presented in Cousin et al. (2003). By contrast, when the stones were neglected and essentially considered similar to the fine soil matrix that has a higher water holding capacity than stones, plant available water was overestimated by 39%.

*1.2.2. Estimating evapotranspiration from stony soil*

Several analytical models have been developed to estimate ET where there are no direct measurements. The most widely used model is a modification of the Penman-

Monteith (PM) equation to estimate a reference ET ($ET_o$), value based on observed meteorological parameters such as net radiation, wind speed, humidity as well as temperature. This $ET_o$ value represents the rate of ET of a mythical short green crop (grass) of uniform height with unlimited water availability that fully covers the ground and has very low and uniform stomatal resistance (Allen et al., 1998). The $ET_o$ is therefore governed by meteorological parameters, and does not depend on soil water availability and vegetation characteristics, the actual ET ($ET_A$) is different from $ET_o$ and is usually less, due to limited soil moisture and actual foliage conditions. Reference ET is often used along with empirical crop coefficients to approximate actual ET from irrigated crops. However, it is difficult to apply such coefficients in natural settings with wide assortment of vegetation where the ET demand is restricted by soil moisture availability (Spano et al., 2009).

Soil moisture dynamics play a role in many ecological and environmental processes including ET (Koster et al., 2004; Miyazawa et al., 2013; Wilson et al., 2001). Numerical models, often referred as Soil-Plant-Atmosphere Continuum (SPAC) models, are able to simulate plant root water uptake and surface evaporation precisely estimating $ET_a$ based on soil moisture dynamics. The HYDRUS-1D numerical model has been widely used for simulating $ET_A$ (Hilten et al., 2008; Hlaváčiková and Novák 2013; Ries et al 2015; Solyu et al., 2011; Sutanto et al., 2012). The HYDRUS-1D software couples a root water uptake model with reference ET equations such as FAO Penman-Monteith and Hargreaves to provide a sink term and soil surface boundary conditions for inversely solving the Richards equation (Feddes et al., 2001; Simunek et al., 2008). The model is able to simulate water flow in and out of the soil when sufficient soil and vegetation parameters are provided.

Moreover, the model can inversely fit the soil hydraulic parameters when temporally-measured soil properties such as water content or matric potential are input (Simunek et al., 2013).

However, obtaining detailed information on soil and vegetation, including stone content, root growth and distribution requires time- and labor-intensive sampling and analysis. Soil stone content distribution is often heterogeneous and affects hydraulic properties, requiring consideration for accurate simulation of root water uptake. Higher stone content is expected to lower the hydraulic conductivity as well as the soil water content of stony soil in comparison to the soil matrix (i.e., composed of particles below 2 mm in diameter; Novak and Knava, 2011; Hlaváčiková et al. 2016). Generally, stone content reduces water available for root uptake and hence may limit the rate and duration of $ET_A$ (Novak and Knava, 2012; Parajuli et al., 2017; Tetegan et al. 2011). This research is aimed at better understanding the impact of stone fragments on estimation of $ET_A$ in montane ecosystems using numerical modeling tools. This method also provides an opening to have improved $ET_A$ information at regional scales using numerical modeling based on meteorological and soil moisture data available from hundreds of Soil Climate Analysis Network (SCAN) and SNOwpack TELemetry (SNOTEL) sites. The SCAN and SNOTEL sites in the state of Utah are shown in Fig. 1.1.

### *1.2.3. Soil parameterization of land surface models*

Land surface models (LSMs) have gradually evolved since the early eighties. They have improved significantly over the past few decades with development in high-performance computing capabilities and taking advantage of increasingly finer temporal

and spatial resolution supported by ground-based measurements and remote sensing (Chen and Dudhia, 2001; Ek et al., 2003; Kumar et al., 2006; Mahrt and Ek 1984; Mahrt and Pan 1984; Niu et al., 2011; Yang et al., 2011). A number of studies have applied LSMs to simulate surface energy and water fluxes using near-surface atmospheric boundary forcing (Ek et al., 2003; Cai et al., 2014a; 2014b; Chen et al., 1996; Long et al., 2014; Gayler et al., 2013,2014). Several studies have applied LSMs to characterize ET, which simulates soil moisture impact on surface evaporation and plant uptake within the soil profile as transpiration (Cai et al., 2014; 2014a; Chen et al., 1996; Long et al., 2014). With the advancement of knowledge in the fields of hydrology, meteorology, bio- and soil-physics, LSMs have become more physically-based (Ek et al., 2003; Mahrt and Ek, 1984; Niu et al., 2011; Yang et al., 2011). Soil hydrology is still poorly represented in LSMs because soil property spatial variability is poorly represented using simplified concepts. The complexities of soil moisture and water flux exchange processes between the land surface and atmosphere are in need of improved representation in LSMs (Koster and Suarez, 1992; Li et al., 2013; Ke et al., 2013).

Noah-Multiparameterization (Noah-MP) LSM is one of the most commonly used LSMs and has incorporated schemes for runoff, leaf dynamics, stomatal resistance, and a soil moisture factor (Niu et al., 2011; Yang et al., 2011; Gayler et al., 2014). Noah-MP is available with multiple options for major land-atmosphere interaction processes, however the model assumes a vertically homogenous soil within its default setting (Cai et al 2014a; Niu et al., 2011; Yang et al., 2011; Barlage et al., 2015). The hydraulic properties are poorly characterized by the soil parameter values which are limited to a number of soil types based on textural class in a soil parameter table. The poorly defined soil texture creates further

limitations for LSMs to accurately simulate soil moisture and water fluxes, as identified in previous studies (Gayler et al., 2013; 2014; Koster et al., 2006; Niu et al., 2011). It is essential for LSMs to account for detailed sub-surface properties in order to advance their capability in simulating fluxes.

### 1.3. Outline

This dissertation uses a multiple-paper format. Chapters 2-4 are each written as independent paper. Chapter 2 presents a binary mixing model for stony-soil that accounts for the stone water retention. It introduces an averaging scheme based on individual water retention properties of stone and soil, which was tested with laboratory measurements using three distinct stone types embedded in soil at various volumetric stone contents. Chapter 3 presents the numerical simulation of the ET using soil moisture dynamics from various climate stations in northern Utah and southern Idaho characterized by stony soils. The stone fragments were found to be vital in modulating the actual ET in stony soil ecosystems, thus chapter 3 highlights the importance of incorporating information regarding hydraulic properties of stones to estimate the ET using soil moisture dynamics in stony soil. Chapter 4 evaluates the potential for improvement in land surface models towards better estimate of evapotranspiration by refining the soil parameterization. Inserting more detailed soil information into the land surface model resulted to a better simulation of soil moisture as well as evapotranspiration. Adding verification to the results in chapter 3, the Noah-MP land surface model with information on stone content resulted in best estimation of ET. Finally, chapter 5 provides overall conclusion for the studies presented in three substantive

chapters. It also reveals the connection between three chapters and their contribution towards advancing ET estimates in montane ecosystems.

**References**

Allen, R. G., Pereira, L. S., Raes, D., & Smith, M. (1998). Crop evapotranspiration-Guidelines for computing crop water requirements-FAO Irrigation and drainage paper 56. *FAO, Rome*, *300*(9), D05109.

Barlage, M., Tewari, M., Chen, F., Miguez-Macho, G., Yang, Z. L., & Niu, G. Y. (2015). The effect of groundwater interaction in North American regional climate simulations with WRF/Noah-MP. *Climatic Change*, *129*(3-4), 485-498.

Bernstein, L., Bosch, P., Canziani, O., Chen, Z., Christ, R., Davidson, O. et al. (2007). Climate change 2007: Synthesis report. Contribution of Working Groups I, II and III to the fourth assessment report of the Intergovernmental Panel on Climate Change. *IPCC: Geneva, Switzerland*.

Blonquist, J. M. Jr., Jones, S. B., Lebron, I., & Robinson, D. A. (2006). Microstructural and phase configurational effects determining water content: Dielectric relationships of aggregated porous media. *Water Resour. Res.*, 42, W05424. doi:10.1029/2005WR004418

Cai, X., Yang, Z. L., David, C. H., Niu, G. Y., & Rodell, M. (2014). Hydrological evaluation of the Noah-MP land surface model for the Mississippi River Basin. *Journal of Geophysical Research: Atmospheres*, *119*(1), 23-38.

Cai, X., Yang, Z. L., Xia, Y., Huang, M., Wei, H., Leung, L. R., & Ek, M. B. (2014a). Assessment of simulated water balance from Noah, Noah-MP, CLM, and VIC over CONUS using the NLDAS test bed. *Journal of Geophysical Research: Atmospheres*, *119*(24).

Chaney, N. W., Wood, E. F., McBratney, A. B., Hempel, J. W., Nauman, T. W., Brungard, C. W., & Odgers, N. P. (2016). POLARIS: A 30-meter probabilistic soil series map of the contiguous United States. *Geoderma*, *274*, 54-67.

Chen, F., Mitchell, K., Schaake, J., Xue, Y., Pan, H. L., Koren, V., & Betts, A. (1996). Modeling of land surface evaporation by four schemes and comparison with FIFE observations. *J. of Geophysical Res.: Atmospheres*, *101*(D3), 7251-7268.

Chen, F., & Dudhia, J. (2001). Coupling an advanced land surface–hydrology model with the Penn State–NCAR MM5 modeling system. Part I: Model implementation and sensitivity. *Monthly Weather Review*, *129*(4), 569-585.

Coile, T. S. (1953). Moisture Content of Small Stones in Soil. *Soil Sci.*, 123, 203-207.

Cousin, I., Nicoullaud, B., & Coutadeur, C. (2003). Influence of rock fragments on the water retention and water percolation in a calcareous soil. *Catena* (53), 97-114.

Ek, M. B., K. E. Mitchell, Y. Lin, E. Rogers, P. Grunmann, V. Koren, G. Gayno, and J. D. Tarpley. (2003). Implementation of Noah land surface model advances in the National Centers for Environmental Prediction operational mesoscale Eta model, *J. Geophys. Res*., 108(D22), 8851, doi: 10.1029/2002JD003296.

Feddes, R. A., Hoff, H., Bruen, M., Dawson, T., de Rosnay, P., Dirmeyer, P., & Pitman, A. J. (2001). Modeling root water uptake in hydrological and climate models. *Bulletin of the American meteorological society*, *82*(12), 2797-2809.

Flint, A. L., & Childs, S. (1984). Physical properties of rock fragments in skeletal soils. In *Erosion and Productivity of Soils Containing Rock Fragments*, (pp 91-103). Madison, WI: Soil Science Society of America

Gayler, S., Ingwersen, J., Priesack, E., Wöhling, T., Wulfmeyer, V., & Streck, T. (2013). Assessing the relevance of subsurface processes for the simulation of evapotranspiration and soil moisture dynamics with CLM3. 5: comparison with field data and crop model simulations. *Environmental earth sciences*, *69*(2), 415-427.

Gayler, S., Wöhling, T., Grzeschik, M., Ingwersen, J., Wizemann, H. D., Warrach-Sagi, K., ... & Wulfmeyer, V. (2014). Incorporating dynamic root growth enhances the performance of Noah-MP at two contrasting winter wheat field sites. *Water Resources Research*, 50(2), 1337-1356.

Hengl, T., de Jesus, J. M., Heuvelink, G. B., Gonzalez, M. R., Kilibarda, M., Blagotić, A., ... & Guevara, M. A. (2017). SoilGrids250m: Global gridded soil information based on machine learning. *PLoS one*, *12*(2), e0169748.

Hilten, R. N., Lawrence, T. M., & Tollner, E. W. (2008). Modeling stormwater runoff from green roofs with HYDRUS-1D. *Journal of Hydrology*, *358*(3-4), 288-293.

Hlaváčiková, H., & Novák, V. (2013). Comparison of daily potential evapotranspiration calculated by two procedures based on Penman-Monteith type equation. *Journal of Hydrology and Hydromechanics*, *61*(2), 173-176.

Hlaváčiková, H., Novák, V., & Šimůnek, J. (2016). The effects of rock fragment shapes and positions on modeled hydraulic conductivities of stony soils. *Geoderma*, *281*, 39-48.

Jahn, R., Blume, H. P., Asio, V. B., Spaargaren, O., & Schad, P. (2006). *Guidelines for soil description* (p. 97). FAO.

Jones, S.B., and D. Or. (1998). Design of porous media for optimal gas and liquid fluxes to plant roots. *Soil Sci. Soc. Am. J.* 62:563 573.

Ke, Y., Leung, L. R., Huang, M., & Li, H. (2013). Enhancing the representation of subgrid land surface characteristics in land surface models. *Geoscientific Model Development*, *6*(5), 1609-1622.

Kool, D., Agam, N., Lazarovitch, N., Heitman, J. L., Sauer, T. J., & Ben-Gal, A. (2014). A review of approaches for evapotranspiration partitioning. *Agricultural and Forest Meteorology*, *184*, 56-70.

Koster, R. D., & Suarez, M. J. (1992). Modeling the land surface boundary in climate models as a composite of independent vegetation stands. *Journal of Geophysical Research: Atmospheres*, *97*(D3), 2697-2715.

Koster, R. D., and Coauthors, 2004: Realistic initialization of land surface states: Impacts on subseasonal forecast skill. *J. Hydrometeor.*, **5,** 1049–1063.

Kumar, S. V., Peters-Lidard, C. D., Tian, Y., Houser, P. R., Geiger, J., Olden, S., ... & Adams, J. (2006). Land information system: An interoperable framework for high resolution land surface modeling. *Environmental modelling & software*, *21*(10), 1402-1415.

Li, H., Wigmosta, M. S., Wu, H., Huang, M., Ke, Y., Coleman, A. M., & Leung, L. R. (2013). A physically based runoff routing model for land surface and earth system models. *Journal of Hydrometeorology*, *14*(3), 808-828.

Liu, S. M., Xu, Z. W., Zhu, Z. L., Jia, Z. Z., & Zhu, M. J. (2013). Measurements of evapotranspiration from eddy-covariance systems and large aperture scintillometers in the Hai River Basin, China. *Journal of hydrology*, *487*, 24-38.

Long, D., Longuevergne, L., & Scanlon, B. R. (2014). Uncertainty in evapotranspiration from land surface modeling, remote sensing, and GRACE satellites. *Water Resources Research*, *50*(2), 1131-1151.

Ma, D., & Shao, M. (2008). Simulating infiltration into stony soils with a dual-porosity model. *European Journal of Soil Science*, *59*(5), 950-959.

Ma, D., Shao, M., Zhang, J., & Wang, Q. (2010). Validation of an analytical method for determining soil hydraulic properties of stony soils using experimental data. *Geoderma*, *159*(3), 262-269.

Mahrt, L., & Ek, M. (1984). The influence of atmospheric stability on potential evaporation. *Journal of Climate and Applied Meteorology*, *23*(2), 222-234.

Mahrt, L., & Pan, H. (1984). A two-layer model of soil hydrology. *Boundary-Layer Meteorology*, *29*(1), 1-20.

Manger, G. E. (1963). *Porosity and Bulk Density of Sedimentary Rocks*. Washington, D.C.: United States Government Printing Office.

Miyazawa, Y., Kobayashi, N., Mudd, R. G., Tateishi, M., Lim, T., Mizoue, N., ... & Kumagai, T. (2013). Leaf and soil-plant hydraulic processes in the transpiration of tropical forest. *Procedia Environmental Sciences*, *19*, 77-85.

Mu, Q., Heinsch, F. A., Zhao, M., & Running, S. W. (2007). Development of a global evapotranspiration algorithm based on MODIS and global meteorology data. *Remote Sensing of Environment, 111*(4), 519-536.

Nagler, P. L., Scott, R. L., Westenburg, C., Cleverly, J. R., Glenn, E. P., & Huete, A. R. (2005). Evapotranspiration on western US rivers estimated using the Enhanced Vegetation Index from MODIS and data from eddy covariance and Bowen ratio flux towers. Remote sensing of environment, 97(3), 337-351.

Niu, G. Y., Z. L. Yang, K. E. Mitchell, F. Chen, M. B. Ek, M. Barlage, A. Kumar, K. Manning, D. Niyogi, E. Rosero, M. Tewari, and Y. L. Xia. 2011. The community Noah land surface model with multiparameterization options (Noah-MP): 1. Model description and evaluation with local-scale measurements. *Journal of Geophysical Research-Atmospheres* **116**: D12109.

Novak, V., & Knava, K. (2012). The influence of stoniness and canopy properties on soil water content distribution: simulation of water movement in forest stony soil. *Eur. J. Forest Res.*, 131(6), 1727–1735.

Novák, V., & Šurda, P. (2010). The water retention of a granite rock fragments in High Tatras stony soils. *J. Hydrol. Hydromech.*, 58(3), 181–187.

Parajuli, K., Kang, K., Shrestha, S. (2014). Application of statistical downscaling in GCMs at constructing the map of precipitation in the Mekong River basin. *Russian Meteorology and Hydrology*, *39*(4), 271-282.

Parajuli, K., Sadeghi, M., & Jones, S. B. (2017). A binary mixing model for characterizing stony-soil water retention. *Agricultural and Forest Meteorology*, *244*, 1-8.

Poesen, J., & Lavee, H. (1994). Rock fragments in top soils: significance and processes. *Catena*, 23(1-2), 1–28.

Ries, F., Lange, J., Schmidt, S., Puhlmann, H., & Sauter, M. (2015). Recharge estimation and soil moisture dynamics in a Mediterranean, semi-arid karst region. *Hydrology and Earth System Sciences*, *19*(3), 1439-1456.

Sakaki, T., & Smits, K. M. (2015). Water Retention Characteristics and Pore Structure of Binary Mixtures. *Vadose Zone J.* doi:10.2136/vzj2014.06.0065

Shrestha, S., Khatiwada, M., Babel, M. S., & Parajuli, K. (2014). Impact of climate change on river flow and hydropower production in Kulekhani hydropower project of Nepal. *Environmental Processes*, *1*(3), 231-250.

Šimůnek, J., M. Šejna, H. Saito, M. Sakai, and M. Th. van Genuchten. (2013). The HYDRUS-1D Software Package for Simulating the Movement of Water, Heat, and Multiple Solutes in Variably Saturated Media, Version 4.17, *HYDRUS Software Series 3*, Department of Environmental Sciences, University of California Riverside, Riverside, California, USA, pp. 343.

Soylu, M. E., Istanbulluoglu, E., Lenters, J. D., & Wang, T. (2011). Quantifying the impact of groundwater depth on evapotranspiration in a semi-arid grassland region. *Hydrology and Earth System Sciences*, *15*(3), 787-806.

Spano, D., Snyder, R.L., Sirca, C., Duce, P., 2009. ECOWAT—A model for ecosystem evapotranspiration estimation. Agric. For. Meteorol. 149(10): 1584-1596.

Sutanto, S. J., Wenninger, J., Coenders-Gerrits, A. M. J., & Uhlenbrook, S. (2012). Partitioning of evaporation into transpiration, soil evaporation and interception: a comparison between isotope measurements and a HYDRUS-1D model. *Hydrology and Earth System Sciences*, *16*(8), 2605-2616.

Tetegan, M., Nicoullaud, B., Baize, D., Bouthier, A., & Cousin, I. (2011). The contribution of rock fragments to the available water content of stony soils: Proposition of new pedotransfer functions. *Geoderma* (165), 40-49.

Ugolini F.C., Corti G., Agnelli A., Certini G. (1998) Under- and overestimation of soil properties in stony soils. *16th World Congress of Soil Science*, Montpellier

Wang, S.-Y., Gillies, R., 2012. Climatology of the U.S. Inter-Mountain West, Modern Climatology, Dr Shih-Yu Wang (Ed.), ISBN: 978-953-51-0095-9

Wang, S., Pan, M., Mu, Q., Shi, X., Mao, J., Brümmer, C., ... & Black, T. A. (2015). Comparing evapotranspiration from eddy covariance measurements, water budgets, remote sensing, and land surface models over Canada. *Journal of Hydrometeorology*, *16*(4), 1540-1560.

Wilcox, B.P., Breshears, D.D., Seyfried, M.S., 2003. Water balance on rangelands. In:Stewart, B.A., Howell, T.A. (Eds.), *Encyclopedia of Water Science*. Marcel Dekker,Inc., New York, pp. 791–794.

Williams, D. G., Cable, W., Hultine, K., Hoedjes, J. C. B., Yepez, E. A., Simonneaux, V., ... & Hartogensis, O. K. (2004). Evapotranspiration components determined by stable isotope, sap flow and eddy covariance techniques. *Agricultural and Forest Meteorology*, *125*(3-4), 241-258.

Wilson, K.B., Hanson, P.J., Mulholland, P.J., Baldocchi, D.D., Wullschleger, S.D., 2001. A comparison of methods for determining forest evapotranspiration and its components: sap-flow, soil water budget, eddy covariance and catchment water balance. Agric. and For. Meteorol. 106(2): 153-168.

Yang, Z.-L., G.-Y. Niu, K. E. Mitchell, F. Chen, M. B. Ek, M. Barlage, L. Longuevergne, K. Manning, D. Niyogi, M. Tewari, and Y. Xia (2011), The community Noah land surface model with multiparameterization options (Noah-MP): 2. Evaluation over global river basins, J. Geophys. Res., 116, D12110, doi:10.1029/2010JD015140.

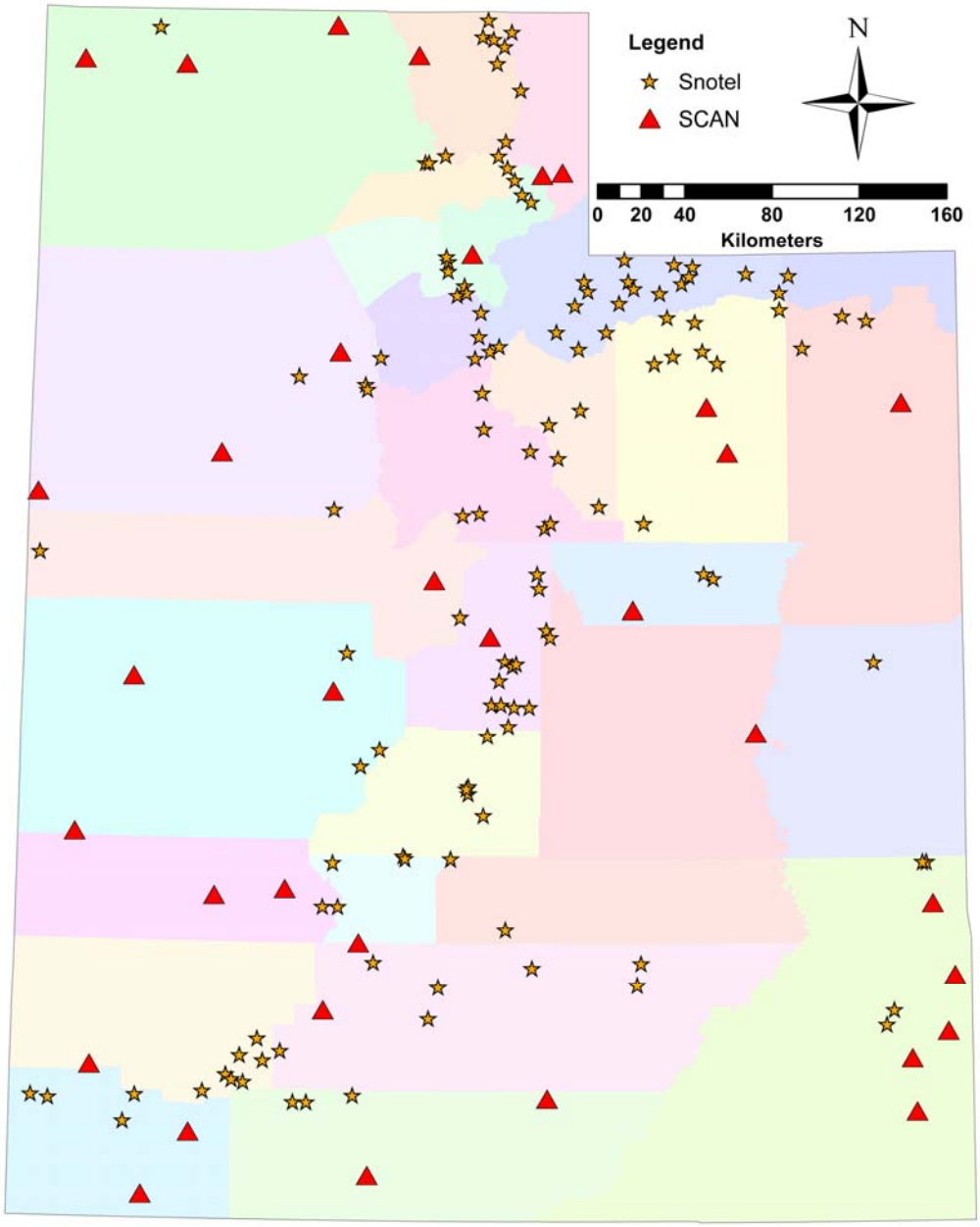


**Fig. 1.1.** Network of USDA Soil Climate Analysis Network (SCAN) and SNOwpack TELemetry (SNOTEL) network sites in Utah.

# CHAPTER 2

# A BINARY MIXING MODEL FOR CHARACTERIZING STONY-SOIL WATER RETENTION[1]


## Abstract

A century of research focused primarily on agricultural soils has largely ignored stony soils, which dominate some forests and are poorly understood in terms of the stone influence on soil hydraulic properties. Motivated by this knowledge gap, this research quantified the influence of soil-containing stone fragments on bulk soil hydraulic properties by determining the water retention curve (WRC) of soil, stone and stone-soil mixtures with varied volumetric stone content. The measured WRC for seven different stone types showed maximum and minimum saturated water contents of 0.55 $m^3$ $m^{-3}$ in pumice and 0.025 $m^3$ $m^{-3}$ in fine sandstone, respectively. The stony soil water retention function was measured using the simplified evaporation method. Contrasting scenarios were studied considering a broad range of stone inclusions; (*i*) negligibly porous, (*ii*) significantly porous but less porous than the background soil, (*iii*) more porous than the background soil. An averaging scheme to describe the WRC of stony soil was proposed based on the individual WRC of the background and stone inclusion which was in good agreement with the experimental data. The HYDRUS-3D model was also employed to simulate the


---

[1] Parajuli K., Sadeghi. M., Jones S. B. (2017). A Binary Mixing Model for Characterizing Stony-Soil Water Retention. *Agricultural and Forest Meteorology*, 244, pp 1-8

evaporation experiment used for the WRC measurements. The model simulations supported the basic assumptions of the proposed averaging scheme.

## 2.1. Introduction

Hydraulic properties of unsaturated soils, namely soil water retention characteristic (WRC) and unsaturated hydraulic conductivity, are critical physical aspects to model study the dynamics of flow and transport in soil (Coile, 1953; Cousin et al., 2003; Elliott et al., 1999; Low, 1954; Sauer and Logsdon, 2002; Schindler et al., 2006; Šimůnek et al., 1998; Yang et al., 2013 etc.). Soil hydraulic properties are mainly affected by the pore-size distribution, which is dictated by the soil particle size distribution (Jones and Or, 1998; Sakaki and Smits, 2015). Stone inclusions embedded in a background soil matrix will likewise alter the bulk hydraulic properties as a result of their pore-size distribution. With an emphasis on arable soils, the soil physics literature has largely focused on the properties of the soil matrix (i.e. particles passing through the 2-mm sieve), neglecting the influence of stones and rock fragments which are quite common in non-arable soils.

Soil containing over 35% stones by volume, i.e., soil particles larger than 2 mm, are classified as stony soil (Jahn et al., 2006; Tetegan et al., 2011; Hlavacikova et al., 2016). Unlike agricultural soils, most non-arable soils commonly have a significant stone content as a result of their formation process and shallow depth underlain by bedrock (Lv et al., 2017; Novak and Surda, 2010; Poesen and Lavee, 1994). Surface soils are commonly formed by the weathering of rock such as limestone, sandstone and quartzite, whose occurrence is spatially variable, both laterally and vertically.

As compared to the soil matrix, stones typically have lower water retention capacity and hydraulic conductivity, depending on their formation processes (Ma and Shao, 2008; Ma et al., 2010). The porosity and the density of different rock types are widely varied (Flint and Childs, 1984). For example, the porosity of sandstone may vary an order of magnitude between 0.03 to around 0.35 (Manger, 1963). There are rocks such as pumice which exhibit porosities greater than 80% that may significantly increase the water holding capacity of the soil (Blonquist et al., 2006) and may augment the water flow through the soil (Coile, 1953; Cousin et al., 2003; Ma et al., 2010). Some studies have shown stone fragments are capable of holding significant amounts of water available to plants (Coile, 1953; Flint and Childs, 1984; Ugolini et al., 1998). Flint and Childs (1984) found that stone fragments contributed an average of 15% to the total available water over the range of 1.6% to 52.1%. Apart from the water retention capacity, the stone fragments can alter the soil water movement by increasing the tortuosity and reducing the available soil-volume for the flow (Childs and Flint, 1990; Ma and Shao, 2008; Mehyus et al., 1975)

Several researchers examined the impact of stones on soil hydraulic properties (Reinhart, 1961; Bouwer and Rice, 1984; Childs and Flint, 1990; Fies et al., 2002; Poesen and Lavee, 1994; Sauer and Logsdon, 2002; Tokunaga et al., 2002, 2003; Cousin et al., 2003; Novák et al., 2011; Boateng et al., 2013; Wang et al., 2013). However, less attention has been paid to creating a predictive model for the hydraulic properties of stony soils. This study is a step toward developing a simple model for estimating the unsaturated hydraulic properties of soil-stone binary porous media. The main objective of this paper was to quantify the impact of stone fragments on the WRC using laboratory measurement techniques and numerical modelling. Three different classes of stone inclusions were

examined; (*i*) low porosity (fine sandstone), (*ii*) medium porosity, i.e., porosity below the background soil matrix (coarse sandstone), (*iii*) high porosity, i.e., porosity above the background soil matrix (pumice).

## 2.2. Theory

The van Genuchten (1980) model is assumed here to continuously represent the discrete WRC data for both the background soils and stone inclusions:

$$S = \frac{\theta - \theta_r}{\theta_s - \theta_r} = \left[1 + \left(\alpha h\right)^n\right]^{-m} \tag{1}$$

where $S$ [-] is the effective degree of saturation, $\theta$ [$L^3L^{-3}$] is the volumetric water content, $h$ [L] is the matric potential (absolute values are used here for convenience), $\theta_r$ and $\theta_s$ are the residual and saturated volumetric water contents, respectively, $\alpha$ [$L^{-1}$] is the scaling parameter and $n$ [-] and $m$ [-] are the shape parameters, assumed to be related as $m = 1 - 1/n$ (van Genuchten, 1980). In the following, the volumetric water content ($\theta$) is distinguished between background soil, stone inclusion and soil-stone mixture as $\theta_{soil}$, $\theta_{stone}$ and $\theta_{mix}$, respectively. Similarly, other variables and parameters are distinguished between different media with subscripts *soil*, *stone* or *mix*.

Our proposed averaging scheme is based on a correction to the following equation, proposed by Bouwer and Rice (1984):

$$\theta_{mix} = \left(1 - v\right)\theta_{soil} \tag{2}$$

where $v$ [$L^3L^{-3}$] is the volumetric stone content.

Equation (2) neglects the porosity of stone fragments, in spite of the fact that some types of stone (e.g., coarse sandstone, pumice) exhibit high porosity and water retention

capacity (Ma et al., 2010; Novak et al., 2011; Wang et al., 2013). Hence, Eq. (2) is corrected here to account for the stone porosity:

$$\theta_{mix} = (1-v)\theta_{soil} + v\theta_{stone} \tag{3}$$

To solve for the WRC of the soil-stone binary mixture, the matric potential between the background and inclusions is assumed to be in equilibrium. This assumption is later evaluated using numerical simulations. Accepting the equilibrium assumption, the WRC of the mixture is obtained using Eq. (3) at any given $h$:

$$\theta_{mix}(h) = (1-v)\theta_{soil}(h) + v\theta_{stone}(h) \tag{4}$$

Equation (4) in conjunction with Eq. (1) can be written in the form of Durner's (1992, 1994) dual-porosity soil WRC:

$$\begin{aligned} &S_{mix} = w_{soil}S_{soil} + w_{stone}S_{stone} = \\ &w_{soil}\left[1+(\alpha_{soil}h)^{n_{soil}}\right]^{-m_{soil}} + w_{stone}\left[1+(\alpha_{stone}h)^{n_{stone}}\right]^{-m_{stone}} \end{aligned} \tag{5}$$

where the weighting factors for soil and stone fractions, $w_{soil}$ and $w_{stone}$, can be solved analytically using Eq. (3) at saturation:

$$w_{soil} = \frac{(1-v)\theta_{s,soil}}{(1-v)\theta_{s,soil} + v\theta_{s,stone}} \tag{6}$$

$$w_{stone} = \frac{v\theta_{s,stone}}{(1-v)\theta_{s,soil} + v\theta_{s,stone}} \tag{7}$$

Equation (5) offers a simple averaging scheme to estimate the WRC of the soil-stone mixture by knowing the individual WRC for soil and stone. Based on the mass balance, the averaging scheme would be physically valid when the soil and stone are in equilibrium (i.e., identical matric potential). Therefore, Eq. (5) is assumed to be applicable

to static (i.e. no flow) condition. For the dynamic case, the validity of Eq. (5) will depend on the $h$ distribution within the mixture. The equilibrium assumption during soil evaporation processes will be discussed later.

As discussed in Gerke and van Genuchten (1993), the stony soil may behave as a dual porosity medium. In a dual-porosity heterogeneous soil system, water from the intra-aggregate pores drain earlier than the inter-aggregate pores. However stony soil may contain a significant overlapping region, described as the overlapping pore domain in Gerke and van Genuchten (1996), where both soil and stone concurrently contribute to the mixture WRC. Equations (5) to (7) provide an anlalytical approach to the empirical coefficients of the mixture WRC, rather than a regression analysis which requires laborious measurements of the soil-stone mixture WRC for any given volumetric stone content, $v$.

## 2.3. Materials and methods

### *2.3.1. Porous materials evaluated*

Various types of stone inclusions, including dolostone (DS), limestone (LS), two coarse sandstones (CSS1 and CSS2), two fine sandstones (FSS1 and FSS2) and pumice (PM), embedded in two different background soils, Millville silt loam and Wedron Silica sand were studied. The bulk density and saturated water content of these materials are presented in Table 2.1.

To determine the bulk density of the stone samples, they were submerged in water for 48 hours followed by exposure to vacuum (0.85 bar) saturation for 30 min to enhance the release of entrapped air inside the pores. After being submerged in water for another 24 hours, the saturated mass of stone samples were obtained. Once the saturated mass was

recorded, the stones were placed in an oven at 110 ºC for 48 hours to obtain the dry mass. The bulk density of each stone sample was computed as:

$$\rho_b = \frac{M_s}{V_t} \tag{8}$$

where $\rho_b$ [$ML^{-3}$] is the bulk density, $M_s$ [M] is the mass of oven dried sample, and $V_t$ [$L^3$] is the total volume of the sample. The saturated water content of the stone samples were calculated as:

$$\theta_s = \frac{\rho_b}{\rho_w}\left(\frac{M_{sat} - M_s}{M_s}\right) \tag{9}$$

where $M_{sat}$ [M] is the mass of the vacuum saturated stone sample and $\rho_w$ [$ML^{-3}$] is the density of water.

*2.3.2. WRC measurement methods*

While historically the most common methods for measuring the WRC have been with pressure plates, pressure flow (Tempe) cells, and hanging water columns, new electronically controlled methods recently developed include use of the dew point and evaporation methods (Dane and Hopmans, 2002; Dane and Topp, 2002; Leong et al., 2003; Scanlon et al., 2002; Schindler et al., 2010a, 2010b; Tuller and Or, 2004). A combination of both traditional and new methods, including the pressure plates, dewpoint potentiometer and simplified evaporation method (SEM), were used in this study to measure the WRC of the soil, stone and mix samples. The pressure plate apparatus was used for measuring WRC of the stone samples only. The dewpoint potentiometer was used for both soil and stone samples. The SEM was used for the mix samples.

The pressure plate apparatus with a 5-bar (500-kPa) plate was used to measure the lower range water potential (i.e. wet end) of the stone samples. The method described in Dane and Hopmans (2002) was followed for using the pressure plate extractor.

A dewpoint potentiometer device (WP4-T, Decagon Devices, Inc.) was used to determine the dry end of the soil and stone WRC, where matric potential is relatively high (i.e. between 1 and 300 MPa; Scanlon et al., 2002). The matric potential in the stone or soil sample was estimated based on equilibrating the vapor-phase water inside the chamber with the liquid-phase water from the sample and estimating the dewpoint temperature of the equilibrated chamber air (Bittelli and Flury, 2009; Tuller and Or, 2005). The corresponding mass was measured using a digital scale with resolution of 100 µg (AL-204, ACCULAB®). The water content was calculated for each measurement after determining the dry mass of the sample. A detailed description of the dewpoint potentiameter is provided in Leong et al. (2003), Macek et al. (2013) and Scanlon et al. (2002).

The SEM (Peters and Durner, 2008; Peters et al., 2015) was used to measure WRC of soil and mix samples. The HYPROP (HYdraulic PROPerty analyzer, Decagon Devices Inc.; Schindler et al., 2010a, 2010b) device for the SEM was used that measures the WRC with simultaneous measurements of matric potential using two miniature tensiometers and sample average water content using mass balance (Macek et al., 2013; Peters et al., 2015; Schindler and Muller, 2006; Šimůnek et al., 1998). The HYPROP-measured WRC is limited to $h < 85$ kPa (Peters and Durner, 2008; Peters et al., 2015; Schindler et al., 2012; Schindler and Muller, 2006). Hence, some additional dry-end measurements for the soils were taken using the WP4-T.

*2.3.3. Sample preparation*

Stone samples were first cut to predetermined dimensions to enable measurement and tracking of changes in stone water content and also to accurately define the volumetric stone content in the mixture. Diamond dust-coated hole saws (2.5 cm i.d.) were used to cut cylindrical stone fragments for measurements in the WP4-T and HYPROP. The cylinders were then sliced to obtain the desired height using a diamond studded lapidary saw. Sample thickness was optimized to allow insertion into the WP4-T dew point potentiameter sample container, which has an internal diameter of 3.8 cm with 1 cm height.

Mixtures of Millville silt loam with CSS1 and FSS1 and mixtures of Wedron sand with pumice were evaluated considering seven different volumetric stone contents ($v$ = 0, 0.05, 0.1, 0.2, 0.3, 0.4 and 1). To prepare the mixtures for the HYPROP, oven-dried soils were packed layer-wise into the HYPROP's sample holder (8 cm diameter and 5 cm height). A packing bulk density of 1.38 and 1.70 g $cm^{-3}$ was considered for the Millville silt loam and Wedron sand, respectively. A regular pattern for embedding the stones within the background soil was considered. Two to three layers of stone were embedded within the soil depending on the stone content, $v$. The prepared mixtures were then saturated using a water supply connected to the bottom of the samples after which they were used for the simplified evaporation experiment.

*2.3.4. Numerical simulation using HYDRUS 3D*

In order to evaluate the validity of the equilibrium assumption, the simplified evaporation experiment was simulated using HYDRUS 3D which numerically solves the Richard's equation (Simunek et al., 2016). A three dimensional simulation was performed

for the mixture of Millville silt loam soil with 40% (i.e. $v$ = 0.4) of the coarse sandstone 1. The soil hydraulic parameters for the Millville silt loam and coarse sandstone were determined by fitting the van Genuchten model, Eq. (1), to their measured WRC data. The initial condition was set to saturated water content for both soil and stone inclusions. The upper boundary condition was set as the temporally variable evaporation rate measured during the evaporation experiment. The bottom boundary condition was set as zero flux.

## 2.4. Results and discussion

### *2.4.1. WRC of soils and stones*

Measured bulk density and porosity of the stone samples are illustrated in Fig. 2.1. Stone bulk density is mainly a function of the mineral composition and the parent rock formation process. A wide variation in the bulk density was observed for different stone samples with the highest values for dolostone in the range of 2.6 g $cm^{-3}$ to 2.65 g $cm^{-3}$ and the lowest values for pumice (~ 1 g $cm^{-3}$). Fig. 2.1 indicates that the physical relationship between saturated water content and bulk density remains similar as that of soil, given as follows:

$$\rho_b = 2.65\left(1-\theta_s\right) \tag{10}$$

where 2.65 (g $cm^{-3}$) is a common value for particle density of soils.

Equation (10) can be applied to estimate porosity or the saturated water content of stones based on bulk density, providing an approximation to the filed-scale saturated water content of the stony soils if the volumetric stone content ($v$) is known.

Fig. 2.2 illustrates measured WRCs for the studied soils and stones. It is evident that saturated water contents ($\theta_s$) for various porous materials varied over a broad range.

The pumice and coarse sandstones both exhibited medium to high values of $\theta_s$. In contrast, the fine sandstones, limestone and dolostone showed values of $\theta_s$ an order of magnitude lower than the higher porosity stones. The parameters $\alpha$ for all stone samples, except for the CSS1, were lower than that of the Millville silt loam, implying a higher air entry value of the inclusions than the background for the Millville mixtures (Fig. 2.3). The CSS1 on the other hand had a higher value of $n$ and a lower air entry-pressure exhibiting the water retention characteristics similar to that of the compact sand.

*2.4.2. Pressure distribution within the stony soil sample*

A basic assumption underlying the proposed averaging scheme, Eq. (5), is the equilibrium condition between the stone inclusions and background soil, i.e., stone fragments have the same matric potential as that of surrounding soil. Illustrating the spatial distribution of matric potential and volumetric water content within the sample during the drying process, Fig. 2.3 indicates the extent to which the equilibrium assumption is valid. The cross-section of the stone-soil mixture in three planes is depicted from the HYDRUS-3D simulation. Fig. 2.3a illustrates the transition in stone and matrix matric potentials during drying, showing equilibrium throughout the mixture of Millville silt loam soil and 40% coarse sandstone 1 through 1.5 days. A visible disparity in the matric potential is observed when stone water content approaches its residual value by day 2, developing a matric potential gradient between stone and soil. The spatial distribution of matric potential at day 2.5 shows an increasing vertical pressure gradient leading to more negative $h$ at the drying front. Based on this result, the proposed averaging method is expected to work well in the wet range of the WRC, but less correlation near the dry end. Errors associated in

applying the mixing model, Eq. (5), depend on the properties of both soil and stone as well as the heterogeneity structure. A discussion on the model error for the studied cases follows.

*2.4.3. WRC of stony soil mixtures*

The measured WRC for three different stone-soil mixtures, each with seven different stone contents, are presented in Fig. 2.4a, b and c, being representative of 3 vastly different mixing scenarios. The range of stone inclusions are; (*i*) low porosity (Fig. 2.4a), (*ii*) medium porosity, i.e., stone less porous than the background soil (Fig. 2.4b), and (*iii*) high porosity, i.e., stone more porous than the background soil (Fig. 2.4c).

A substantial difference between the various stone contents is evident, indicating the potentially significant role of stone fragments on the WRC of stony soils. These results contradict several past studies (e.g., Novak and Knava, 2012; Hlaváčiková et al., 2016) in which the WRC of stony soils were approximated based on the assumption of zero stone porosity. Fig. 2.4 highlights the fact that neglecting the porosity and water holding capacity of the stone fragments may result in a substantial underestimation of the actual water retention of stony soils. When low porosity stones are present in the soil, such as fine sandstone, the overall contribution to stony soil WRC is indeed negligible. In this case, the assumption of zero porosity for the stone fragments may provide a reasonable approximation. However, highly porous stones such as pumice (Fig 2.4c), if neglected, can for example lead to significant errors in modeling water flow processes.

Fig. 2.4 also presents estimates of the proposed averaging scheme, Eq. (5), in comparison with the measured data. The estimated WRCs are in a good agreement with the

observations for the case of Millville silt loam mixed with fine and coarse sandstones. However, modeled estimates of SWC for the Wedron sand and pumice mixture are not as consistent with measurements. To quantify the estimation errors, measured water contents for all mixtures were compared against the estimated water contents using Eq. (5). The total root mean squared error (RMSE) for Figs. 2.4a, 2.4b and 2.4c were obtained 0.015, 0.014 and 0.039 cm $cm^{-3}$, respectively.

This mismatch in the sand-pumice mixture is partly due to the narrow pore-size distribution of the sand leading to a step-like WRC coupled with a broad variation in the porosity of the pumice stone samples (air-entrapment in pumice). The step-like function minimized the mixing range of $h$ for the pumice samples and the variation in porosity of the pumice samples may not have been well-represented by the few samples providing the stone WRC. In addition, air entrapment in pumice fragments in the stone soil mixtures, would result in lower measured saturated water contents than what would be modeled.

Despite relatively poor performance of Eq. (5) for the case of Fig. 2.4c, it was able to accurately model the shape of WRC for the Wedron sand-pumice mixture, as illustrated in Fig. 2.5, where a least-squares fit of Eq. (5) to the measured data is shown. The WRCs were developed with the van Genuchten parameters, $\theta_r$, $\alpha$ and $n$ fitted to individual Wedron sand and pumice measurements (Fig. 2.2), whereas $w_{soil}$, $w_{stones}$ and $\theta_s$ were fitted to match the measurements in Fig. 2.5. The fitted weighting factor $w_{soil}$ and $w_{stones}$ in Fig. 2.5 were approaching the calculated values using Eqs. (6) and (7). However, $\theta_s$ values were smaller than the values calculated based on the weighted average as defined by Eq. (3), supporting the assumption of air entrapment during the process of saturation. These results illustrate

how small adjustments in the model parameters can produce a well-modeled WRC describing the soil-stone mixture using the Durner dual-porosity model.

**2.5. Summary and conclusion**

Our experimental data along with the numerical simulations demonstrated that stones can play an important role in the bulk stony-soil water retention characteristic. An averaging scheme based on individual water retention properties of stone and of soil was introduced and tested with laboratory measurements using three distinct stone types embedded in a background soil at various volumetric stone contents ($v$ = 0, 0.05, 0.1, 0.2, 0.3, 0.4 and 1). All WRC measurements presented here demonstrated the extent to which the stone fragments contributed to water retention and holding capacity of the stony soil. Stones exhibiting low porosity (FSS1, CSS1) contributed less to water retention than the background soil (Millville silt loam) leading to a reduced water retention with increased volumetric stone content. However, the bulk stony soil water retention was increased significantly with the increased volume fraction of stones exhibiting medium and high porosity. It is evident from this analysis that the WRC estimated without considering the holding capacity of stone inclusions may result in underestimation of water retention for highly porous stones such as pumice and coarse sandstone. This study has demonstrated, how stones present in soil can alter the effective hydraulic properties. Because stone hydraulic properties (i.e., porosity, pore-size distribution, etc.) vary widely, there is a need to expand studies on stony soils, emphasizing stone porosity and fraction of stone content in order to better estimate the resulting soil hydraulic properties. Developing more accurate averaging schemes to estimate the WRC (e.g., under non-equilibrium condition) as well as

predictive models for unsaturated hydraulic conductivity of stony soils are part of ongoing research.

**References**

Bouwer, H., & Rice, R. C. (1984). Hydraulic properties of stony vadose zones. *Ground Wate*r, 22(6), 696-705.

Bittelli, M., & Flury, M. (2009). Errors in Water Retention Curves Determined with Pressure Plates. *Soil Sci. Soc. Am. J.*, 73(5), 1453-1460.

Blonquist, J. M. Jr., Jones, S. B., Lebron, I., & Robinson, D. A. (2006). Microstructural and phase configurational effects determining water content: Dielectric relationships of aggregated porous media. *Water Resour. Res.*, 42, W05424. doi:10.1029/2005WR004418

Boateng, E., Yangyuoru, M., Breuning-Madsen, H., & MacCarthy, D. S. (2013). Characterization of soil-water retention with coarse fragments in the densu basin of Ghana. *West Afr. J. Appl. Ecol.*, 21(1), 31-46.

Childs, S. W., & Flint, A. L. (1990). Physical properties of forest soils containing rock fragments. *Sustained productivity of forest soils/edited by SP Gessel...[et. al.]*.

Coile, T. S. (1953). Moisture Content of Small Stones in Soil. *Soil Sci.*, 123, 203-207.

Cousin, I., Nicoullaud, B., & Coutadeur, C. (2003). Influence of rock fragments on the water retention and water percolation in a calcareous soil. *Catena* (53), 97-114.

Durner, W. (1992). Predicting the unsaturated hydraulic conductivity using multi-porosity water retention curves. *Indirect methods for estimating the hydraulic properties of unsaturated soils. Univ. of California, Riverside*, 185-202.

Durner, W. (1994). Hydraulic conductivity estimation for soils with heterogeneous pore structure. *Water Resour. Res.,* 30(2), 211-223, doi: 10.1029/93WR02676

Dane, J. H., & Topp, G. C. (2002). *Methods of Soil Analysis, Part 4: Physical Methods*. Madison, WI, USA: Soil Science Society of America.

Dane, J. H., & Hopmans J. W. (2002). Pressure Plate Extractor. In *Methods of Soil Analysis, Part 4: Physical Methods*. (pp. 688-690) Madison, WI, USA: Soil Science Society of America.

Elliott, E. T., Heil, J. W., Kelly, E. F., & Monger, H. C. (1999). Soil structural and other physical properties. In *Standard Soil Methods for Long-Term Ecological Research* (pp. 73-88). New York: Oxford University Press.

Fies, J., Louvigny, N. D., & Chanzy, A. (2002). The role of stones in soil water retention. *Eur. J. Soil Sci.*, *53*(1), 95-104.

Flint, A. L., & Childs, S. (1984). Physical properties of rock fragments in skeletal soils. In *Erosion and Productivity of Soils Containing Rock Fragments*, (pp 91-103). Madison, WI: Soil Science Society of America

Gerke, H. H., & van Genuchten, M. T. (1993). A dual-porosity model for simulating the preferential movement of water and solutes in structured porous media. *Water Resour. Res.*, *29*(2), 305-319.

Gerke, H. H., & van Genuchten, M. T. (1996). Macroscopic representation of structural geometry for simulating water and solute movement in dual-porosity media. *Adv. Water Resour.*, *19*(6), 343-357.

Hlaváčiková, H., Novák, V., & Šimůnek, J. (2016). The effects of rock fragment shapes and positions on modeled hydraulic conductivities of stony soils. *Geoderma*, *281*, 39-48.

Jahn, R., Blume, H. P., Asio, V. B., Spaargaren, O., & Schad, P. (2006). *Guidelines for soil description* (p. 97). FAO.

Jones, S.B., and D. Or. 1998. Design of porous media for optimal gas and liquid fluxes to plant roots. *Soil Sci. Soc. Am. J.* 62:563 573.

Leong, E. C., Tripathy, S., & Rahardjo, H. (2003). Total suction measurement of unsaturated soils with a device using the chilled-mirror dew-point technique. *Géotechnique*, 53(2), 173-182.

Low, A. J. (1954). The study of soil structure in the field and the laboratory. *J. Soil Sci.*, 5(1), 57-74.

Lv, L., S.B. Jones and L.E. Hipps. 2017. Evapotranspiration estimates in four common mountain vegetation species of the Intermountain West. Under review in *Ag. Forest Met*.

Ma, D., & Shao, M. (2008). Simulating infiltration into stony soils with a dual-porosity model. *European Journal of Soil Science*, *59*(5), 950-959.

Ma, D., Shao, M., Zhang, J., & Wang, Q. (2010). Validation of an analytical method for determining soil hydraulic properties of stony soils using experimental data. *Geoderma*, *159*(3), 262-269.

Macek, M., Smolar, J., & Petkovsek, A. (2013). Extension of measurement range of dew-point potentiometer and evaporation method. In *Proceedings of the 18th International Conference on Soil Mechanics and Geotechnical Engineering* (pp. 1137–1142). Paris.

Manger, G. E. (1963). *Porosity and Bulk Density of Sedimentary Rocks*. Washington, D.C.: United States Government Printing Office.

Mehuys, G.R., Stolzy, L.H., Letey, J. & Weeks, L.V. 1975. Effect of stones on the hydraulic conductivity of relatively dry desert soils. *Soil Science Society of America Proceedings*, **39**, 37–42.

Novak, V., & Knava, K. (2012). The influence of stoniness and canopy properties on soil water content distribution: simulation of water movement in forest stony soil. *Eur. J. Forest Res.*, 131(6), 1727–1735.

Novák, V., Kňava, K., & Šimůnek, J. (2011). Determining the influence of stones on hydraulic conductivity of saturated soils using numerical method. *Geoderma* (161), 177-181.

Novák, V., & Šurda, P. (2010). The water retention of a granite rock fragments in High Tatras stony soils. *J. Hydrol. Hydromech.*, 58(3), 181–187.

Peters, A., & Durner, W. (2008). Simplified evaporation method for determining soil hydraulic properties. *J. Hydrol.*, 356(1-2), 147–162.

Peters, A., Iden, S. C., & Durner, W. (2015). Revisiting the simplified evaporation method: Identification of hydraulic functions considering vapor, film and corner flow. *J. Hydrol.*, 527, 531–542.

Poesen, J., & Lavee, H. (1994). Rock fragments in top soils: significance and processes. *Catena*, 23(1-2), 1–28.

Reinhart, K. G. (1961). The Problem of Stones in Soil-Moisture Measurement. *Soil Sci. Soc. Am. J.*, 25(4), 268-270.

Sakaki, T., & Smits, K. M. (2015). Water Retention Characteristics and Pore Structure of Binary Mixtures. *Vadose Zone J.* doi:10.2136/vzj2014.06.0065

Sauer, T. J., & Logsdon, S. D. (2002). Hydraulic and Physical Properties of Stony Soils in a Small Watershed. *Soil Sci. Soc. Am. J.,* (66), 1947-1956.

Scanlon, B. R., Andraski, B. J., & Bilskie, J. (2002). Miscellaneous Methods for Measuring Matric or Water Potential. In *Methods of Soil Analysis Part 4: Physical Methods* (pp. 643-673). Madison, WI: Soil Science Society of America.

Schindler, U., Durner, W., von Unold, G., Mueller, L., & Wieland, R. (2010a). The evaporation method: Extending the measurement range of soil hydraulic properties using the air-entry pressure of the ceramic cup. *J. Plant Nutr. Soil Sci.*, 173(4), 563–572.

Schindler, U., Durner, W., von Unold, G., & Müller, L. (2010b). Evaporation method for measuring unsaturated hydraulic properties of soils: Extending the measurement range. *Soil Sci. Soc. Am. J.*, 74(4), 1071-1083.

Schindler, U., & Muller, L. (2006). Simplifying the evaporation method for quantifying soil hydraulic properties. *J. Plant Nutr. Soil Sci.*, (169), 623–629.

Schindler, U., Mueller, L., da Veiga, M., Zhang, Y., Schlindwein, S., & Hu, C. (2012). Comparison of water-retention functions obtained from the extended evaporation method and the standard methods sand/kaolin boxes and pressure plate extractor. *J. Plant Nutr. Soil Sci.*, 175(4), 527–534.

Šimůnek, J., van Genuchten, M. T., & Wendroth, O. (1998). Parameter estimation analysis of the evaporation method for determining soil hydraulic properties. *Soil Sci. Soc. Am. J.,* 62(4), 894-905.

Šimůnek, J., van Genuchten, M. T., & Šejna, M. (2016). Recent developments and applications of the HYDRUS computer software packages. *Vadose Zone J.*, *15*(7).

Tetegan, M., Nicoullaud, B., Baize, D., Bouthier, A., & Cousin, I. (2011). The contribution of rock fragments to the available water content of stony soils: Proposition of new pedotransfer functions. *Geoderma* (165), 40-49.

Tokunaga, T. K., Olson, K. R., & Wan, J. (2003). Moisture Characteristics of Hanford Gravels: Bulk, Grain-surface and Intergranular Components. *Vadose Zone J.* (2), 322-329.

Tokunaga, T. K., Wan, J., & Olson, K. R. (2002). Saturation-matric potential relations in gravel. *Water Resour. Res.*, 38(10), 1214.

Tuller, M., & Or, D. (2004). Retention of water in soil and the soil water characteristic curve. *Encyclopedia of Soils in the Environment*, *4*, 278-289.

Tuller, M., and D. Or (2005), Water films and scaling of soil characteristic curves at low water contents, Water Resour. Res., 41, W09403, doi:10.1029/2005WR004142.

Ugolini F.C., Corti G., Agnelli A., Certini G. (1998) Under- and overestimation of soil properties in stony soils. *16th World Congress of Soil Science*, Montpellier

Van Genuchten M. T. (1980) A closed-form equation for predicting the hydraulic conductivity of unsaturated soils. *Soil Sci. Soc. Am. J.,* 44, 892–898

Wang, H., Xiao, B., Wang, M., & Shao, M. (2013). Modeling the Soil Water Retention Curves of Soil-Gravel Mixtures with Regression Method on the Loess Plateau of China. *PLoS ONE*, 8(3), e59475.

Yang, Y.-F., Wang, Q.-J., & Zhuang, J. (2013). Estimating hydraulic parameters of stony soils on the basis of one-dimensional water absorption properties. *Acta* Agr. Scand. B – S. P., 63(4), 304-313.

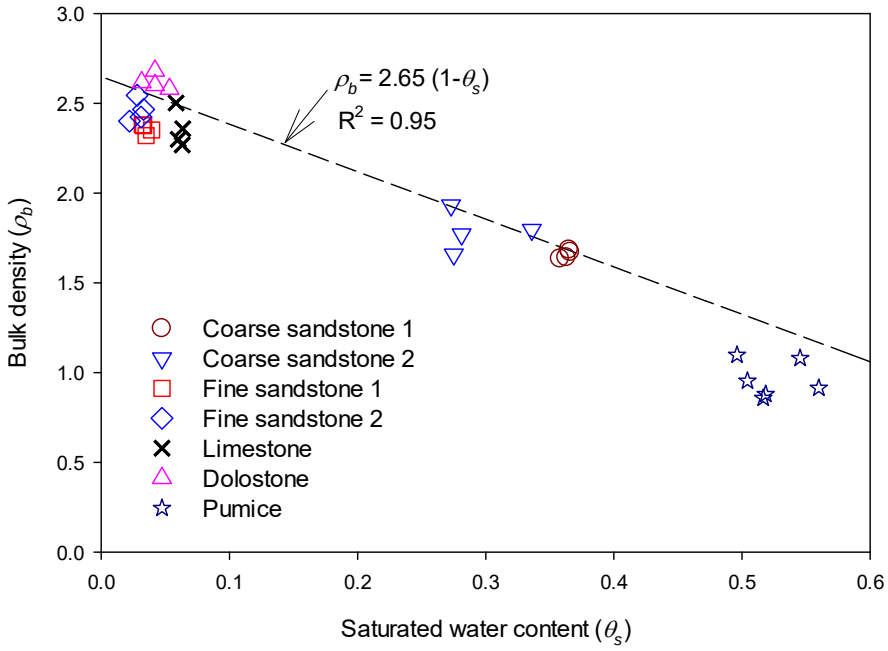


**Fig. 2.1.** Relationship between stone bulk density and saturated water content for different stone types. The relationship is in agreement with the physical relation of Eq.10) with the determination coefficient R2 of 0.95.

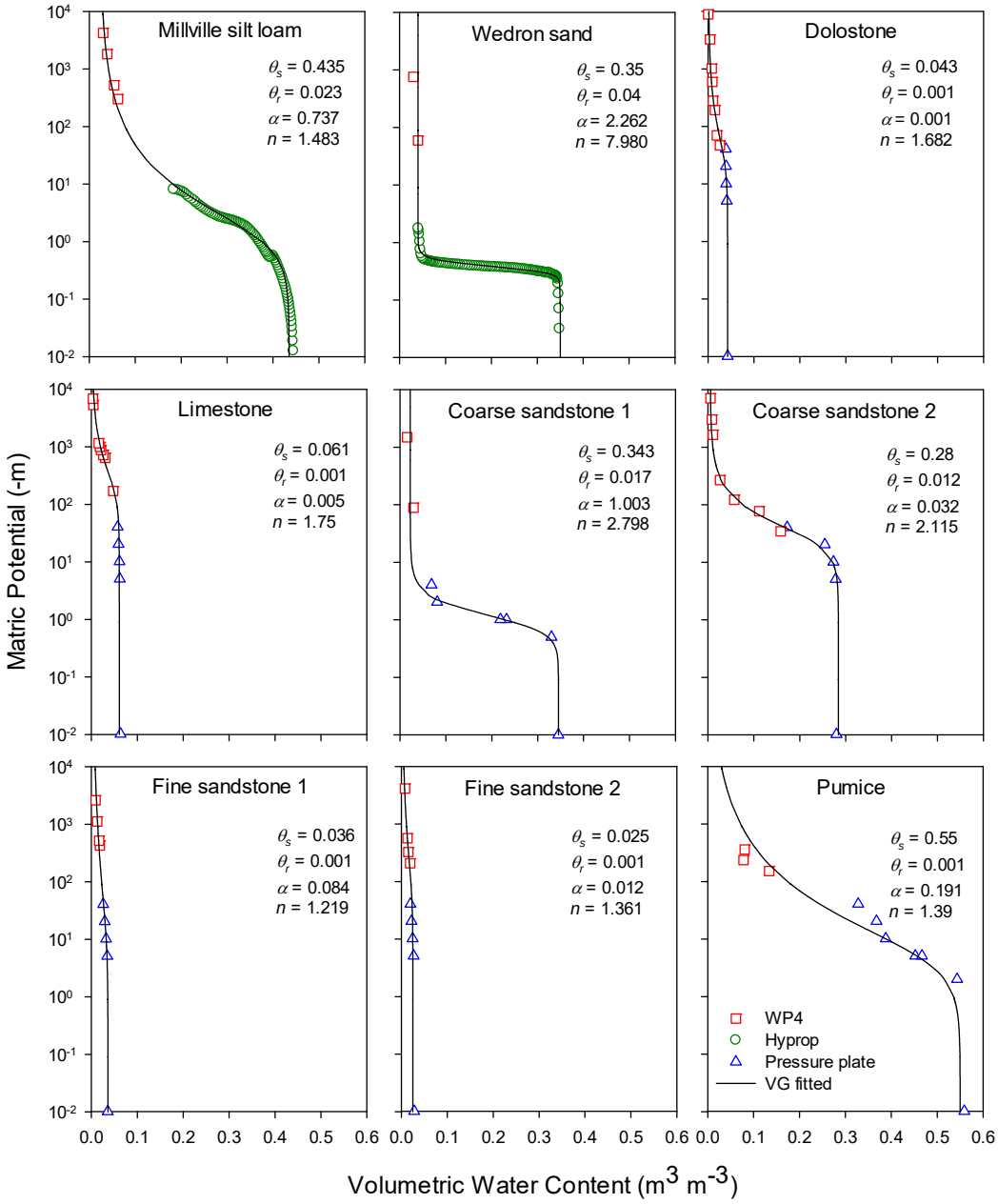


**Fig. 2.2.** Water retention data (points) and fitted van Genuchten (VG) curves (solid lines) for different soil samples Millville silt loam and Wedron sand and the stone samples including coarse sandstones, fine sandstones, limestone, dolostone and pumice measured using the pressure plate, dew point potentiometer (WP4) and HYPROP.

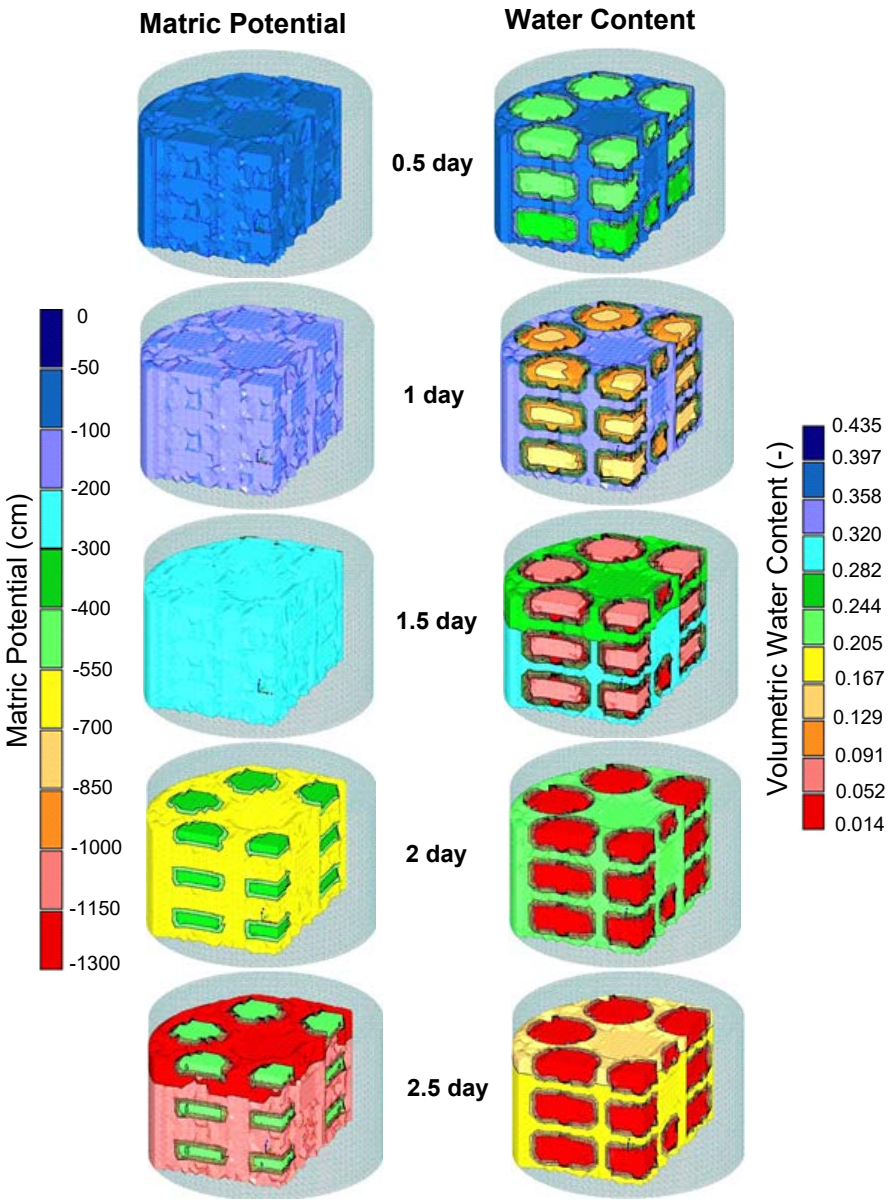


**Fig. 2.3.** HYDRUS-3D simulation results for distribution of matric potential and volumetric water content in Millville silt loam mixed with 40% coarse sandstone 1 during soil drying.

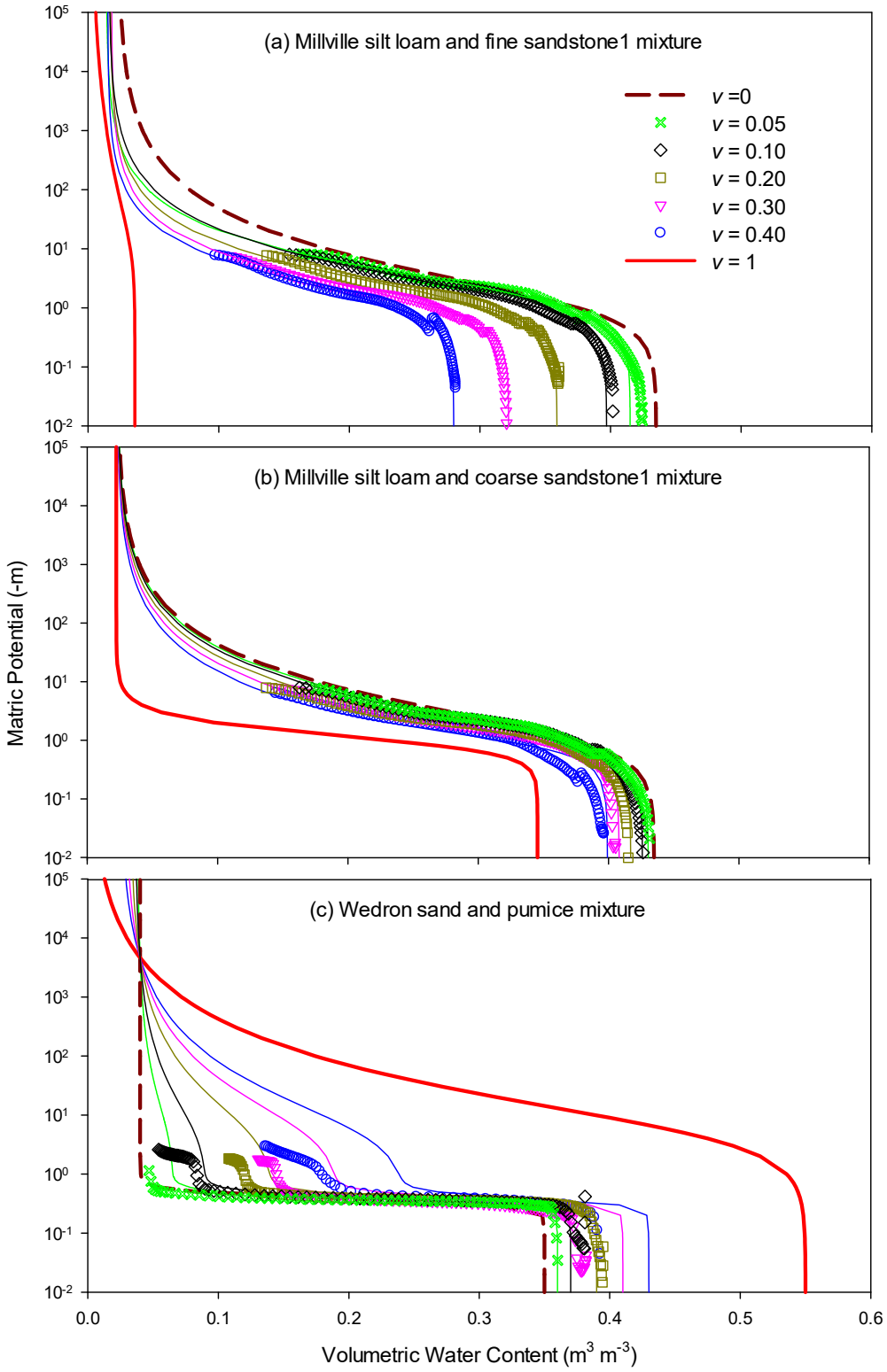


**Fig. 2.4.** Measured (points) and estimated [lines, Eq. (5)] water retention curves for different mixtures with various volumetric stone content ($v$).

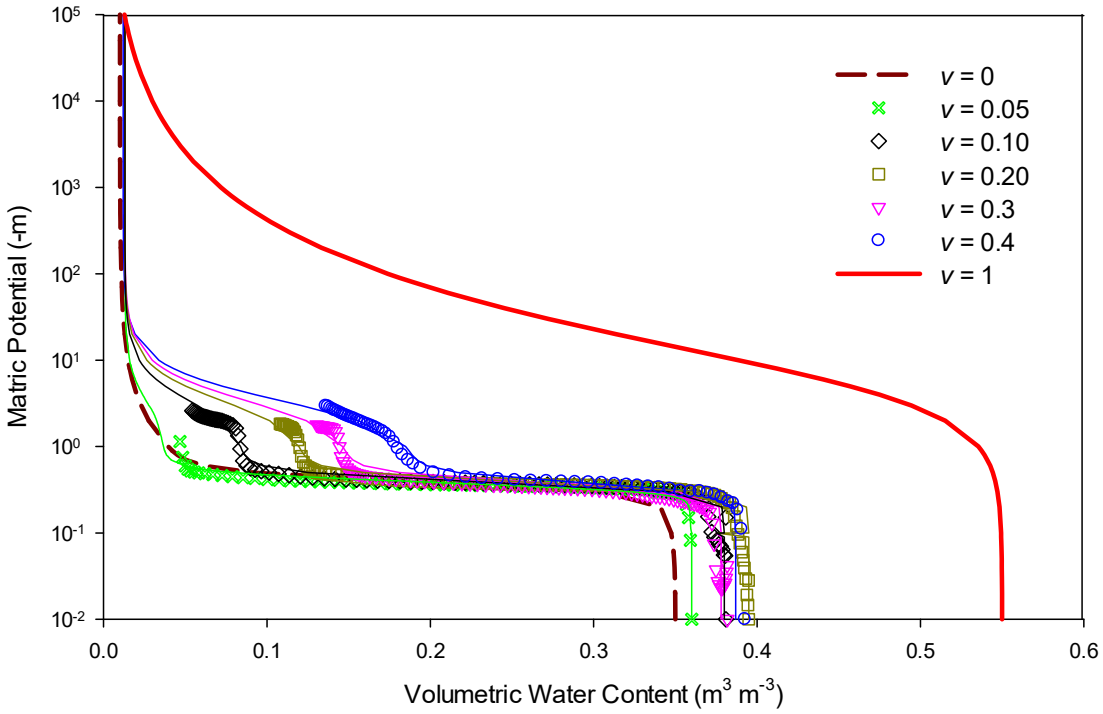


**Fig. 2.5.** Measured (points) water retention curves and the best fit of Eq. (5) (lines) for different mixtures of Wedron sand and pumice with various volumetric stone content ($v$).

**Table 2.1.** Physical properties of the studied background soils (Millville silt loam and Wedron silica sand) and stone inclusions (DS, LS, CSS, FSS and PM). The bulk density ($\rho_b$) and saturated water content ($\theta_s$) for each stone type were estimated as the mean of six different samples.

| **Porous material** | **Source** | $\rho_b$ **(g cm$^{-3}$)** | $\theta_s$ |
|---|---|---|---|
| Millville silt loam | Greenville Farm* | 1.38 | 0.437 |
| Wedron silica sand | Wedron silica Co. | 1.7 | 0.350 |
| Dolostone, DS | Canyon mouth† | 2.6 | 0.042 |
| Limestone, LS | Tony Grove† | 2.3 | 0.061 |
| Coarse sandstones 1, CSS1 | TWDEF ‡ | 1.65 | 0.363 |
| Coarse sandstones 2, CSS2 | Franklyn Basin† | 1.8 | 0.291 |
| Fine sandstones 1, FSS1 | TWDEF ‡ | 2.35 | 0.034 |
| Fine sandstones 2, FSS2 | Franklyn Basin† | 2.45 | 0.028 |
| Pumice, PM | Different Sources§ | 0.96 | 0.523 |

*North Logan, UT.
†Logan Canyon, Cache National Forest, Northern UT.
‡T.W. Daniel Experimental Forest, Cache National Forest, Northern UT.
§Coso range, California; Pocatello, Idaho.

# CHAPTER 3

# ESTIMATING EVAPOTRANSPIRATION FROM STONY-SOILS IN MONTANE ECOSYSTEMS [2]


## Abstract

Quantification of evapotranspiration (ET) is crucial for understanding the water balance and efficient water resources planning. Agricultural settings have received much attention regarding ET measurements while there is less knowledge for actual ET ($ET_A$) in natural ecosystems. This study is focused on modelling $ET_A$ from stony soil in montane ecosystems where we account for the contribution of stone water retention properties in soil. We employed a numerical model (HYDRUS-1D) to simulate $ET_A$ in natural settings in northern Utah and southern Idaho during the 2015 and 2016 growing season based on meteorological and soil moisture measurements at a range of depths. We simulate $ET_A$ under three different scenarios, considering soil with (i) no stones, (ii) highly porous stones, and (iii) negligibly porous stones. The simulation results showed significant overestimation of modeled $ET_A$ when neglecting stones, in comparison to $ET_A$ measured by eddy covariance. The modeled $ET_A$ estimates with negligibly porous stone were much lower in all stations due to the substantial decrease in soil water storage compared with estimates made considering highly porous stone. Assumptions of highly porous or negligibly porous stones in the soil, lead to reductions in simulated $ET_A$ of between 10% and 30%,


[2] Coauthored by Kshitij Parajuli, Scott B. Jones, David G. Tarboton, Gerald N. Flerchinger, Lawrence E. Hipps, L. Niel Allen, Mark S. Seyfried

respectively, when compared with the no stone condition. These results reveal the important role played by stones, common in many forest soils, in modulating water balance by affecting $ET_A$ in montane ecosystems.

### 3.1. Introduction

Evapotranspiration (ET) is the largest outward flux of water and a key component of the hydrological cycle and is therefore essential in quantifying the water budget and planning water resources (Baldocchi and Ryu, 2011; Mu et al., 2007; Schelde et al., 2011; Sheffield et al., 2010). Water flux to the atmosphere by the process of ET constitutes up to 95% of the water balance in arid regions (Kool et al., 2014; Wilcox et al., 2003). However, ET remains a major uncertainty in eco-hydrological systems, and this uncertainty motivates research on more accurate quantification of ET within large-scale irrigated projects and natural ecosystems. Forests have been recognized as a fundamental part of ecosystems that play a key part in regulating hydrological balance by altering streamflow and ET (Andreassia 2004; Ice and Stednick, 2004; Sun et al., 2008). Despite the fact that many studies have been conducted on ET estimation across different spatial scales ranging from point- to basin-scale (Parajuli 2015; Senay et al., 2011; Schelde et al., 2011), very few focused on the natural ecosystems as compared to agricultural settings. Accurate quantification of ET in natural ecosystems is essential to evaluate the effects of land management and global change on availability of water, streamflow, and ecosystem productivity (Andreassia 2004; Sun et al., 2008; Zhou et al, 2008).

Correct information about temporal and spatial variations in ET is critical for better understanding of the interactions between land surfaces and the atmosphere and solving

the water and energy balances used in hydrological and climate models (Kumar et al., 2006; Mu et al., 2007; Niu et al.,2011; Yang et al.,2011). Better estimates of ET are furthermore important to improve management of water resources and agricultural systems by assisting in decision making processes related to water allocations (Allen et al., 1998; Kumar et al., 2006; Mu et al., 2007, Raziei & Pereira, 2013). However, it is challenging to calculate ET over land surfaces characterized by heterogeneity in soil and vegetation type and other parameters affecting the ET phenomenon (Mu et al., 2007; Senay et al., 2011; Sheffield et al., 2010; Sun et al., 2008).

A number of techniques to estimate ET such as the catchment water budget method direct measurements using soil and plant weighing lysimeters, Bowen ratio and eddy covariance have been developed and applied at different scales (Prueger et al., 1997; Wilson et al., 2001). Watershed ET measurements that are based on a catchment scale water budget approach where ET is calculated as the residual of the water balance (Baldocchi and Ryu, 2011) depend on the reliability and accuracy of measurements or estimates of other parameters such as precipitation, runoff, drainage and infiltration. Lysimeters on the other hand can provide actual ET ($ET_A$) by measuring the weight change, though their installation and maintenance costs are high. The surface energy balance approach and eddy covariance technique provide alternatives to measure $ET_A$ at spatial- and point-scales, while their applications are limited due to the requirement of intensive measurements and information about energy balance components (Law et al., 2002; Wilson et al., 2001). The latent heat flux data collected at eddy covariance towers are considered as validation of the results from hydrologic models at point as well as regional scales (Baldocchi et al., 1988; Wilson et al., 2001).

Various analytical models have been developed to estimate ET where there are no direct measurements. A widely used model is the Penman-Monteith (PM) equation that calculates ET for a leaf or complete cover canopy based on observed meteorological parameters such as net radiation, wind speed and saturation deficit. The equation also includes turbulence characteristics by considering aerodynamic resistance and physiology via stomatal resistance. Both are however, diffcult to determine. The PM equation can be used to estimate reference ET ($ET_o$), which represents a mythical ET of a short green crop (grass) with unlimited water availability that fully covers the ground, and has arbitrarily low stomatal resistance (Allen et al., 1998). The $ET_o$ is estimated based on meteorological parameters and does not depend on soil water and vegetation. The actual ET ($ET_A$) will differ and is usually less due to limited soil moisture or stomatal responses to environment in natural ecosystems. As available soil moisture affects many ecological and environmental processes including ET, in principle, ET can be quantified by studying the soil moisture dynamics (Cai et al., 2017; Koster et al., 2004; Lv et al., 2014; Miyazawa et al., 2013; Wilson et al., 2001).

There are numerical modeling approaches that can estimate $ET_A$ by accounting for soil moisture dynamics in the simulation of plant root water uptake and surface evaporation. HYDRUS-1D is one such model that has been widely used for simulating $ET_A$ (Hilten et al., 2008; Hlaváčiková and Novák 2013; Ries et al 2015; Solyu et al., 2011; Sutanto et al., 2012). The HYDRUS-1D software couples a root water uptake model with an $ET_o$ equation based on a simplified Penman-Monteith, or Hargreaves equation to inversely solve the Richards equation (Feddes et al., 2001; Simunek et al., 2008). The model is able to simulate water flow in and out of the soil when adequate soil and

vegetation parameters are provided. Both soil and vegetation are however, extremely diverse in montane ecosystems. Soil hydraulic properties vary horizontally and vertically due to non-uniformity in soil types, representation of which requires detailed information on soil parameters to simulate the soil water flow and root water uptake (Mohanty 2013). An advantage of the HYDRUS-1D model is that it can inversely fit the soil hydraulic parameters when the measured soil water content or matric potential is provided (Simunek et al., 2008).

Apart from the variation in soil texture, non-arable soils contain significant quantities of stone fragments (particles with diameter >2 mm) that modify the water storage capacity of soil. Stones furthermore alter the soil hydraulic transport properties, which in turn affect the available water for root uptake (Cousin et al., 2003; Novak and Knava, 2012). Higher stone content is expected to lower the soil water storage of stony soils in comparison to the fine soils (soil particles that are less than 2 mm in diameter; Hlaváčiková et al. 2016; Novak et al., 2011). Stones reduce the water available for root uptake of soil water and hence limit the rate of ET (Novak and Knava, 2012; Parajuli et al., 2017; Tetegan et al. 2011). Many studies in the past have neglected the presence of stone fragments in soil while simulating soil moisture dynamics. Two different approaches are common while dealing with stony soils. One approach assumes the stones as a non-porous system, hence any water held by the stones is not accounted for. This leads to reduced water estimation per unit volume as pointed out by Cousin et al. (2003) and Ugolini et al. (1998). Plant available soil water in such cases may be underestimated by up to 34% as reported in Cousin et al. (2003). By contrast, the second approach essentially considers the stones as behaving similar to the fine soil matrix, which typically has a higher water holding capacity

than stones. In Cousin et al. (2003), plant available water was overestimated by 39%. It may therefore be important to consider the contribution of stone fragments to soil water storage when simulating soil moisture dynamics involving ET estimation, especially when soil stone content is significant.

The objectives of this research involved: (i) Modelling $ET_A$ using the physically based numerical model, HYDRUS-1D, and validating its output against eddy covariance measurements. (ii) Examining the effect of stone content on estimation of $ET_A$ from natural vegetation in stony soils. (iii) Comparing simulated $ET_A$ while neglecting the presence of stone with the simulations considering the soil stone content with highly and negligibly porous stones.

### 3.2. Site description

In this study, we selected four climate stations in northern Utah and one in southern Idaho as shown in Fig. 3.1. The location and general vegetation around the stations are presented in Table 3.1. The stations in Utah are part of the innovative Urban Transitions and Arid region Hydro-sustainability (iUTAH) project. The iUTAH project has developed and installed several weather- and aquatic-stations to monitor and understand Utah's water resources. These are referred to as GAMUT sites as they are intended to quantify processes on a Gradient Along Mountain to Urban Transition (GAMUT). These stations measure different aspects of climate, hydrology, and water quality in three watersheds (Logan River-, Red Butte Creek- and Provo River-Watersheds).

The climate of northern Utah and southern Idaho is typical of the montane semi-arid intermountain west and varies widely with four distinct seasons, cold snowy winter,

hot dry summer and transition periods of spring and autumn. The majority of precipitation occurs as snowfall. The higher elevation weather stations are covered with snow until May or June whereas early snowmelt occurs at the weather stations in lower elevation. Patches of sagebrush surround the observation sites at Tony Grove, Beaver Divide and Soapstone, while the station at the Knowlton Fork is located in a sloping meadow with tall ferns. The meteorological parameters required for calculating $ET_o$ (reference ET), such as air temperatures, saturation deficit, net radiation and wind speed were recorded every fifteen minutes. In addition, the soil moisture and temperature were measured at depths of 5-, 10-, 20-, 50-, and 100- cm using time-domain-transmissometry (TDT) at the same time step as the meteorological parameters (iUTAH 2014). Blonquist et al., (2005) and Jones et al., (2005) have detailed description about the principles of TDT, where the calibration to moisture is based on the method given in Topp et al. (1980).

The Low Sage site in southern Idaho is part of the Critical Zone Observatory (CZO) located in Reynolds Creek Experimental Watershed of southwestern Idaho, approximately 80 km southwest of Boise, Idaho, USA. The site was equipped with sensors to collect meteorological and soil data along with an eddy covariance tower to quantify water and carbon fluxes in a sagebrush ecosystem. Short and long wave radiation, air temperature and humidity were collected at the eddy covariance station every 30 minutes using a four-component net radiometer (CNR-1, Kipp & Zonen, Delft, The Netherlands), and a temperature/humidity probe (HMP155C, Vaisala, Helsinki, Finland). Ground heat flux was measured with six heat flux sensors (HFT3, REBS, Seattle, WA) installed 0.08-m deep within the soil and three sets of self-averaging thermocouples installed at 0.02 and 0.06-m deep (Fellows et al., 2017). The meteorological station near the EC tower includes

measurements of air temperature, humidity, wind speed and direction and solar radiation. Weather and soil data were processed at 30-minute intervals. Precipitation was measured using a dual-gauge system especially designed for windy and snow dominated conditions and aggregated hourly. Volumetric soil water content was recorded every hour at mean depths of 5-, 15-, 30-, 60-, and 90- cm.

During the process of soil moisture sensor installation in each station, the excavated soil was analyzed in order to determine the soil texture, root distribution and stone content (Parajuli et al., 2017a; Patton et al., 2018). The soil description for the selected stations exhibited a high degree of heterogeneity along the depth with significant volumetric stone content ($v$). The vertical distribution of stone content and root density derived from the root information obtained from soil pit description at different sites is presented in Fig. 3.2.

The soil pit descriptions extended to a 100 cm depth in most of the stations. The stone content in the bottommost layer was assumed to be valid and constant down to 200 cm. As shown in Fig. 3.2, Low Sage, Tony Grove, Knowlton Fork and Soapstone exhibited around 0.45 $m^3\ m^{-3}$ volumetric stone content between the depth of 40- to 80-cm. Average stone content within a one-meter soil profile ranged from 0.07 $m^3\ m^{-3}$ at Knowlton Fork to 0.38 $m^3\ m^{-3}$ at Tony Grove. The majority of stones collected from soil pits in iUTAH stations were sandstone varying in terms of their porosities. Sandstones with coarser grains had higher porosities, close to thirty percent and exhibited water retention properties similar to sandy soil. However, fine grained sandstones were negligibly porous with porosities between three to five percent. The water retention properties of the stones were measured by Parajuli et al. (2017) and are presented in Table 3.2.

## 3.3. Theoretical considerations

### *3.3.1. HYDRUS-1D numerical modeling*

A physically based numerical model, HYDRUS-1D (Šimůnek et al., 2008; 2009) was applied to simulate the root water uptake, by coupling with different reference ET equations (eg. Allen et al., 1998; Hargreaves and Samani 1985). HYDRUS-1D solves the Richards equation (Richards, 1931) inversely for the sink term that represents root water uptake and surface evaporation (Simunek et al., 2008; 2013). The Richards equation used to simulate water flow in soil is expressed as:

$$\frac{\partial \theta(h)}{\partial t} = \frac{\partial}{\partial z}\left[ K(h)\left\{\frac{\partial h}{\partial z} + 1\right\}\right] - S \qquad (1)$$

where, $\theta$ is volumetric water content [$m^3\ m^{-3}$], $z$ is the vertical coordinate [m], $t$ is time [s], $h$ is matric potential [m], $K(h)$ is the unsaturated hydraulic conductivity as a function of matric potential [$m\ s^{-1}$], i.e. product of relative hydraulic conductivity $K_r$ (dimensionless) and the saturated hydraulic conductivity $K_s$ [$m\ s^{-1}$] and $S$ is a sink term representing root water uptake or some other source or sink [$m^3\ m^{-3}\ s^{-1}$].

The sink term, $S$, can be computed as the volume of water lost from the soil in unit time due to root water uptake (Feddes et al., 1978) as

$$S(h,z) = \alpha(h,z)\, b(z) \cdot T_p \qquad (2)$$

where $\alpha(h,z)$ is defined as the reduction coefficient for root water uptake (Feddes et al., 1974, 1978) with the depth. Water uptake is zero when it is close to the pressure corresponding to saturation and wilting point. Hence uptake is optimum at $\alpha(h,z)=1$, and $T_p$ is the potential water uptake rate when uptake is optimum. The normalized water uptake distribution function, $b(z)$, describes the spatial variation of $S$ over the root zone. There are

three ways to express $b(z)$: Constant with depth, Linear (Feddes et al., 1978), or the Hoffman and van Genuchten distribution, (1983). A detailed explanation is available in Simunek et al. (2013). The $b(z)$ function was estimated using the Hoffman and van Genuchten (1983) root distribution function in this study.

The reference evapotranspiration ($ET_o$) was calculated in HYDRUS-1D using the FAO simplified Penman-Monteith combination equation using meteorological parameters (Allen et al., 1998; FAO, 1990) as:

$$ET_o = \frac{1}{\lambda}\left[\frac{\Delta\left(R_n - G\right) + \left\{\rho c_p \left(e_a - e_d\right)/r_a\right\}}{\Delta + \gamma\left(1 + r_c/r_a\right)}\right] \tag{3}$$

where $\lambda$ is latent heat of vaporization [MJ kg$^{-1}$], $R_n$ is net radiation at surface [MJ m$^{-2}$ d$^{-1}$], $G$ is soil heat flux [MJ m$^{-2}$ d$^{-1}$], $\rho$ is atmospheric density [kg m$^{-3}$], $c_p$ is specific heat of moist air [i.e., 1.013 kJ kg$^{-1}$ $^{o}$C$^{-1}$], $e_a$ is saturation vapor pressure at temperature T [kPa], $e_d$ is actual vapor pressure [kPa], $r_c$ is crop canopy resistance [s m$^{-1}$], and $r_a$ is aerodynamic resistance [s m$^{-1}$], $\Delta$ is slope of the vapor pressure curve, [kPa $^{o}$C$^{-1}$] and $\gamma$ is psychrometric constant [kPa $^{o}$C$^{-1}$].

As suggested by Ritchie (1972), $ET_o$, was partitioned into potential evaporation $(E_p)$ and potential transpiration ($T_p$) fluxes using Beer's Law assuming a canopy structure as follows:

$$T_p = ET_o \cdot \left(1 - e^{-k \cdot LAI}\right) = ET_o \cdot SCF \tag{4}$$

$$E_p = ET_o \cdot \left(e^{-k \cdot LAI}\right) = ET_o \cdot \left(1 - SCF\right) \tag{5}$$

where, soil cover fraction, *SCF=1-exp(-k LAI)*, *k* is radiation extinction coefficient and is function of sun angle, distribution of plants and arrangement of leaves [-] and *LAI* is leaf area index (Simunek et al., 2008; 2013).

The root water uptake or the actual transpiration ($T_a$) can be then obtained by integrating the sink term in Eq. (2) over the root zone ($L_r$),

$$T_a = \int_{L_r} S(h,z)\, dz = T_p \int_{L_r} \alpha(h,z) b(z)\, dz \tag{6}$$

The variable boundary condition in HYDRUS-1D is governed by the effective precipitation. Some precipitation gets intercepted by the canopy before it infiltrates to the soil. Hence, the maximum infiltration rate at the soil surface was computed as the difference between precipitation ($P$), and interception ($I$) where, $I$, is calculated as (Braden 1985; Schwärzel et al., 2006; van Dam et al., 1997):

$$I = a \cdot LAI \left[ 1 - 1 \Big/ \left( 1 + \frac{SCF \cdot P}{a \cdot LAI} \right) \right] \tag{7}$$

where, $a$ is an empirical coefficient [m]. Parameter $a$ is assumed to be 0.25 (Simunek et al., 2008).

The initial conditions were described by the initial moisture content along the soil profile at time $t$ = 0. The surface boundary condition of the soil domain was set to the atmospheric boundary condition with surface runoff. The actual flux exchange at the soil-atmosphere interface was driven by the atomospheric demand and controlled by the near-surface soil moisture, expressed as (Simunek et al., 2008):

$$\left| -K\left(\frac{\partial h}{\partial z} + 1\right) \right| \leq E \tag{8}$$

$$h_a \le h \le h_s \quad (9)$$

where, $E$ is the maximum rate of infiltration or evaporation under given atmospheric conditions [$LT^{-1}$]; $h_a$ and $h_s$ are minimum and maximum pressure heads, [L] at the soil surface, respectively. The value of $h_a$ can be computed from the relative humidity in the air (Feddes, et al., 1974).

The lower boundary condition was set as a free drainage boundary, assuming an infinitely deep soil profile with no effect of ground water table. For every station, a 200 cm soil profile was used for simulation, which was divided into five layers according to the soil textural classification with one soil moisture sensor in each layer.

The initial hydraulic parameters of each layer were estimated based on the soil texture information obatined from the soil pit analysis. The soil parameters for van Genuchten-Maulem Model (Mualem 1976; van Genuchten 1980) were calibrated for each layers using inverse modelling in HYDRUS-1D. The van Genuchten (1980) model is expressed as;

$$S_e = \frac{\theta - \theta_r}{\theta_s - \theta_r} = \left[1 + \left(\alpha |h|\right)^n\right]^{-m} \quad (10)$$

where, $S_e$ is the effective degree of saturation [-], $\theta_r$ and $\theta_s$ are the residual and saturated volumetric water contents [$m^3\ m^{-3}$], $\alpha$ is the factor related to the inverse of air entry pressure [$m^{-1}$], $n$ and $m$ are empirical fitting parameters that gives measure of pore-size distribution.

The inverse simulations were carried out based on the measured soil moisture values at each measured depth. The optimization process using the HYDRUS-1D simulation was interative until it achieved the highest correlation between simulated and measured soil moisture content (Simunek et al., 2008). The primary objective of inverse

modeling was to optimize the hydraulic parameters for the van Genuchten model for each layer of soil to fit the observed and simulated volumetric water contents for the soil. The HYDRUS-1D model takes consideration of the root density along the soil profile while simulating root water uptake. However the rock fragments in the soil may alter the soil water retention properties and thus affect water availability for $ET_A$, as described subsequently.

*3.3.2. Accounting for stone content in the HYDRUS-1D simulation*

In order to address the impact of stone content on soil hydraulic properties and thus estimation of $ET_A$, the stony soil was assumed to be a binary porous medium allowing two different water retention properties for stone and fine soil in each layer. The dual porosity model (Durner 1994) within the HYDRUS-1D software was applied to satisfy the algorithm suggested by Parajuli et al., (2017) to account for the effect of stone fragments in the soil.

$$\frac{\theta_{mix}-\theta_{r_{mix}}}{\theta_{s_{mix}}-\theta_{r_{mix}}} = w_{soil}\left[1+\left(\alpha_{soil}h\right)^{n_{soil}}\right]^{-m_{soil}} + w_{stone}\left[1+\left(\alpha_{stone}h\right)^{n_{stone}}\right]^{-m_{stone}} \quad (11)$$

where the parameters with subscript *soil*, *stone* and *mix* are van Genuchten parameters for background soil, stone inclusion and soil-stone mixture respectively. The weighting factors for soil and stone fractions, $w_{soil}$ and $w_{stone}$, at saturation are defined as:

$$w_{soil} = \frac{\left(1-v\right)\theta_{s,soil}}{\left(1-v\right)\theta_{s,soil}+v\theta_{s,stone}} \quad (12)$$

$$w_{stone} = \frac{v\theta_{s,stone}}{\left(1-v\right)\theta_{s,soil}+v\theta_{s,stone}} \quad (13)$$

where, *v* is the ratio of the stone fragment volume to the total soil volume (or volume fraction of the stone content).

In order to understand the impact of variably porous stones in simulation of $ET_A$, two scenarios were studied where all the stones were considered as either coarse sandstones (highly porous) or fine sandstones (negligibly porous) with water retention properties expressed in Table 3.2.

The unsaturated hydraulic conductivity as function of effective saturation of the stony soil is defined by combining Eq. (11) with Mualem's (1976) pore-size distribution model as:

$$K(S_e) = K_s \frac{(w_1 S_{e_1} + w_2 S_{e_2})^l (w_1 \alpha_1 [1-(1-S_{e_1}^{1/m_1})^{m_1}] + w_2 \alpha_2 [1-(1-S_{e_2}^{1/m_2})^{m_2}])^2}{(w_1 \alpha_1 + w_2 \alpha_2)^2} \quad (14)$$

where subscripts *1* and *2* represent parameters for soil and stones respectively, *l* is empirical parameter of the hydraulic function.

## 3.4. Results

### *3.4.1. Calibration of the HYDRUS-1D model*

The simulation period started following snowmelt, when the soil moisture was near field capacity. The Low Sage station in Idaho had early snowmelt allowing us to initialize the model on DOY 100 (10 April 2015), while iUTAH stations in Northern Utah were snow covered until about the middle to the latter part of May. In order to compare the same time period, simulations started on DOY 148 (28 May 2015) at all iUTAH stations running until the September (DOY 274). The same period was selected for both years to have better comparison of ET estimates under different conditions. Daily precipitation plotted in Fig. 3.3 shows that 2016 experienced much less rainfall than 2015. The four iUTAH stations

illustrated in Fig. (3.1) have recorded similar rainfall patterns over the period. There were several rain events during the simulation period in 2015, but 2016 remained relatively dry with one major precipitation event towards the end of September (DOY 268).

The HYDRUS-1D numerical model was initialized using the soil hydraulic parameters obtained from field measurements. The initial soil hydraulic parameters were estimated using Rosetta Lite v1.1 software in HYDRUS-1D, based on the sand, silt and clay fraction of soil obtained from soil pit descriptions (Parajuli et al., 2017a; Patton et al., 2018). Model calibration was achieved primarily by inversely fitting the soil hydraulic parameters and trial-and-error adjustment of the vegetation parameters such as the water stress reduction function to minimize the root mean squared error (RMSE) and improve graphical fit between simulated and measured volumetric water content for each soil layer.

Volumetric water content measured using time-domain-transmissometry (TDT) and HYDRUS-1D simulations of water content at soil profile depths of 5-, 15-, 30-, 60-, and 90-cm from the Low Sage station are presented in Fig. 3.4. Variation in rainfall is expected to alter the soil moisture dynamics in both years. The volumetric water content approached the saturation level during spring snowmelt, but these montane soils drain quickly to field capacity once snowmelt ceases. Rain events during the summer of 2015 are able to recharge the soil profile to a depth of 30 cm as shown in Fig. 3.4. There was no significant rain event during the simulation period in 2016, and the soil dried down towards the end of the growing season.

Simulation results for the four iUTAH sites using HYDRUS-1D are compared withTDT measured soil moisture content at 5-, 10-, 20-, 50-, and 100-cm in Fig. 3.5. Soil moisture dropped rapidly from a near-saturated condition at the beginning of the growing season/simulation period. As in Fig. 3.4, the sensors at depths 5-, 10- and 20-cm reflected the effect of rainfall with rapid rise in moisture content readings during 2015; however, the amount of precipitation was not enough to wet the sensors below 20 cm throughout the growing season.

The goodness of fit to the measured soil moisture values with the HYDRUS-1D simulation are expressed in terms of coefficients of determination ($R^2$) and root mean squared errors (RMSE) shown in Table 3.3. The calibrated HYDRUS-1D simulation results compared well with measured soil moisture at each depth for both years. The coefficients of determination ($R^2$) were greater than 0.8 for most depths, while a few of the simulation depths had $R^2$ as low as 0.65 (Table 3.3). The RMSE remained less than 0.04 $m^3\ m^{-3}$ on average for all the stations. The few $R^2$ values below 0.8 and RMSE values greater than 0.03 $m^3\ m^{-3}$ for individual depths are bolded for clarity in Table 3.3. The match between simulated and observed water contents at different depths in all stations suggests the HYDRUS-1D model hydraulic parameters were well calibrated to represent the soil hydrodynamics.

*3.4.2. Simulation of actual evapotranspiration*

Root water uptake and evaporative fluxes from soil and plants were simulated by HYDRUS-1D to provide an estimate of the $ET_A$. Daily $ET_A$ estimates simulated by HYDRUS-1D were compared with eddy covariance measurements of $ET_A$ at the Low Sage

station as illustrated in Fig. 3.6. The daily $ET_A$ simulated by the HYDRUS-1D model followed the seasonal patterns of eddy covariance measured $ET_A$ very well (Fig. 3.6). The correlation was reasonable with $R^2$ values of 0.78 and 0.76 for year 2015 and 2016, respectively (Fig. 3.7, Table 3.4). The RMSE values for 2015 and 2016 were 0.64 mm/day and 0.51 mm/day, respectively (Table 3.4). The HYDRUS-1D model periodically overestimated $ET_A$ compared to the eddy covariance measurements mostly around rain events. The cumulative $ET_A$ measured by eddy covariance for the period DOY 101 (10 April) to DOY 273 (30 September) was 305 mm and 221 mm in 2015 and 2016, whereas the HYDRUS-1D simulation estimated 332 mm and 198 mm in 2015 and 2016, respectively. This overestimation of $ET_A$ simulated by HYDRUS-1D in 2015 and the underestimation in 2016 is also evident from the scatter plot in Fig. 3.7. However, the seasonal total $ET_A$ values from HYDRUS-1D were in good agreement with the eddy covariance results.

*3.4.3. Effect of stone content on evapotranspiration*

With the aim of analyzing the impact of stone content on $ET_A$, we simulated three different scenarios assuming soil for all five sites with: no stones; highly porous stones (Coarse Sandstone); and negligibly porous stones (Fine Sandstone). The average stone content for each layer was estimated based on the soil pit description also presented in Fig. 3.2. The water retention parameters for the highly and negligibly porous stone considered for this study were measured in the laboratory (Parajuli et al., 2017) and are presented in Table 3.2.

The simulation in the Low Sage site where the average stone content was 0.18 $m^3$ $m^{-3}$ showed substantial improvement in estimation of $ET_A$, when the stones were considered as negligibly porous stones. The $R^2$ values increased slightly while RMSE values were lower under the negligibly porous stone scenario for both years (Table 3.4). The result supported our assumption, namely, that if we could quantify the stone content in the soil properly and include that in the soil moisture simulation, the $ET_A$ from stony soil would be estimated more accurately.

Fig. 3.8 shows the cumulative $ET_A$ simulated by HYDRUS-1D under the three different scenarios considering soil with no stone, highly porous stone and negligibly porous stone at each station. With the purpose of comparing $ET_A$ over the same period for each site, the cumulative ET is presented from DOY 148 (28 May) to DOY 273 (30 September) for all stations. In general, the cumulative $ET_A$ over the same period in 2016 is much less than that from 2015 for all stations providing us with the impression that the available soil moisture limited the $ET_A$. The year 2016 was considerably drier than 2015, resulting in reduced soil water storage, which is also implicit in Fig. 3.4 and 3.5.

The simulations under different conditions revealed significant reductions in cumulative $ET_A$ at the Tony Grove and Soapstone stations. The percent changes in simulated actual transpiration ($T_A$), evaporation ($E_A$) and $ET_A$ for conditions with highly porous stones and negligibly porous stones with reference to soil without stones, is presented in Table 3.5. The cumulative $ET_A$ was reduced by 10% and 21% at Tony Grove and 1% and 17% at Soapstone for assumptions of highly- and negligibly-porous stones, respectively (Table 3.5). However, there was not any noticeable change in cumulative $ET_A$ at the Knowlton Fork station where the average stone content was 0.07 $m^3$ $m^{-3}$. The Low Sage station that

has average stone contents of 0.16 $m^3 m^{-3}$, exhibited a slight reduction in cumulative $ET_A$, about 4% and 10% when considering stony soil with negligibly porous and highly porous stones. Similarly, the Beaver Divide station with average stone content of 0.18 $m^3 m^{-3}$, showed reduction in $ET_A$ by nearly 3% while assuming highly porous stone, the $ET_A$ reduced by 7% under consideration of negligibly porous stones for both years. In contrast, the $ET_A$ simulations for Beaver Divide in 2016 showed incremental changes when considering either stone type.

## 3.5. Discussion

### *3.5.1. Soil moisture dynamics and model calibration*

HYDRUS-1D model was able to simulate the soil moisture remarkably well in all five stations with significant correlation of $R^2$ greater than 0.8 and RMSE less than 0.04 $m^3 m^{-3}$, averaged for over the depth at five stations for both years (Table 3.3). Some discrepancies were observed such as at depth 20 cm in Beaver Divide and Soapstone that showed relatively lower $R^2$ of 0.651 and higher RMSE of 0.05 $m^3 m^{-3}$ and 0.04 $m^3 m^{-3}$ respectively. The source of discrepancies between measured and simulated soil moisture is likely due to the inability of HYDRUS-1D model to account for the complexity caused by soil heterogeneity, which is quite common in forest soil (Flinn and Marks, 2007; Hawley et al., 1983). Though the soil texturevaried extremely along the depth with significant amount of stones, the soil profile at each station within the simulation domain (2m deep) were clustered into five distinct layers based on textural information obtained from the soil pit description. This simplification of soil representation has likely increased errors in previous simulations of soil moisture to some extent.

*3.5.2. Simulation of actual evapotranspiration*

The HYDRUS-1D simulation for 2015 and 2016 suggested that the $ET_A$ was strongly correlated to the soil moisture availability during the growing season as 2016 showed lower cumulative $ET_A$ corresponding to the drier soil profile (Fig. 3.4; 3.5; 3.8). The $ET_A$ measured by the eddy covariance system at the Low Sage station and simulated by HYDRUS-1D followed the same trend (Fig. 3.6). However, the HYDRUS-1D model overestimated the peak values noticeably, usually after the rain events in 2015. Despite the difference between spatial scales of the eddy covariance footprint and the point scale simulation of HYDRUS-1D, the results validate the potential of quantifying $ET_A$ using soil moisture dynamics in natural settings.

Slight differences between modeled daily $ET_A$ and values measured by eddy covariance were expected. The eddy covariance method does not always provide energy balance closure consistently, which may lead to underestimation of latent heat flux or $ET_A$ (Wilson et al., 2002). When comparing the sum of latent heat flux and sensible heat with available energy (Rn - G), Wilson et al. (2002) reported an average error of 20% from 22 FLUXNET (a network of eddy covariance sites) sites. Although the energy budget ratio at the Low Sage site over the two years during snow-free, non-freezing periods was 0.96, weekly values over the simulation period in Fig. 3.6 were as low as 0.80. Moreover, error in HYDRUS-1D simulation may result from inaccuracy of model parameterization of soil hydraulics. Soils in natural settings are highly heterogeneous within the profile with extremely variable hydraulic properties. Limitation of the HYDRUS-1D model to represent soil complexity might have resulted into incorrect estimations of water balance leading to erroneous $ET_A$ estimates in some cases.

*3.5.3. Accounting for stone content*

The magnitude of the effects of stone content on the $ET_A$ simulation was dependent upon the type of stones and their hydraulic properties. As presented in Durner (1994), prediction of both the water retention and hydraulic conductivity function near saturation may be highly unreliable and subject to large estimation error with even in the best quality measurements. Acknowledging this, we assumed the saturated hydraulic conductivity of the stony soil was similar to that of the fine soil matrix while the unsaturated hydraulic conductivity for stony soil was defined by Eq. (14) as a function of effective saturation. Several studies suggest reduction in hydraulic conductivity due to increase in stone content, while conversely, the hydraulic conductivity has also been shown to increase in stony soil near saturation (Beckers et al., 2016; Sauer and Logsdon, 2002). Our assumption of soil with lower porosity stone have a tendency to simulate $ET_A$ that matched well with the eddy covariance observations (Fig. 3.6). Consideration of stony soil with negligibly porous stone reduced the simulation of total cumulative $ET_A$ considerably in all stations for both years except for Knowlton Fork, which exhibited the lowest average stone content (Fig. 3.2). However, the higher porosity stone, with water retention behavior similar to coarse sandstone had the least effect on $ET_A$ simulation. The cumulative $ET_A$ over the simulation period was reduced by up to 30% for the Soapstone site in 2016 when accounting for the stones as negligibly porous stones (Table 3.5). This correlates well with results in Cousin et al. (2003) that showed overestimation of available water content by 39% while the presence of stones in the soil were not accounted for.

## 3.6. Conclusion

In this study, we demonstrated the influence of soil stone content on the uptake of water as evapotranspiration (ET) using stony-soil moisture dynamics. The soil moisture and $ET_A$ simulated by HYDRUS-1D were found to be in good agreement with directly measured soil moisture and $ET_A$ using the eddy covariance system indicating that the model is efficient in simulating the boundary fluxes including $ET_A$. The simulated root water uptake from stony soil was found to be sensitive to stone content, showing significant reduction in cumulative simulated $ET_A$ over the simulation period up to 30% percent of the total $ET_A$ computed without accounting for the stone content. The simulated $ET_A$ values were least affected when considering soil with highly porous stones, while estimates were reduced significantly for the stations with higher average stone content, when considering soil with negligibly porous stones. It was revealed that lower- and higher-porosity stones might reduce $ET_A$ by 30% and 10%, respectively, suggesting the overestimation of $ET_A$ while the stone content is neglected in the simulation. It is hence important to incorporate the hydraulic properties of stones to estimate $ET_A$ using soil moisture dynamics in stony soil. This study thus provides backing for potential application of numerical simulation of soil moisture dynamics to estimate $ET_A$ from montane forest ecosystems with stony soils.

**References**

Allen, R. G., Pereira, L. S., Raes, D., & Smith, M. (1998). Crop evapotranspiration-Guidelines for computing crop water requirements-FAO Irrigation and drainage paper 56. *FAO, Rome*, *300*(9), D05109.

Andréassian, V. (2004). Waters and forests: from historical controversy to scientific debate. *Journal of hydrology*, *291*(1-2), 1-27.

Baldocchi, D. D., & Ryu, Y. (2011). A Synthesis of Forest Evaporation Fluxes –from Days to Years – as Measured with Eddy Covarience. In *Forest Hydrology and Biogeochemistry: Synthesis of Past Research and Future Directions* (Vol. 216, pp. 101-116). Springer.

Baldocchi, D. D., Hincks, B. B., & Meyers, T. P. (1988). Measuring Biosphere-Atmosphere Exchanges of Biologically Related Gases with micrometeeorological methods. *Ecology*, 69(5), 1331-1340.

Beckers, E., Pichault, M., Pansak, W., Degré, A., & Garré, S. (2016). Characterization of stony soils' hydraulic conductivity using laboratory and numerical experiments. *Soil*, *2*(3), 421-431.

Blonquist, J.M.J., Jones, S.B., Robinson, D.A., (2005). Standardizing characterization of electromagnetic water content sensors. Vadose Zone J. 4(4): 1059-1069.

Cai, X., Pan, M., Chaney, N. W., Colliander, A., Misra, S., Cosh, M. H., ... & Wood, E. F. (2017). Validation of SMAP soil moisture for the SMAPVEX15 field campaign using a hyper-resolution model. *Water Resources Research*, *53*(4), 3013-3028.

Cousin, I., Nicoullaud, B., & Coutadeur, C. (2003). Influence of rock fragments on the water retention and water percolation in a calcerous soil. *Catena* (53), 97-114.

Durner, W. (1994). Hydraulic conductivity estimation for soils with heterogeneous pore structure. *Water resources research*, *30*(2), 211-223.

Feddes, R. A., Bresler, E., & Neuman, S. P. (1974). Field test of a modified numerical model for water uptake by root systems. *Water Resources Research*, *10*(6), 1199-1206.

Feddes, R. A., Kowalik, P. J., & Zaradny, H. (1978). *Simulation of field water use and crop yield*. Centre for Agricultural Publishing and Documentation.

Feddes, R. A., Hoff, H., Bruen, M., Dawson, T., de Rosnay, P., Dirmeyer, P., & Pitman, A. J. (2001). Modeling root water uptake in hydrological and climate models. *Bulletin of the American meteorological society*, *82*(12), 2797-2809.

Fellows, Aaron W.; Flerchinger, Gerald N.; Seyfried, Mark S.; and Lohse, Kathleen. (2017). *Data for Partitioned Carbon and Energy Fluxes Within the Reynolds Creek Critical Zone Observatory* [Data set]. Retrieved from https://doi.org/10.18122/B2TD7V

Food and Agriculture Organization (FAO) of the United Nations (1990). Expert consultation on revision of FAO methodologies for crop water requirements, ANNEX V, FAO Penman-Monteith Formula, Rome, Italy.

Flinn, K.M., Marks, P.L., 2007. Agricultural legacies in forest environments: tree communities, soil properties, and light availability. Ecol. Appl. 17(2): 452-463.

Hargreaves, G. H., & Samani, Z. A. (1985). Reference crop evapotranspiration from temperature. *Appl. Eng. Agric*, *1*(2), 96-99.

Hawley, M.E., Jackson, T.J., McCuen, R.H., 1983. Surface soil moisture variation on small agricultural watersheds. J. Hydrol. 62(1–4): 179-200.

Hilten, R. N., Lawrence, T. M., & Tollner, E. W. (2008). Modeling stormwater runoff from green roofs with HYDRUS-1D. *Journal of Hydrology*, *358*(3-4), 288-293.

Hlaváčiková, H., & Novák, V. (2013). Comparison of daily potential evapotranspiration calculated by two procedures based on Penman-Monteith type equation. *Journal of Hydrology and Hydromechanics*, *61*(2), 173-176.

Hlaváčiková, H., Novák, V., & Šimůnek, J. (2016). The effects of rock fragment shapes and positions on modeled hydraulic conductivities of stony soils. *Geoderma*, *281*, 39-48.

Hoffman, G. J., & Van Genuchten, M. T. (1983). Soil properties and efficient water use: water management for salinity control. *Limitations to efficient water use in crop production*, (*limitations to ef*.), 73-85.

Ice, G. G., & Stednick, J. D. (2004). century of forest and wildland watershed lessons. Society of American Foresters.

iUTAH GAMUT Working Group . (2014). iUTAH GAMUT Network Raw Data. Retrieved from iUTAH Modeling & Data Federation: http://repository.iutahepscor.org/dataset/

Jones, S.B., Blonquist, J.M., Robinson, D.A., Rasmussen, V.P., Or, D., (2005). Standardizing characterization of electromagnetic water content sensors. Vadose Zone J. 4(4): 1048-1058.

Kool, D., Agam, N., Lazarovitch, N., Heitman, J. L., Sauer, T. J., & Ben-Gal, A. (2014). A review of approaches for evapotranspiration partitioning. *Agricultural and Forest Meteorology*, *184*, 56-70.

Koster, R. D., Dirmeyer, P. A., Guo, Z., Bonan, G., Chan, E., Cox, P., ... & Liu, P. (2004). Regions of strong coupling between soil moisture and precipitation. *Science*, *305*(5687), 1138-1140.

Kumar, S. V., Peters-Lidard, C. D., Tian, Y., Houser, P. R., Geiger, J., Olden, S., ... & Adams, J. (2006). Land information system: An interoperable framework for high resolution land surface modeling. *Environmental modelling & software*, *21*(10), 1402-1415.

Law, B. E., Falge, E., Gu, L. V., Baldocchi, D. D., Bakwin, P., Berbigier, P., ... & Goldstein, A. (2002). Environmental controls over carbon dioxide and water vapor exchange of terrestrial vegetation. *Agricultural and Forest Meteorology*, *113*(1), 97-120.

Lv, L., Franz, T. E., Robinson, D. A., & Jones, S. B. (2014). Measured and Modeled Soil Moisture Compared with Cosmic-Ray Neutron Probe Estimates in a Mixed Forest. *Vadose Zone Journal*, *13*(12), vzj2014-06.

Miyazawa, Y., Kobayashi, N., Mudd, R. G., Tateishi, M., Lim, T., Mizoue, N., ... & Kumagai, T. (2013). Leaf and soil-plant hydraulic processes in the transpiration of tropical forest. *Procedia Environmental Sciences*, *19*, 77-85.

Mohanty, B. P. (2013). Soil hydraulic property estimation using remote sensing: A review. *Vadose Zone Journal*, *12*(4).

Mu, Q., Heinsch, F. A., Zhao, M., & Running, S. W. (2007). Development of a global evapotranspiration algorithm based on MODIS and global meteorology data. *Remote Sensing of Environment*, 111(4), 519-536.

Mualem, Y. (1976). A new model for predicting the hydraulic conductivity of unsaturated porous media. *Water Resour. Res.,* 12, 513–522.

Niu, G. Y., Yang, Z. L., Mitchell, K. E., Chen, F., Ek, M. B., Barlage, M., ... & Tewari, M. (2011). The community Noah land surface model with multiparameterization options (Noah-MP): 1. Model description and evaluation with local-scale measurements. *Journal of Geophysical Research: Atmospheres*, *116*(D12).

Novak, V., & Knava, K. (2012). The influence of stoniness and canopy properties on soil water content distribution: simulation of water movement in forest stony soil. *Eur. J. Forest Res.*, 131(6), 1727–1735.

Novák, V., Kňava, K., & Šimůnek, J. (2011). Determining the influence of stones on hydraulic conductivity of saturated soils using numerical method. *Geoderma* (161), 177-181.

Parajuli, K. (2015). Spatial Analysis of Actual Evapotranspiration Estimates from the iUTAH Climate Station Network. In Karvazy, K., & Webster, V. L. (Eds.), *World Environmental and Water Resources Congress 2015: Floods, Droughts, and Ecosystems,* Paper presented at World Environmental and Water Resources Congress, Austin, TX, (pp. 2252-2260). ASCE-EWRI.

Parajuli, K., Jones, S. B., & Hipps, L. (2015a). Numerical Modeling of Evapotranspiration from Montane Vegetation with Verification from Actual Surface Energy Balance Measurements. In *SSSA Annual Meeting 2015, Minneapolis, MN*.

Parajuli, K., Sadeghi, M., & Jones, S. B. (2017). A binary mixing model for characterizing stony-soil water retention. *Agricultural and Forest Meteorology*, *244*, 1-8.

Parajuli, K., S. B. Jones, J. Lawley (2017a). Soil Description for GAMUT Weather Stations, HydroShare, http://www.hydroshare.org/resource/4dc603691c964c0-7a766f00638024776

Patton, Nicholas R.; Lohse, Kathleen A.; Seyfried, M.S.; Will, Ryan M.; and Benner, Shawn. (2018). *Dataset for Coarse Fraction Adjusted Bulk Density Estimates for Dryland Soils Derived from Felsic and Mafic Parent Materials* [Data set]. Retrieved from https://doi.org/10.18122/B22M6Q

Prueger, J. H., Hatfield, J. L., Aase, J. K., & Pikul, J. L. (1997). Bowen-ratio comparisons with lysimeter evapotranspiration. *Agronomy Journal*, *89*(5), 730-736.

Raziei, T., & Pereira, L. S. (2013). Estimation of ETo with Hargreaves–Samani and FAO-PM temperature methods for a wide range of climates in Iran. *Agricultural Water Management, 121*, 1-18.

Richards, L. A. (1931). Capillary conduction of liquids through porous mediums. *J. Applied Physics*, 1(5), 318-333.

Ries, F., Lange, J., Schmidt, S., Puhlmann, H., & Sauter, M. (2015). Recharge estimation and soil moisture dynamics in a Mediterranean, semi-arid karst region. *Hydrology and Earth System Sciences*, *19*(3), 1439-1456.

Ritchie, J. T. (1972). Model for predicting evaporation from a row crop with incomplete cover. *Water resources research*, *8*(5), 1204-1213.

Sauer, T. J., & Logsdon, S. D. (2002). Hydraulic and physical properties of stony soils in a small watershed. *Soil Science Society of America Journal*, *66*(6), 1947-1956.

Schelde, Kirsten, Ringgaard, Rasmus, Herbst, Mathias, Thomsen, Anton, Friborg, Thomas, Søgaard, Henrik (2011). Comparing evapotranspiration rates estimated from atmospheric flux and TDR soil moisture measurements. *Vadose Zone Journal* 10:78-83

Schwärzel, K., Šimůnek, J., van Genuchten, M. T., & Wessolek, G. (2006). Measurement modeling of soil-water dynamics evapotranspiration of drained peatland soils. Journal of Plant Nutrition and Soil Science, 169(6), 762-774.

Senay, G. B., Leake, S., Nagler, P. L., Artan, G., Dickinson, J., & Glenn, J. T. (2011). Estimating basin scale evapotranspiration (ET) by water balance and remote sensing methods. *Hydrological Processes, 25*, 4037-4049.

Sheffield, J., Wood, E. F., & Arriola, F. M. (2010). Long-Term Regional Estimates of Evapotranspiration for Mexico Based on Downscaled ISCCP Data. *Journal of Hydrometeorology, 11*, 253-275.

Simunek, J., & Genuchten, M. T. (2008). Modeling Nonequilibrium Flow and Transport Processes Using HYDRUS. *Vadose Zone Journal, 7*(2), 782-792.

Šimunek, J., Sejna, M., Saito, H., Sakai, M., van Genuchten, M. T. (2009). *The HYDRUS-1D Software Package for Simulating the Movement of Water. Heat, and Multiple Solutes in Variably Saturated Media,* Version, 4.08.

Šimůnek, J., M. Šejna, H. Saito, M. Sakai, and M. Th. van Genuchten. (2013). The HYDRUS-1D Software Package for Simulating the Movement of Water, Heat, and Multiple Solutes in Variably Saturated Media, Version 4.17, *HYDRUS Software Series 3*, Department of Environmental Sciences, University of California Riverside, Riverside, California, USA, pp. 343.

Soylu, M. E., Istanbulluoglu, E., Lenters, J. D., & Wang, T. (2011). Quantifying the impact of groundwater depth on evapotranspiration in a semi-arid grassland region. *Hydrology and Earth System Sciences*, *15*(3), 787-806.

Sun, G., Noormets, A., Chen, J., & McNulty, S. G. (2008). Evapotranspiration estimates from eddy covariance towers and hydrologic modeling in managed forests in Northern Wisconsin, USA. *Agricultural and forest Meteorology*, *148*(2), 257-267.

Sutanto, S. J., Wenninger, J., Coenders-Gerrits, A. M. J., & Uhlenbrook, S. (2012). Partitioning of evaporation into transpiration, soil evaporation and interception: a comparison between isotope measurements and a HYDRUS-1D model. *Hydrology and Earth System Sciences*, *16*(8), 2605-2616.

Tetegan, M., Nicoullaud, B., Baize, D., Bouthier, A., & Cousin, I. (2011). The contribution of rock fragments to the available water content of stony soils: Proposition of new pedotransfer functions. *Geoderma* (165), 40-49.

Topp, G.C., Davis, J.L., Annan, A.P., 1980. Electromagnetic determination of soil water content: Measurements in coaxial transmission lines. Water Resour. Res. 16(3): 574-582.

Ugolini F.C., Corti G., Agnelli A., Certini G. (1998) Under- and overestimation of soil properties in stony soils. *16th World Congress of Soil Science*, Montpellier

van Dam, J. C., J. Huygen, J. G. Wesseling, R. A. Feddes, P. Kabat, P. E. V. van Walsum, P. Groenendijk, and C. A. van Diepen, Theory of SWAP version 2.0, Report 71, Dept. of Water Resour., Wageningen Agricultural University, Wageningen, the Netherlands, 1997.

Van Genuchten, M. T. (1980). A closed-form equation for predicting the hydraulic conductivity of unsaturated soils. *Soil science society of America journal*, *44*(5), 892-898.

Wilcox, B. P., Breshears, D. D., & Allen, C. D. (2003). Ecohydrology of a resource-conserving semiarid woodland: Effects of scale and disturbance. *Ecological Monographs*, *73*(2), 223-239.

Wilson, K. B., Hanson, P. J., Mulholland, P. J., Baldocchi, D. D., & Wullschleger, S. D. (2001). A comparison of methods for determining forest evapotranspiration and its components: sap-flow, soil water budget, eddy covariance and catchment water balance. *Agricultural and forest Meteorology*, *106*(2), 153-168.

Wilson, K., Goldstein, A., Falge, E., Aubinet, M., Baldocchi, D., Berbigier, P., ... & Grelle, A. (2002). Energy balance closure at FLUXNET sites. *Agricultural and Forest Meteorology*, *113*(1), 223-243.

Yang, Z. L., Niu, G. Y., Mitchell, K. E., Chen, F., Ek, M. B., Barlage, M., ... & Xia, Y. (2011). The community Noah land surface model with multiparameterization options (Noah-MP): 2. Evaluation over global river basins. *Journal of Geophysical Research: Atmospheres*, *116*(D12).

Zhou, Guoyi, Ge Sun, Xu Wang, Chuanyan Zhou, Steven G. McNulty, James M. Vose, and Devendra M. Amatya, 2008. Estimating Forest Ecosystem Evapotranspiration at Multiple Temporal Scales With a Dimension Analysis Approach. Journal of the American Water Resources Association (JAWRA) 44(1):208-221. DOI: 10.1111/j.1752-1688.2007.00148.x

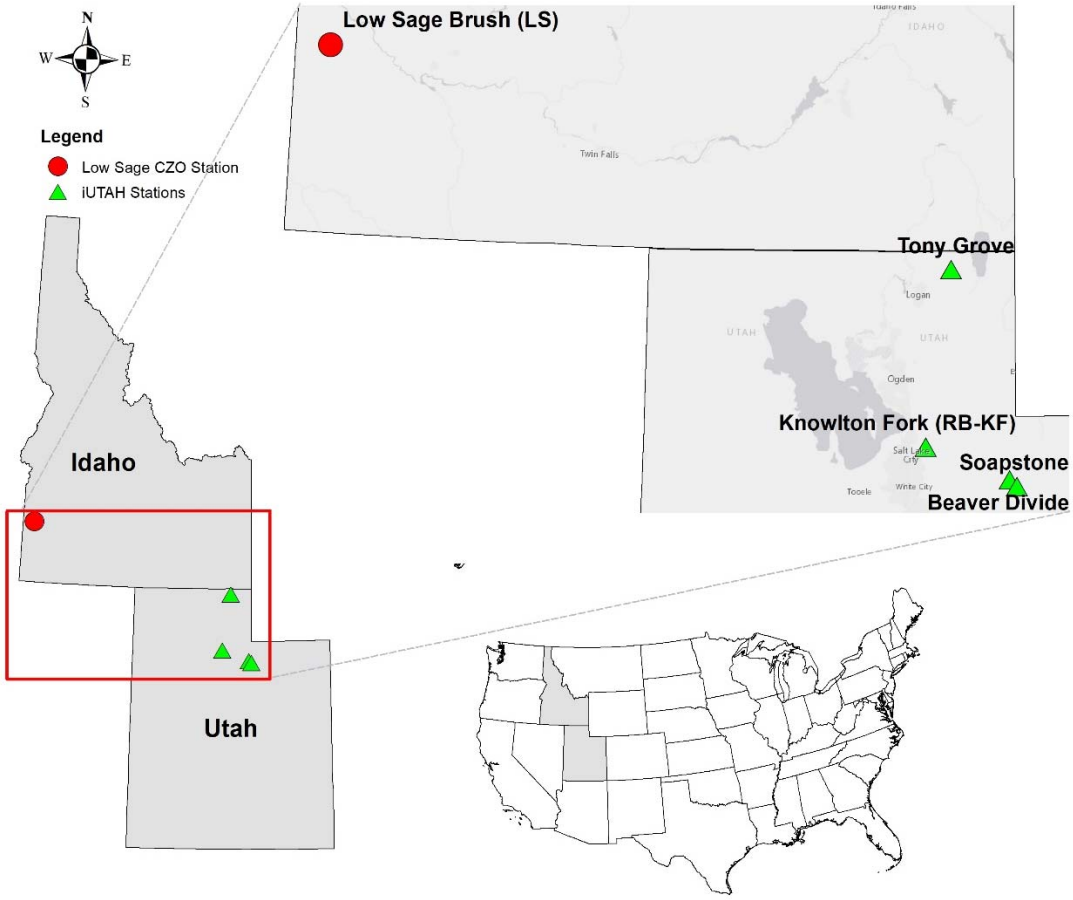


**Fig. 3.1.** Selected climate stations in Northern Utah and Reynolds Creek, Idaho installed by iUTAH and the Critical Zone Observatory (CZO) respectively. All stations have measurements of meteorological parameters including volumetric soil water content. The Low Sage station is furthermore equipped with an eddy covariance tower.

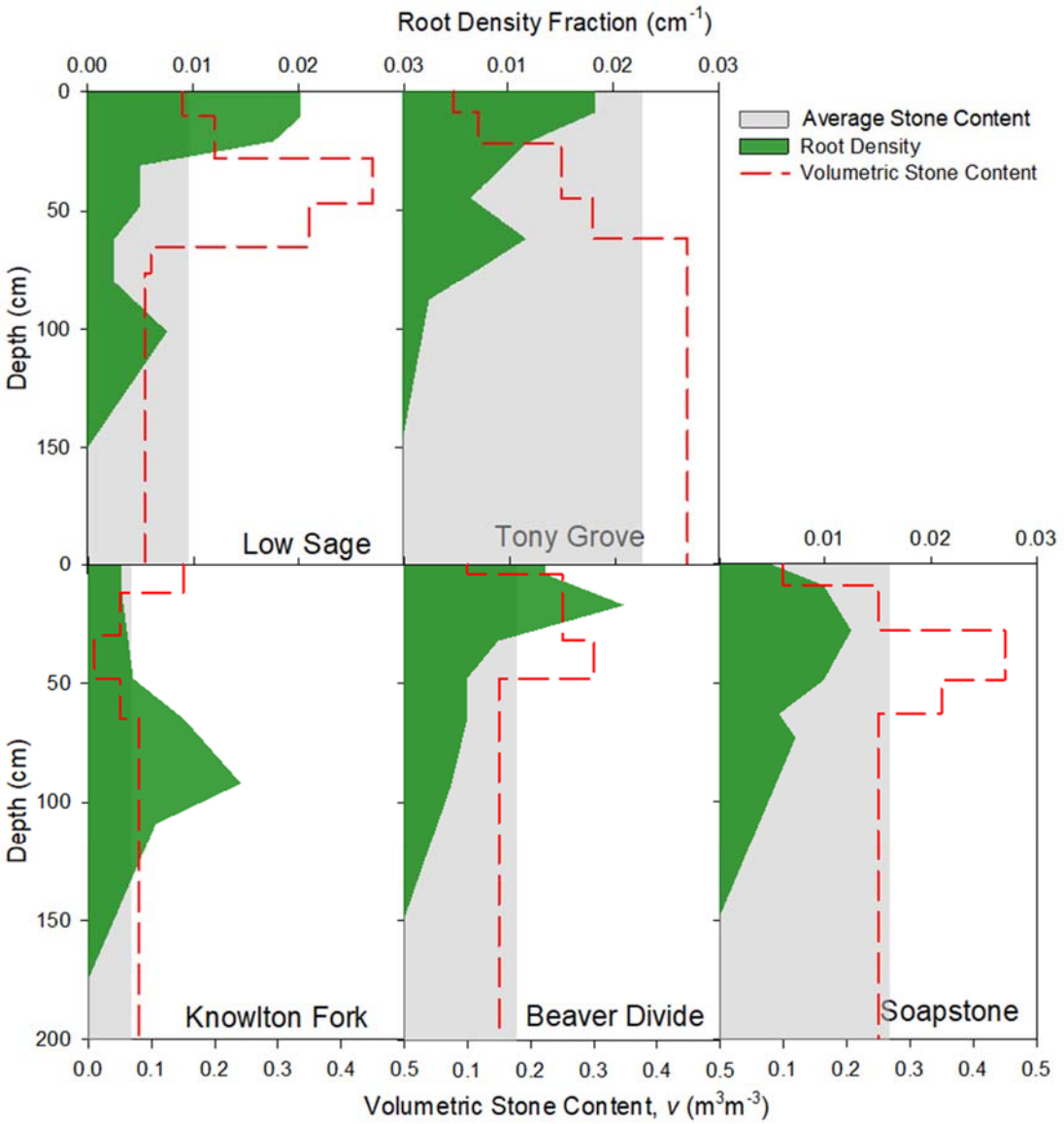


**Fig. 3.2**. Root density distribution and volumetric stone content along the soil profile at (a) Low Sage, (b) Tony Grove, (c) Knowlton Fork, (d) Beaver Divide and (e) Soapstone weather stations. The root density fraction and stone content were obtained from the soil pit description during the installation of climate stations. Information on stone content was available to the depth of around 100 cm. Below that depth the stone content is considered similar to the stone content in the bottom most layer from the soil pit description. The average stone content is taken from stone distribution in the entire 200 cm soil profile.

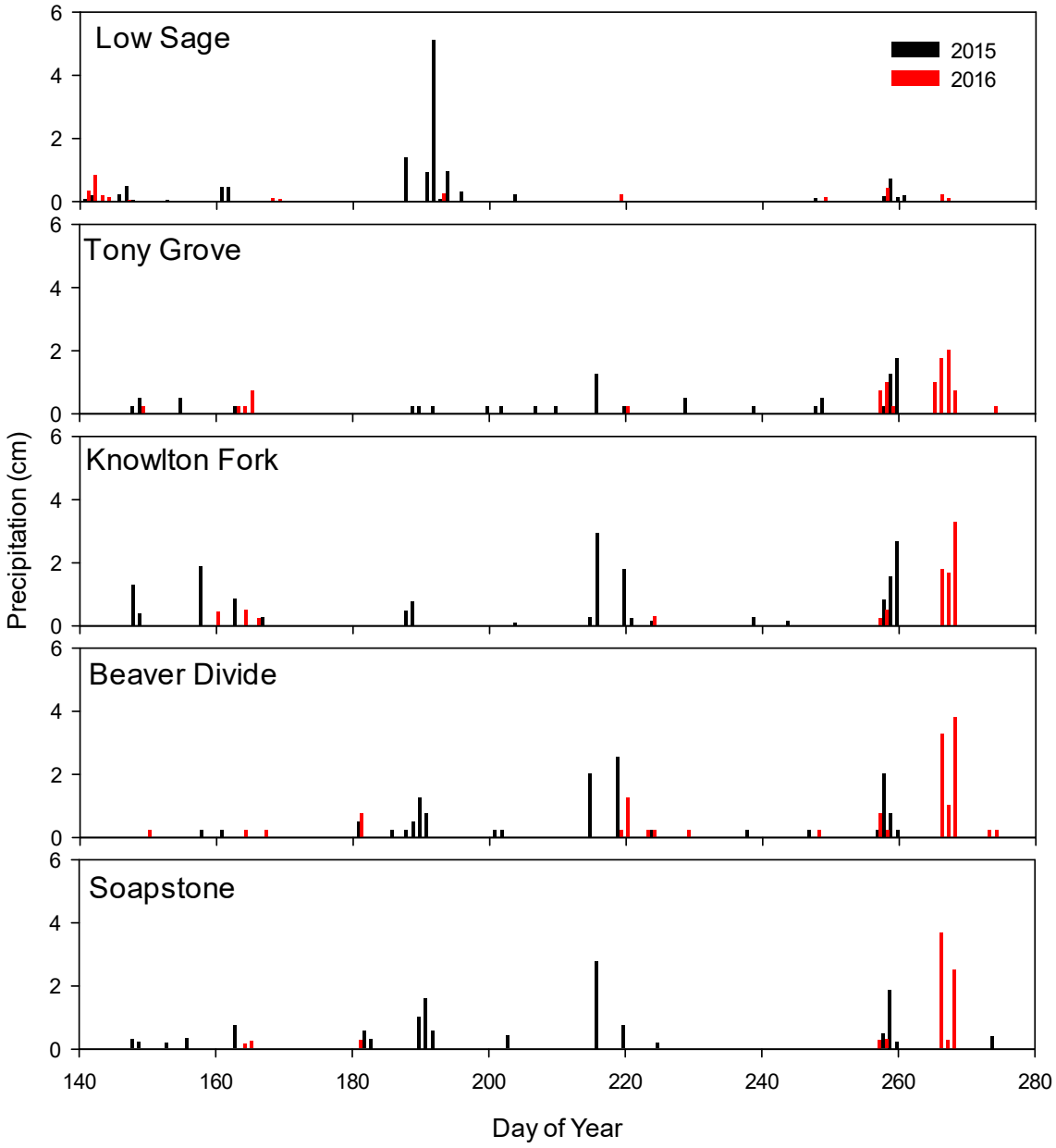


**Fig. 3.3.** Daily precipitation during the HYDRUS-1D simulation period in the selected sites for 2015 and 2016.

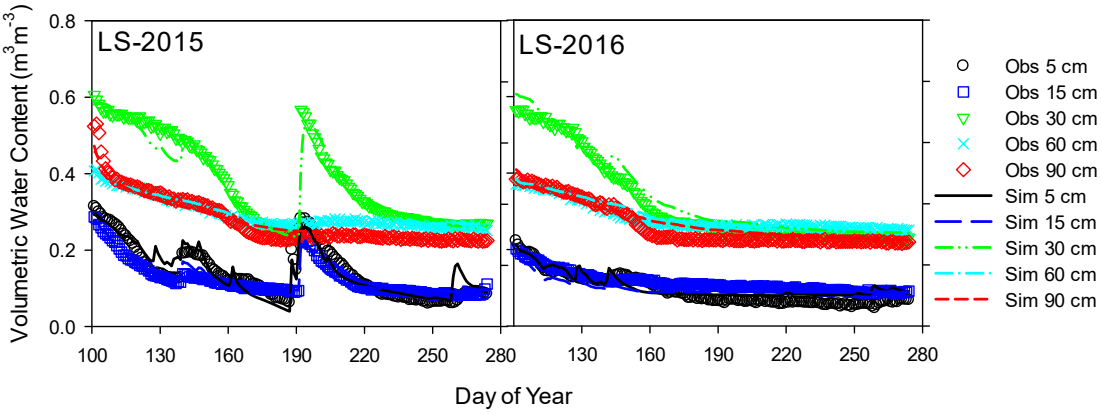


**Fig. 3.4.** Volumetric water content reported by Hydraprobe sensors (points) at different depths and as simulated by HYDRUS-1D (lines) after calibration for the growing seasons of 2015 and 2016 at the low sage station. The simulation period was between DOY 100 (10 April) and DOY 273 (30 September).

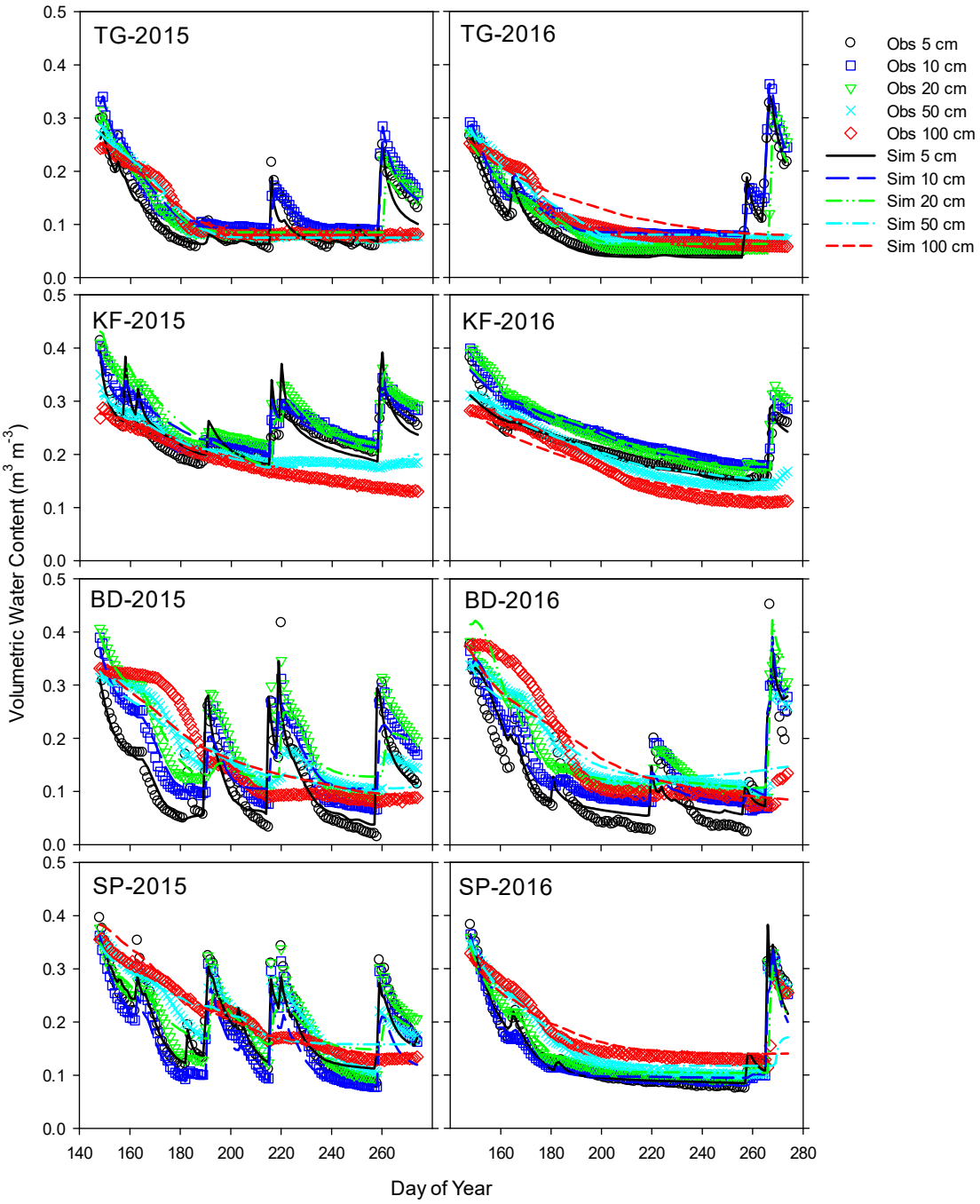


**Fig. 3.5.** Volumetric water content reported by TDT sensor (points) at different depths and as simulated by HYDRUS-1D (lines) after calibration for the growing season of 2015 and 2016 at Tony Grove (TG), Knowlton Fork (KF), Beaver Divide (BD) and Soapstone (SP). The simulation period was between DOY 147 (27 May) and DOY 273 (30 September).

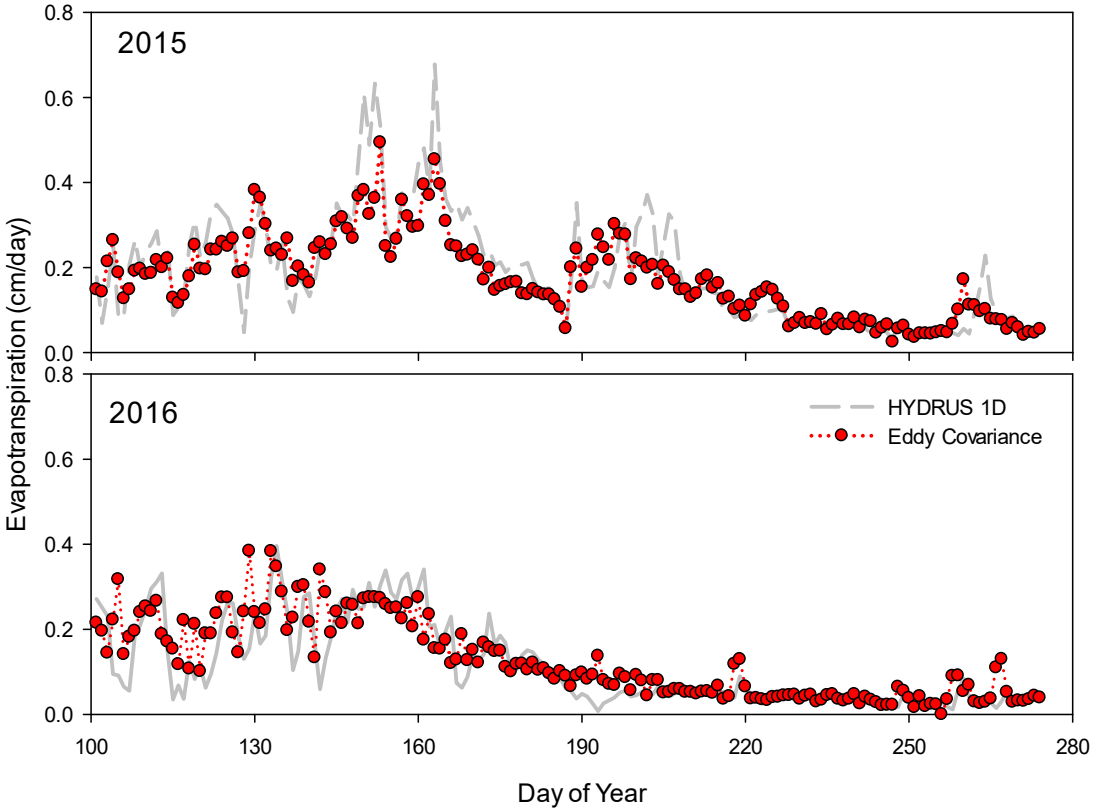


**Fig. 3.6.** Actual evapotranspiration measurements from the eddy covariance system compared with actual evapotranspiration simulated using HYDRUS-1D at the Low Sage station in Reynolds Creek Watershed for the year 2015 and 2016.

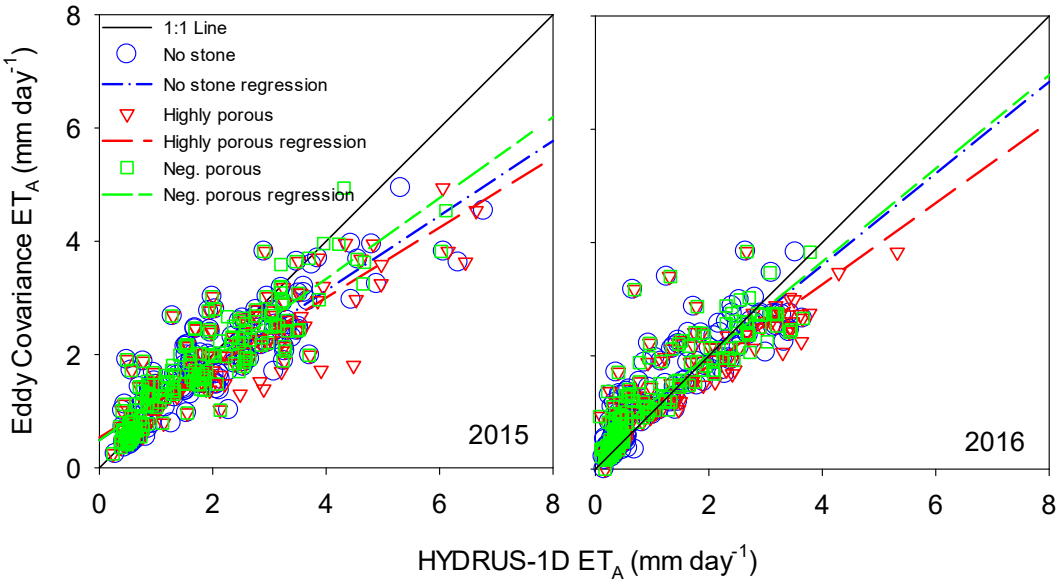


**Fig. 3.7.** Scatter plot between the evapotranspiration measured by the Eddy Covariance tower at the low sage station and the HYDRUS-1D simulations of actual evapotranspiration assuming no stones, highly porous and negligibly porous stones along with their regression line for 2015 and 2016.

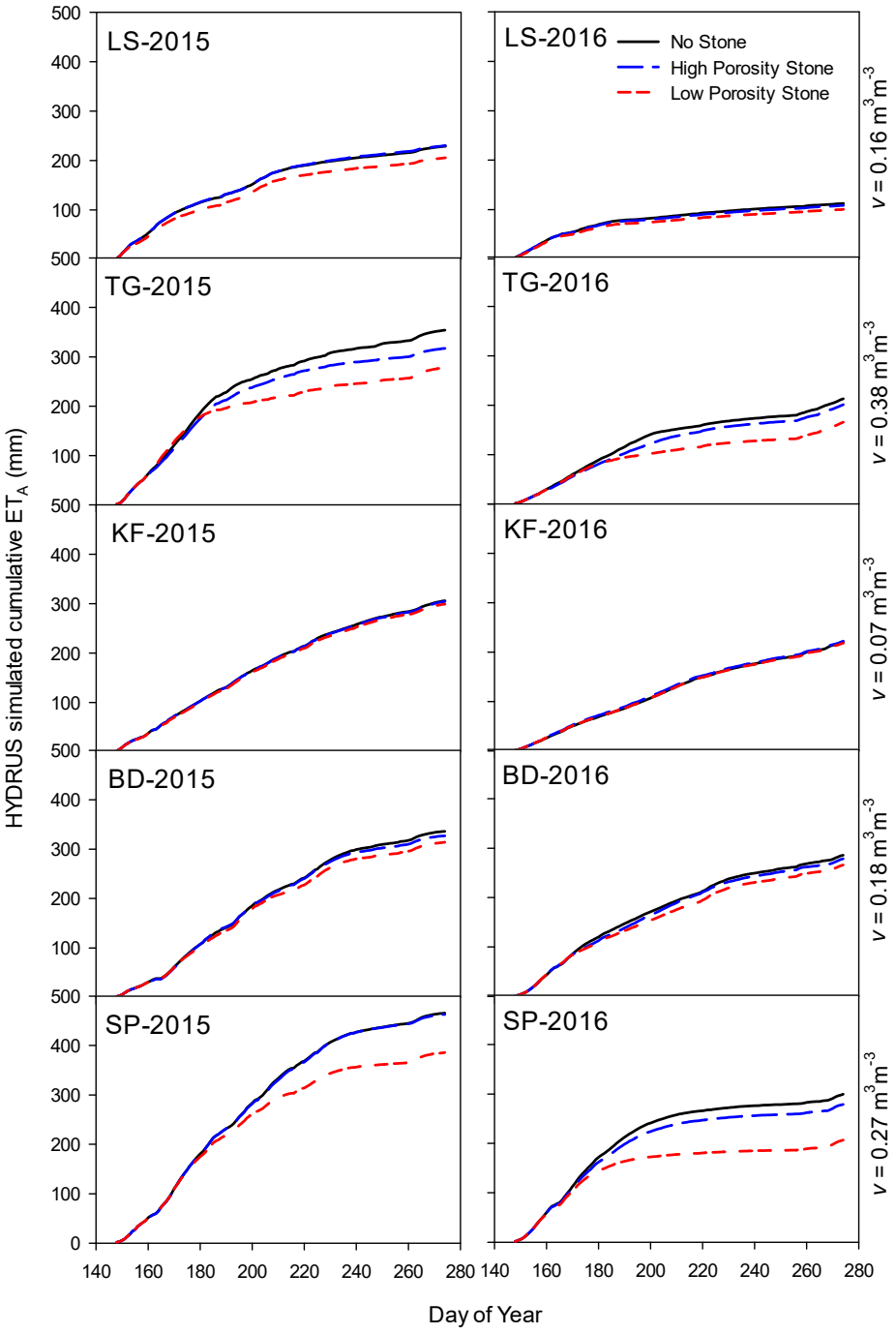


**Fig. 3.8.** Cumulative evapotranspiration simulated by HYDRUS-1D under three different scenarios considering soil with -no stone, -highly porous stone and -negligibly porous stone at the Low Sage (LS), Tony Grove (TG), Knowlton Fork (KF), Beaver Divide (BD) and Soapstone (SP) stations for 2015 and 2016. The ET is cumulative from DOY 148 (28 May) to DOY 273 (30 September). The stone content along the soil profile is presented in Fig. 3.2. Average stone content ($v$) for each site is presented on the right side of each plot.

**Table 3.1.** Location and description of weather stations

| Station | Watershed, State | Lat | Lon | Elev (m) | Vegetation |
|---|---|---|---|---|---|
| Low Sage (LS) | Reynolds Creek, ID | 43.14 | -116.74 | 1608 | Sagebrush |
| Tony Grove (TG) | Logan River, UT | 41.89 | -111.57 | 1928 | Sagebrush, Grass |
| Knowlton Fork (KF) | Red Butte Creek, UT | 40.81 | -111.77 | 2178 | Grass, Fern |
| Beaver Divide (BD) | Provo River, UT | 40.61 | -111.10 | 2508 | Sagebrush, Grass |
| Soapstone (SP) | Provo River, UT | 40.57 | -111.04 | 2388 | Sagebrush, Grass |

**Table 3.2.** Measured water retention parameters: saturated water content ($\theta_s$), residual water content ($\theta_r$), shape parameters $\alpha$ and $n$ for the stone fragments obtained from Parajuli et al., (2017).

| Parameters | Highly Porous Stone (Coarse Sandstone) | Negligibly Porous Stones (Fine Sandstone) |
|---|---|---|
| $\theta_s$ [$m^3\ m^{-3}$] | 0.28 | 0.036 |
| $\theta_r$ [$m^3\ m^{-3}$] | 0.012 | 0 |
| $\alpha$ [$m^{-1}$] | 0.032 | 0.084 |
| $n$ | 2.115 | 1.219 |

**Table 3.3.** Goodness of fit for measured soil moisture content with the HYDRUS-1D simulation, expressed in terms of the coefficients of determination ($R^2$) and root mean squared errors (RMSE)

| Year | Sensor Depth | Low Sage | | Sensor Depth | Tony Grove | | Knowlton Fork | | Beaver Divide | | Soapstone | |
|---|---|---|---|---|---|---|---|---|---|---|---|---|
| | | $R^2$ | RMSE ($m^3\ m^{-3}$) | | $R^2$ | RMSE ($m^3\ m^{-3}$) | $R^2$ | RMSE ($m^3\ m^{-3}$) | $R^2$ | RMSE ($m^3\ m^{-3}$) | $R^2$ | RMSE ($m^3\ m^{-3}$) |
| 2015 | 5 cm | 0.853 | 0.025 | 5 cm | 0.927 | 0.021 | **0.667** | 0.028 | **0.671** | **0.047** | 0.927 | 0.025 |
| | 15 cm | 0.931 | 0.013 | 10 cm | 0.951 | 0.014 | 0.853 | 0.017 | 0.889 | **0.032** | 0.873 | **0.035** |
| | 30 cm | 0.957 | 0.028 | 20 cm | 0.903 | 0.019 | 0.839 | 0.025 | **0.651** | **0.052** | **0.651** | **0.042** |
| | 60 cm | 0.975 | 0.006 | 50 cm | 0.989 | 0.006 | 0.962 | 0.008 | 0.866 | 0.026 | 0.638 | **0.039** |
| | 90 cm | 0.967 | 0.019 | 100 cm | 0.976 | 0.009 | 0.994 | 0.005 | 0.936 | **0.033** | 0.976 | 0.014 |
| | Average | 0.937 | 0.018 | | 0.949 | 0.014 | 0.863 | 0.017 | 0.803 | **0.038** | 0.813 | 0.031 |
| 2016 | 5 cm | 0.817 | 0.016 | 5 cm | 0.989 | 0.011 | 0.893 | 0.017 | **0.771** | **0.044** | 0.966 | 0.015 |
| | 15 cm | 0.837 | 0.022 | 10 cm | 0.990 | 0.007 | 0.974 | 0.010 | 0.875 | 0.030 | 0.978 | 0.012 |
| | 30 cm | 0.984 | 0.026 | 20 cm | 0.989 | 0.014 | 0.942 | 0.016 | 0.919 | 0.029 | 0.913 | 0.022 |
| | 60 cm | 0.957 | 0.012 | 50 cm | 0.985 | 0.012 | 0.986 | 0.012 | 0.807 | **0.036** | **0.705** | **0.041** |
| | 90 cm | 0.935 | 0.022 | 100 cm | 0.947 | 0.027 | 0.980 | 0.015 | 0.904 | **0.040** | **0.707** | **0.034** |
| | Average | 0.906 | 0.020 | | 0.980 | 0.014 | 0.955 | 0.014 | 0.855 | **0.036** | 0.854 | 0.024 |

**Table 3.4.** Goodness of fit for evapotranspiration measured by eddy covariance with HYDRUS-1D simulation considering soil with: (1) no stones, (2) highly porous stones, and (3) negligibly porous stones, expressed in terms of coefficients of determination ($R^2$) and root mean squared errors (RMSE)

| | 2015 | | 2016 | |
|---|---|---|---|---|
| | $R^2$ | RMSE (mm/day) | $R^2$ | RMSE (mm/day) |
| No Stone | 0.78 | 0.64 | 0.76 | 0.51 |
| Highly Porous Stone | 0.76 | 0.73 | 0.78 | 0.54 |
| Negligibly Porous Stone | 0.79 | 0.55 | 0.79 | 0.49 |

**Table 3.5.** HYDRUS-1D simulated actual-Transpiration ($T_A$) , -Evaporation ($E_A$) and -Evapotranspiration ($ET_A$) reported as mm of water loss at different sites in years 2015 and 2016 under three different scenarios considering soil with no stones, highly porous stones and negligibly porous stones. The numbers on right hand side are percent change while considering the highly- and negligibly-porous stones as compared to no stone condition.

| Year | Scenario | Component | Low Sage | | Tony Grove | | Knowlton Fork | | Beaver Divide | | Soapstone | |
|---|---|---|---|---|---|---|---|---|---|---|---|---|
| | | | (mm) | Change(%) | (mm) | Change(%) | (mm) | Change(%) | (mm) | Change(%) | (mm) | Change(%) |
| **2015** | No Stone | $T_A$ | 134 | | 262 | | 228 | | 267 | | 384 | |
| | | $E_A$ | 95 | | 92 | | 78 | | 69 | | 81 | |
| | | $ET_A$ | 229 | | 354 | | 306 | | 336 | | 466 | |
| | Highly Porous Stone | $T_A$ | 130 | *-3.06* | 258 | *-1.61* | 226 | *-0.84* | 265 | *-0.54* | 384 | *-0.22* |
| | | $E_A$ | 101 | *5.97* | 59 | *-35.27* | 79 | *0.84* | 62 | *-11.14* | 80 | *-2.36* |
| | | $ET_A$ | 231 | *0.70* | 317 | *-10.35* | 305 | *-0.41* | 327 | *-2.72* | 463 | *-0.60* |
| | Negligibly Porous Stone | $T_A$ | 124 | *-6.97* | 180 | *-31.46* | 228 | *-0.12* | 247 | *-7.40* | 307 | *-20.22* |
| | | $E_A$ | 81 | *-14.57* | 99 | *7.25* | 72 | *-8.02* | 67 | *-3.62* | 79 | *-2.85* |
| | | $ET_A$ | 206 | *-10.13* | 278 | *-21.41* | 299 | *-2.14* | 314 | *-6.62* | 386 | *-17.19* |
| **2016** | No Stone | $T_A$ | 103 | | 156 | | 165 | | 172 | | 245 | |
| | | $E_A$ | 9 | | 57 | | 56 | | 114 | | 54 | |
| | | $ET_A$ | 112 | | 213 | | 221 | | 286 | | 299 | |
| | Highly Porous Stone | $T_A$ | 99 | *-4.56* | 148 | *-5.07* | 163 | *-1.44* | 196 | *14.02* | 226 | *-7.64* |
| | | $E_A$ | 10 | *10.17* | 54 | *-6.41* | 60 | *7.48* | 83 | *-27.56* | 52 | *-3.30* |
| | | $ET_A$ | 109 | *-3.38* | 202 | *-5.43* | 222 | *0.81* | 278 | *-2.58* | 279 | *-6.85* |
| | Negligibly Porous Stone | $T_A$ | 92 | *-11.31* | 111 | *-28.76* | 165 | *-0.16* | 180 | *5.07* | 160 | *-34.74* |
| | | $E_A$ | 9 | *-0.52* | 55 | *-3.80* | 54 | *-3.45* | 86 | *-25.00* | 47 | *-13.80* |
| | | $ET_A$ | 101 | *-10.44* | 166 | *-22.05* | 218 | *-0.99* | 266 | *-6.94* | 207 | *-30.95* |

# CHAPTER 4

# EVALUATING THE NOAH-MP LAND SURFACE MODEL FOR SIMULATION OF EVAPOTRANSPIRATION AND HYDRODYNAMICS IN STONY SOILS[3]


## Abstract

There has been considerable advancement in spatiotemporal resolution of remote sensing and ground-based measurements enabling refinements to the parameters used in land surface models for simulating surface fluxes. However, inadequate representation of subsurface processes and soil parameters still create limitations for land surface model simulation. This study investigates the performance of the Noah-Multiphysics (Noah-MP) land surface model for simulating soil moisture and evapotranspiration under various soil parameterizations. A comprehensive field data set including soil profile property measurements, micrometeorological data and soil moisture from different depths from the Low Sagebrush eddy covariance tower at Reynolds Creek watershed in Southwestern Idaho was employed to drive Noah-MP and assess the simulation results. We evaluated the performance of Noah-MP considering four different scenarios: 1-layer soil profile with (i) Noah-MP default hydraulic parameters, and 5-layer soil profile with -(ii) soil hydraulic parameters from look up table that Noah-MP uses and SSURGO/STATSGO soils information at the depth corresponding to each layer, -(iii) hydraulic parameters from field observations –(iv) hydraulic parameters from field, accounting for stone content in each


[3] Coauthored by, Kshitij Parajuli, Lin Zhao, Scott B. Jones, David G. Tarboton, Lawrence E. Hipps, Alfonso Torres-Rua, Morteza Sadeghi, Gerald N. Flerchinger

layer. Additional simulations were performed using the HYDRUS-1D numerical model employing more detailed representation of soil hydraulic functions. These included 5- layer soil profile -(i) neglecting the presence of stones and -(ii) considering the effect of stone content. Each experiment was forced with the same set of initial conditions, atmospheric forcing and vegetation parameters. The best simulation fit to measured soil moisture was obtained with the HYDRUS-1D numerical model. Significant improvement in the Noah-MP soil moisture simulation was achieved using the improved soil parameters. The Noah-MP model incorporating stone content effects and using detailed soil properties as obtained from field observations provided the better estimation of evapotranspiration compared to eddy covariance measurements. We conclude that improvement in representation of soil properties along with stone content information can substantially improve the ability of land surface models to simulate soil water flow and boundary fluxes.

Keywords: Land surface models, Soil hydrology, Noah-MP, Evapotranspiration, Stony soil

## 4.1. Introduction

Land surface models (LSMs) have been used widely in studying interactions between soil, vegetation and the atmosphere continuum, in addition to predicting water- and energy- fluxes. Understanding of the land-atmosphere interaction enhances the capability of weather and climate predictions (Barlage et al., 2015; Chen et al., 2001; Gao et al., 2015; Kumar et al., 2014). Detailed land-atmosphere processes and vegetation characteristics are incorporated in state-of-the-art versions of LSMs for improved prediction of soil-atmosphere boundary fluxes (Chen and Dudhia 2001; Gayler et al., 2013, Niu et al., 2011; Oleson et al., 2013). In additon, high-performance computing facilities

and improved spatiotemporal resolution of remote sensing and ground-based measurements have contributed to enhancement of these models. This has resulted in extensive applications of LSMs to characterize evapotranspiration (ET) and soil moisture dynamics at regional scales (Cai et al., 2014; 2014a; Gayler et al., 2013; Koster and Suarez, 1992; Chen et al., 1996; Long et al., 2014). Nevertheless, inadequacy in simulating water- and energy- fluxes from soil still exist due to poor representation of subsurface processes and soil parameters (Gayler et al., 2013; 2014; Koster et al., 2009; Zheng et al., 2015).

Soil moisture is a key variable and fundamental in governing the exchange of water- and energy-flux at the soil-atmosphere boundary (Dirmeyer and 1994; Dirmeyer 1995; Gayler et al., 2014; Poltoradnev et al., 2018; Zheng et al., 2015). Soil moisture content interacts with atmospheric proceses and directly influences the energy partitioning into sensible and latent heat flux (Goodrich et al., 1994; Heathman et al., 2009). Despite being a prime variable in controlling the transfer of water and energy fluxes from land surfaces, past studies have reported the inability of LSMs to accurately simulate soil moisture (Chen et al., 2013; Dirmeyer et al. 2006; Xia et al. 2014; Koster et al., 2009; Xue et al., 2013). Soil moisture dynamics computed within LSMs are dependent on the specified soil hydraulic properties. These are often simplified and therefore poorly characterized in LSMs because the soil parameter values may be limited to a number of soil types based on textural class in a soil parameter lookup table. Soils are highly heterogeneous spatially and vertically with distinct plant-dependent root systems, soil textures, organic matter content and stone fragment distributions (Chen et al., 2013;2016; Yang et al., 2005; Zheng et al., 2015; 2017; Cousin et al., 2003). These contrasting physical and hydraulic properties

augment complexities in calculating heat and water transfer within the soil (Koster and Suarez, 1992; Li et al., 2013; Gayler et al., 2013; Ke et al., 2013). Poorly defined soil parameters have been identified as one of the limitations for LSMs to accurately simulate soil moisture and water fluxes in previous studies (Gayler et al., 2013; 2014; Koster et al., 2006; Niu et al., 2011). Soil moisture content simulated by LSMs is therefore highly dependent on the model and are inconsistent among different models even when the models are driven with precisely the same boundary forcing due to differences in soil parameters and model physics accunting for the subsurface processes (Dirmeyer et al. 2006; Koster et al., 2009; Zheng et al., 2015). This necessitates more detailed accounting for subsurface processes with improved soil parameterization in LSMs in order to enhance simulation of soil moisture and water- and energy-fluxes between the land surface and atmosphere (Koster and Suarez, 1992; Li et al., 2013; Ke et al., 2013).

Current LSMs use soil information from soil maps generated by the National Resources Conservation Service (NRCS), State Soil Geographic (STATSGO) and the Food and Agricultural Organization (FAO) soil databases. These were developed in the early 90s at 1 km resolution for the contiguous United States (CONUS) and at 10 km resolution elsewhere (FAO, 1991; Yang et al., 2011; ). These maps provide two soil layers; 0-30 cm and 30-100 cm. There has been notable improvement in soil mapping in recent years. For example, a new soil database known as POLARIS has remapped the Soil Survey Geographic (SSURGO) database using high-resolution geospatial environmental data and machine learning algorithms to obtain soil parameters at various depths for CONUS at a 30-m spatial resolution (Chaney et al., 2016). SoilGrids250m is another noteworthy

resource that provides global prediction for several soil properties such as organic carbon, bulk density, pH, soil texture fractions and coarse fragments at seven standard depths (0, 5, 15, 30, 60, and 200 cm), with 250-m resolution (Hengl et al., 2017). These soil datasets have delivered options for including detailed soil information in order to improve soil parmeterization in LSMs at regional scales.

In natural settings, the complexity in representing soils is amplified by the extreme heterogeneity in stone distribution and content (particle size greater than 2 mm) throughout the soil profile (Cousin et al., 2003; Novak and Surda, 2010; Parajuli et al., 2017). Stone content in soil disturbs the soil physical properties affecting available water content and soil hydrodynamics, which further impacts root water uptake and ET (Cousin et al., 2003). Stone content in the soil alters the soil hydraulic properties and usually reduces soil water storage. The magnitude of this effect depends upon the type and origin of stones, the volumetric fraction of stone content and the size and porosity of stones (Cousin et al., 2003; Parajuli et al., 2017). The majority of studies cited above disregard the presence of stones in the soil. In order to close this knowledge gap, the main motivation of this study has been to address the effects of stone content on soil moisture dynamics and ET simulated by LSMs.

This study applies one of the most widely used LSMs, Noah-Multiphysics (Noah-MP). The specific objective of this study was to investigate the potential improvement in the Noah-MP LSM soil moisture and ET simulations through improved soil hydraulic parameterization and accouting for the stone content. We first simulate ET using Noah-MP with default soil parameters from the lookup table with single soil type for the whole soil

profile. Then, we estimate ET by accounting for vertical heterogeneity in the soil using five distinct layers. First we use soil hydraulic parameters from a lookup table for soil type defined by USDA soil textural class. Then we adjust soil parameters based on textural and stone content information obtained from field observations for each layers. We also compare the Noah-MP soil moisture and ET simulations with those of the HYDRUS-1D numerical model, that employs a more accurate parameterization of soil hydraulic functions and root water uptake.

## 4.2. Materials and methods

### *4.2.1. Site description and data*

The data for this study were collected from the lower sage station (43.14$^{o}$N, 116.74$^{o}$ E) at Reynolds Creek experimental watershed in southwestern Idaho, USA. The site is located at an altitude of 1600 m above sea level and is part of the Reynolds Creek Critical Zone Observatory (CZO). Climate in Reynolds creek watershed varies with the montane elevation gradient, while the mean annual temperature and precipitation for the lower sage station were 8.5 ℃ and 345 mm (Fellows et al., 2017).

Meteorological observations, including humidity, air temperature, wind speed, pressure, precipitation, incoming short- and long-wave radiation were obtained from an established eddy covariance station. These variables were used as atmospheric forcing data to drive a one-dimensional Noah-MP simulation in an offline mode. The data were collected every 15 minutes and processed at 30-minute intervals. Precipitation was measured using a dual-gauge system especially designed for windy and snow dominated conditions and processed hourly. Volumetric soil water content and soil temperature were

recorded every hour at depths of 5-, 15-, 30-, 60-, and 90- cm using Hydra-probe II soil moisture sensors (Stevens Water Monitoring System, Inc., Portland, OR).

The site was further instrumented with an eddy covariance (EC) tower with the system mounted at a height of 2.09 m above the ground surface to measure water and carbon fluxes within the sagebrush ecosystem. Short- and long-wave radiation, air temperature and humidity were collected at the eddy covariance station every 30 minutes using a four-component net radiometer (CNR-1, Kipp & Zonen, Delft, The Netherlands), and a temperature/humidity probe (HMP155C, Vaisala, Helsinki, Finland). Soil heat flux was determined using six soil heat flux sensors (HFT3, REBS, Seattle, WA) installed 0.08-m deep within the soil along with three sets of self-averaging thermocouples installed at 0.02 and 0.06 m (Fellows et al., 2017). A three-dimensional sonic anemometer (Model CSAT3, Campbell Scientific, Inc., Logan UT) and an open path infrared gas analyzer (IRGA; Model LI-7500a, LI-COR, Inc., Lincoln, NE) were sampled at 10 Hz as part of the eddy covariance system.

During the process of soil moisture sensor installation, the excavated soil was analyzed in order to determine soil texture, bulk density, root distribution, stone content etc. The site was highly heterogeneous in terms of soil distribution with significant stone content within the profile. The soil description for the site was obtained from Patton et al. (2018), presented in Table 4.1.

The soil textural analysis was performed for multiple horizons at increments of nearly 10 cm. However, only five distinct soil layers were assumed for the improved Noah-MP

simulation. Soils collected from the site had high stone content within the soil depth with nearly 40% stones by volume between 30 and 80 cm (Table 4.1, Fig. 4.1).

*4.2.2. Noah-MP land surface model*

Noah-MP is one of the most commonly used LSMs and has incorporated schemes for runoff, leaf dynamics, stomatal resistance, and a soil moisture factor (Niu et al., 2011, Yang et al., 2011). In addition to the previously available Noah LSM, Noah-MP has added biophysical processes such as; unconfined aquifer for groundwater storage and a dynamic water table, interactive vegetation canopy, multilayer snowpack, and a simple TOPMODEL-based (TOPography based hydrological MODEL) runoff production function (Dickinson et al., 1998; Niu et al., 2005, 2007; Yang and Niu, 2003 in Cai et al 2014a). While Noah-MP has mostly been used as a component of the Weather Research and Forecasting (WRF) model, it is also available as a stand alone one-dimensional model (Noah-MP v2.0), which we have used in this study.

The soil water flow component in the Noah-MP LSM is simulated using the diffusivity form of the Richards' equation or, more accurately to say, Richardson-Richards equation (Raats and Knight, 2018):

$$\frac{\partial \theta}{\partial t} = \frac{\partial}{\partial z}\left( D(\theta)\frac{\partial \theta}{\partial z} \right) + \frac{\partial K(\theta)}{\partial z} + S(\theta) \qquad (1)$$

where $D$ is soil water hydraulic diffusivity [$m^2\ s^{-1}$], $S$ represents sources and sinks (i.e. precipitation, $P$, evapotranspiration, $ET$, and runoff, $R$) and is expressed as: $S = P + ET + R$. The soil hydraulic diffusivity for one-dimensional vertical flow in soil is expressed in

terms of the soil hydraulic conductivity ($K$), matric potential ($h$), and volumetric water content ($\theta$):

$$D = K(\theta)\left(\frac{dh}{d\theta}\right) \tag{2}$$

Note that, for the sake of simplicity, absolute value of $h$ is considered in Eq. (2) and the following equations.

The Clapp-Hornberger parameterization of water retention and hydraulic conductivity functions (Clapp and Hornberger, 1978) are used with Eq. (1) to simulate the soil water flow (Chen and Dudhia, 2001; Cosby et. al., 1984):

$$h(\theta) = h_s\left(\frac{\theta}{\theta_s}\right)^{-b} \tag{3}$$

$$K(\theta) = K_s\left(\frac{\theta}{\theta_s}\right)^{2b+3} \tag{4}$$

where $h_s$ is matric potential at air entry, often referred as "*bubbling pressure*" [m], $K_s$ is saturated soil hydraulic conductivity [m $s^{-1}$] and $b$ is a fitting parameter related to the soil pore-size distribution. The parameters in this study were determined from the Noah-MP soil parameter lookup table for the soil type based on soil textural class. The $K(\theta)$ and $D(\theta)$ functions are non-linearly dependent on $\theta$ and vary by several orders of magnitude for small variation in $\theta$ as the soil gets drier.

In Noah-MP, the latent heat flux (*LE*) is calculated in terms of potential evapotranspiration ($ET_o$) using a Penman-Monteith (Monteith 1973; Penman, 1953) energy balance approach written (Bonan 2008; Mahrt and Ek, 1984; Cai et al 2014a):

$$\lambda ET_o = \frac{\Delta\left(R_n - G_o\right) + \rho_a c_p \left(e_s - e_a\right) \Big/ r_a}{\Delta + \gamma\left(1 + r_c \Big/ r_a\right)} \tag{5}$$

where $R_n$ is the net radiation [W m$^{-2}$], $G$ is the soil heat flux [W m$^{-2}$], $e_s$ and $e_a$ are saturated and actual vapor pressure [kPa], respectively, $\rho_a$ is the mean air density at constant pressure [kg m$^{-3}$], $c_p$ is the specific heat of the air [J kg$^{-1}$ K$^{-1}$], $\Delta$ is the slope of the saturated vapor pressure curve [kPa K$^{-1}$], $\lambda$ is the latent heat of vaporization [J kg$^{-1}$], $\gamma$ is the psychrometric constant [-], $r_c$ and $r_a$ are the canopy- and aerodynamic- resistances [s m$^{-1}$], respectively.

The actual ET is then computed as the sum of these three components, which are soil evaporation ($E_{dir}$), evaporation of intercepted precipitation by the canopy ($E_c$), and transpiration through the vegetation ($E_t$). The evaporation from the top soil layer is calculated as:

$$E_{dir} = (1 - f_c)\left(\frac{\theta_1 - \theta_{wp}}{\theta_s - \theta_{wp}}\right)^{f_x} E_o \tag{6}$$

where, $f_c$ is the fractional vegetation cover [-], $f_x$ is an empirical constant assumed equal to 2.0 [-], $\theta_s$ is the saturated soil moisture content [m$^3$ m$^{-3}$], $\theta_{wp}$ is the soil moisture content at wilting point [m$^3$ m$^{-3}$], and $\theta_1$ is the soil moisture content in the first soil layer

[$m^3$ $m^{-3}$]. The direct evaporation of rain intercepted by the plant canopy is determined as (Huang 2016):

$$E_c = f_c E_o \sqrt{\frac{CMC}{CMC_{\max}}} \tag{7}$$

where, $CMC$ and $CMC_{\max}$ are the actual and maximum canopy moisture contents [kg $m^{-2}$]. Similarly, the transpiration from the plant is determined as:

$$E_t = f_c P_c \left(1 - \sqrt{\frac{CMC}{CMC_{\max}}}\right) E_o \tag{8}$$

where $P_c$ is the plant coefficient [-].

*4.2.3. HYDRUS-1D numerical model*

HYDRUS-1D (Šimůnek et al., 2016) is a physically-based numerical modelling software package used to simulate unsaturated hydrodynamics including root water uptake, by inversely solving the sink term ($S$) in Richards' equation (Eq. 1). The soil hydraulic functions were defined by the van Genuchten (1980) model:

$$\Theta = \frac{\theta - \theta_r}{\theta_s - \theta_r} = \left[1 + (\alpha h)^n\right]^{-m} \tag{9}$$

where $\Theta$ is effective degree of saturation [-], $\theta_r$ and $\theta_s$ are the residual and saturated volumetric water contents [$m^3$ $m^{-3}$], $\alpha$ is a scaling factor related to the inverse of air entry pressure [$m^{-1}$], $n$ and $m$ are empirical fitting parameters related to the soil pore-size distribution.

The unsaturated hydraulic conductivity of the soil is described by the van Genuchten-Mualem (VGM) model expressed as (Mualem, 1976; van Genuchten, 1980):

$$K(h) = K_s \left[ \frac{\left\{ 1 - (\alpha h)^{n-1} \left[ 1 + (\alpha h)^n \right]^{-m} \right\}^2}{\left[ 1 + (\alpha h)^n \right]^{m/2}} \right] \tag{10}$$

*4.2.4. Experimental design*

In this study, four numerical experiments were designed to evaluate the performance of the Noah-MP LSM for simulating soil moisture and ET under different soil parameterization (summarized in Table 4.2). Each experiment was forced with the same set of atmospheric forcing conditions and vegetation parameters between 15 April and 28 September 2015. The first simulation (NMP I) was performed using default settings where a single soil type was considered for the entire soil profile, represented by a single set of soil parameters ($\theta_s$, $K_s$, $h_s$, and $b$) obtained from the Noah-MP soil parameter lookup table. In the second simulation (NMP II), five soil layers were used. However, the soil parameters were obtained from the soil parameter lookup table based on general soil classification defined by United States Department of Agriculture (USDA) soil textural class. The third simulation (NMP III) used the same five soil layers with more descriptive soil parameters derived for each soil layer using a pedotransfer function based on textural information of sand-, silt-, clay-percentage and bulk density. The saturated water content ($\theta_s$) was estimated by neural network prediction (Rosetta Lite v. 1.1; Schaap et al., 2001; Schaap and Bouten, 1996; Schaap et al., 1998; Simunek et al., 2008) that required the same information on sand-, silt-, and clay-percentage and bulk density of the soil. Other

parameters $K_s$, $h_s$, and $b$ in Eqs. (3) and (4) were estimated by pedotransfer functions of Clapp and Hornberger (1978). Finally, in the fourth simulation (NMP IV) we accounted for the stone content by adjusting the total water holding capacity of the soil (i.e. saturated water content) for each layer based on the volumetric stone content as shown in Table 4.1. The stone's porosity was considered to be 15% assuming an average between highly porous (coarse sandstones) and negligibly porous (fine sandstones) stones as presented in Parajuli et al. (2017). The effective water content at saturation for stony soil was calculated as a weighted average:

$$\theta_{mix} = (1 - v)\theta_{soil} + v\theta_{stone} \tag{11}$$

where $\theta_{mix}$, $\theta_{soil}$, and $\theta_{stone}$ are volumetric water contents for stony soil, background soil, and stone fragments ($m^3\ m^{-3}$) and $v$ is the volumetric stone content ($m^3\ m^{-3}$).

Two additional numerical experiments were performed using a one-dimensional numerical model HYDRUS-1D, (i) neglecting the stone content (H1D I) and (ii) assuming stones with 15% porosity (H1D II). The van Genuchten soil parameters as shown in Eq. (9) in HYDRUS-1D were obtained from the Rosetta Lite software. Furthermore, $\alpha$, $n$ and $K_s$ were optimized by inverse simulation in HYDRUS-1D, yielding the best fit of the simulated soil moisture to the measured soil moisture values.

In order to account for the effect of stone fragments in the soil, the dual porosity model (Durner 1994) within the HYDRUS-1D software was applied to satisfy the algorithm suggested by Parajuli et al. (2017):

$$\frac{\theta_{mix}-\theta_{r,mix}}{\theta_{s,mix}-\theta_{r,mix}} = w_{soil}\left[1+\left(\alpha_{soil}h\right)^{n_{soil}}\right]^{-m_{soil}} + w_{stone}\left[1+\left(\alpha_{stone}h\right)^{n_{stone}}\right]^{-m_{stone}} \quad (12)$$

where the parameters with subscript *soil*, *stone* and *mix* are van Genuchten parameters for background soil, stone inclusion and soil-stone mixture, respectively. The weighting factors for soil and stone fractions, $w_{soil}$ and $w_{stone}$, at saturation are defined as:

$$w_{soil} = \frac{(1-v)\theta_{s,soil}}{(1-v)\theta_{s,soil}+v\theta_{s,stone}} \quad (13)$$

$$w_{stone} = \frac{v\theta_{s,stone}}{(1-v)\theta_{s,soil}+v\theta_{s,stone}} \quad (14)$$

## 4.3. Results

### *4.3.1. Simulation of soil moisture*

The time series of daily average measured soil moisture is shown in Fig. 4.2 along with the different numerically simulated values from Noah-MP and HYDRUS-1D as described in Section 3.3. The Hydraprobe measurements of soil volumetric water content and simulations from Noah-MP and HYDRUS-1D for depths 5, 15, 30, 60 and 90 cm are compared (Fig. 4.2). The soil is distinctly drying down from the beginning of the simulation period (15 April) with a recharge up to the depth of 30 cm in mid-July. When considering a single soil type for the entire soil profile (NMP I), the Noah-MP simulation showed less dry-down of the soil. Under this consideration, overestimation of soil moisture in the top two layers can be perceived from Fig. 4.2 contrasting with Zheng et al. (2015), where underestimation of soil moisture for the two upper soil layers (depth 5 cm and 25 cm) were reported. A simlar trend is observed in the second simulation (NMP II), where the soil

profile is divided into five different layers based on a general soil texural class in each layer. The soil moisture simulation showed significant improvement when the soil parameters were derived from the pedotransfer function based on actual observation of sand, silt and clay fraction and bulk density in the third experiment (NMP III).

While considering the presence of stone content in NMP IV, soil moisture was underestimated due to significant reduction in maximum water holding capacity caused by the presence of stone content (NMP IV). A notable disagreement in measured and simulated soil moisture was detected at the 30-cm depth for all four simulations. A low $K_s$ value for the clay layer above the depth of 30 cm could be a possible reason for restriction of water flow to the lower layers. Thus, the impact of rain events was not well-represented by the Noah-MP model at 30 cm.

The HYDRUS-1D without stone inclusion (H1D I) was able to simulate soil moisture at all depths with the best fit (Fig. 4.2). The performance of HYDRUS-1D in accurately simulating soil moisture is due to its ability to inversely fit the soil hydraulic parameters optimized to fit simulated soil moisture with measured one in process of simulation. Simulated soil moisture with consideration of stone content under H1D II was underestimated considerably at the 30 cm depth, where the maximum water content value was controlled by reduced saturated water content as in Noah-MP. However, HYDRUS-1D was able to capture the trend of soil moisture in both simulations (H1D I and H1D II) unlike Noah-MP. The scatter plot between the measured soil moisture at depths of 5, 15, 30, 60 and 90 cm are compared with the simulated values under four different simulations (NMP I, NMP II, NMP III and NMP IV) using Noah-MP LSM and two different

simulations (H1D I and H1D II) using the HYDRUS-1D numerical model, shown in Fig. 4.3. It is evident from the Fig. that HYDRUS-1D is most efficient in simulating soil moisture at all depths. The Noah-MP simulation with improved soil parameters (NMP III) improved the match between measured and simulated soil moisture.

Table 4.3 presents the error statistics in terms of root mean square error (RMSE) and coefficient of determination ($R^2$) computed between the measured soil moisture at the 5, 15, 30, 60 and 90 cm depths with those simulated from four Noah-MP and two HYDRUS-1D experiments. The low RMSE values closer to zero represent the better fit, whereas higher $R^2$ infer better correlation between observation and model results. As depicted in Fig. 4.3, the greatest correlation and least RMSE were found for H1D I simulation with the average RMSE and $R^2$ for five depths to be 0.02 $m^3$ $m^{-3}$ and 0.91, respectively. Among the Noah-MP simulations the third experiment (NMP III) where the soil parameters were derived from actual physical properties of the soil with detailed layering was able to simulate the most accurate soil moisture. The highest $R^2$ of 0.79 and least RMSE of 0.04 $m^3m^{-3}$ between observations and simulations were obtained in NMP III. The values of $R^2$ decreased in NMP IV and H1D II compared with similar simulations neglecting stone content (i.e. NMP III and H1D I) due the underestimation of soil moisture in both cases.

*4.3.2. Evaluation of evapotranspiration estimates*

The daily averaged values of measured latent heat flux were compared with the simulated values produced by the four Noah-MP simulations and the two HYDRUS-1D simulations as presented in Fig. 4.4. The Noah-MP simulated latent heat flux under NMP

I and NMP II showed overestimation towards the beginning of the simulation period but were able to match the observations during drier periods. The Noah-MP simulations with improved soil paramaters (NMP III) and with stone content information (NMP IV) matched the eddy covariance estimates agreeably. The overestimation of ET can be observed following rain events in mid July for NMP I and NMP II. For the same period, NMP III, NMP IV and both HYDRUS-1D simulations (H1D I and H1D II) performed well. The H1D and H1D II simulations slightly overestimated the latent heat flux at the beginning of June.

Comparison between the measured and simulated latent heat flux under different experiments is presented by scatter plots in Fig. 4.5. The error statistics between the measured and simulated latent heat fluxes are shown in terms of RMSE and $R^2$. The scatter plot in Fig. 4.5 and $R^2$ values in Table 4.3 exhibit a significant correlation between the measured latent heat flux with those simulated by Noah-MP and HYDRUS-1D. The HYDRUS-1D simulations showed better correlation as compared to the Noah-MP results (Fig. 4.5; Table 4.3). However, the HYDRUS-1D RMSE values were higher than NMP III and NMP IV. The lowest RMSE of 13.4 W $m^{-2}$ (0.5 mm $day^{-1}$, Table 4.3) suggests the improved soil paramterization with consideration of stone content more accurately simulated latent heat fluxes or evapotranspiration using LSMs.

Box plots showing measured daily evapotranspiration along with different simulated values for each month are shown in Fig. 4.6. The middle line within the box represents the median value, which is the $50^{th}$ percentile of daily ET. The box represents the middle 50% of ET values (from $25^{th}$ to $75^{th}$ percentile) and the whiskers represent

values outside the middle 50% of ET estimates. The measured ET was maximum during May and June with monthly averages of 2.6 mm $day^{-1}$. The lowest ET occurred during September with less than 1 mm $day^{-1}$ on average. The Noah-MP simulation considering stone content (NMP IV) showed reasonable consistency in predicting daily ET. The HYDRUS-1D simulations were able to predict ET closer to the mean value, however, with more fluctuations towards maximum and minimum values of daily ET.

The cumulative ET simulated under NMP IV (Noah-MP with stone content) over the simulation period (15 Apr – 28 Sep 2018) produced the closest match with the measured cumulative ET of 302 mm. The cumulative ET simulated in H1D II was 306 mm while that of H1D I was 329 mm. The monthly cumulative ET (Fig. 4.7a) showed that NMP IV estimates of ET were much lower than the actual measurements until July. On the other hand, the H1D I and H1D II simulations showed better estimation of cumulative ET for all months except June, where considerable overestimation of daily ET is observed (Fig. 4.4).

**4.4. Discussion**

Soil moisture has substantial influence on the surface energy balance as it dictates the partitioning of available energy into latent and sensible heat fluxes. Soil moisture also affects the soil heat conductivity inducing the heat flow into the soil as soil heat flux. Hence, all the components of energy balance are reliant on available soil moisture, meaning that the simulation of soil moisture has direct influence on the simulation of heat fluxes and ET. Soil moisture simulations were substantially improved using the modified soil hydraulic parameterization with some uncertainties as expressed by average RMSE of 0.04 $m^3m^{-3}$ and 0.07 $m^3m^{-3}$ under the NMP III and NMP IV, respectively (Table 4.3). The RMSE

between soil moisture measured by the Hydraprobe sensor at the 30 cm depth and predicted by the NMP III and NMP IV simulations for respective layer were 0.1 $m^3m^{-3}$ and 0.17 $m^3m^{-3}$ (Table 4.3). Similarly, for the same depth the RMSE increased from 0.02 $m^3m^{-3}$ in the H1D I simulation to 0.15 $m^3m^{-3}$ in the H1D II output. The increased RMSE was due to underestimation of soil moisture (Fig.s 4.2 and 4.3) when the effect of stone content was accounted for in the Noah-MP and HYDRUS-1D models. This under-estimation of soil moisture resulted from high stone content (0.38 $m^3m^{-3}$) at the 30 cm depth, which seems that have significantly reduced water storage for the respective soil layer. In reality, soil moisture content recorded by the Hydraprobe sensors is more representative of the fine soil matrix than of the total soil volume including stones (at different soil moisture) because the sensors are generally only embedded within the soil matrix, minimizing contact with the stones. This placement likely overestimates the average moisture content for the whole layer, which contains almost 40% stone. A comprehensive investigation on the effect of stone content on the soil moisture sensors is required to have better understanding of soil moisture measurements and their interpretation for stony soils. However, this is beyond the scope of the current study.

The latent heat flux simulated by the Noah-MP model depends on water availability in the root zone, thus the modification in soil parametrization has significantly influenced the ET estimation. Adjustment of the soil parameters to account for the stone content within Noah-MP (NMP IV) resulted in improved simulation of ET, yielding the closest estimates to the eddy covariance measured values. The RMSE values were reduced to 13 $Wm^{-2}$ from 20 $Wm^{-2}$ in NMP I and 14.3 $Wm^{-2}$ in NMP III. Although HYDRUS-1D simulations of soil

moisture showed greater accuracy than Noah-MP simulations, overestimation of ET values were observed for both H1D I and H1D II simulations. The HYDRUS-1D simulations, however, showed the best correlations and the RMSE was lower than that of NMP IV. This discrepancy likely resulted from over estimation of ET during the month of June, which is clear from Fig. 4.7(a). The over prediction of the median value as compared to the eddy covariance measurement for the month of June under H1D I is evident also from the box plot in Fig. 4.6. The error in HYDRUS-1D simulations may result from inaccuracy of soil hydraulic parameters estimates. On the other hand, though eddy covariance represents the most direct and accurate measurements of latent heat flux or ET at the local scale, there are limitations of its application as the flux footprint varies with the wind speed and direction. The flux footprint of eddy covariance measurements extends well beyond the point scale simulations using Noah-MP and HYDRUS-1D but for 1-dimensional vertical fluxes these should be highly correlated. Furthermore, instrumentation error and site condition can affect the flux measurements. Ryu et al. (2008) reported the uncertainty in ET measured by eddy covariance over a California grassland to be nearly 9% at the 90% confidence level. The NMP IV simulations of ET yielded an $R^2$ value of 0.76 while achieving the lowest RMSE within the 95% confidence prediction interval (Fig. 4.5). Regardless of the difference between spatial scales of the eddy covariance footprint and the single column simulation of Noah-MP, the results suggest that the improvement in soil parameterization with effects of stone content can significantly advance estimates of ET in the natural settings using Land Surface Models.

## 4.5. Conclusions

Performance of Noah-MP in simulating soil moisture and evapotranspiration was evaluated using various representations of soil and stone content. These revealed mixed influences of stones and soil details for simulating measured soil moisture with better results generally coming from more detailed information. Results showed significant enhancement in the ability to simulate soil moisture as well as evapotranspiration with improved soil parameters in Noah-MP LSM. Distinct bias in simulated soil moisture was observed while accounting for the presence of stone fragments. On the other hand, accounting for stone content improved the evapotranspiration estimates using Noah-MP as well as the HYDRUS-1D numerical model. Both models are dependent on parameter sets with combinations of alternative equations for different processes. Nevertheless, HYDRUS-1D with more detailed soil parametrization was able to simulate the soil moisture with greater accuracy for all depths, while significant biases were observed in simulated evapotranspiration as compared to the eddy covariance measurements. Noah-MP on the other hand effectively improved the simulation of evapotranspiration predicting the closest cumulative value for the simulation period when considering the soil stone content. This suggested the substantial role of stones in modulating soil moisture dynamics and evapotranspiration. Thus, apart from detailed representation of subsurface processes, it is equally important to incorporate the presence of stone content that could possibly have greater impact on soil moisture dynamics and evapotranspiration for larger scale simulations.

**References**

Barlage, M., Tewari, M., Chen, F., Miguez-Macho, G., Yang, Z. L., & Niu, G. Y. (2015). The effect of groundwater interaction in North American regional climate simulations with WRF/Noah-MP. *Climatic Change*, *129*(3-4), 485-498.

Bernstein, L., Bosch, P., Canziani, O., Chen, Z., Christ, R., Davidson, O., ... & Kundzewicz, Z. (2007). Climate change 2007: Synthesis report. Contribution of Working Groups I, II and III to the fourth assessment report of the Intergovernmental Panel on Climate Change. *IPCC: Geneva, Switzerland*.

Bonan, G. B. (2008). Forests and climate change: forcings, feedbacks, and the climate benefits of forests. *science*, *320*(5882), 1444-1449.

Brooks, R. H., & Corey, A. T. (1964). Hydraulic properties of porous media and their relation to drainage design. *Transactions of the ASAE*, *7*(1), 26-0028.

Brutsaert, W., Hsu, A. Y., & Schmugge, T. J. (1993). Parameterization of surface heat fluxes above forest with satellite thermal sensing and boundary-layer soundings. *Journal of Applied Meteorology, 32*(5), 909-917.

Brutsaert, W. (1998). Land-surface water vapor and sensible heat flux: Spatial variability, homogeneity, and measurement scales. *Water Resources Research*, *34*(10), 2433-2442.

Cai, X., Yang, Z. L., David, C. H., Niu, G. Y., & Rodell, M. (2014). Hydrological evaluation of the Noah-MP land surface model for the Mississippi River Basin. *Journal of Geophysical Research: Atmospheres*, *119*(1), 23-38.

Cai, X., Yang, Z. L., Xia, Y., Huang, M., Wei, H., Leung, L. R., & Ek, M. B. (2014a). Assessment of simulated water balance from Noah, Noah-MP, CLM, and VIC over CONUS using the NLDAS test bed. *Journal of Geophysical Research: Atmospheres*, *119*(24).

Chaney, N. W., Wood, E. F., McBratney, A. B., Hempel, J. W., Nauman, T. W., Brungard, C. W., & Odgers, N. P. (2016). POLARIS: A 30-meter probabilistic soil series map of the contiguous United States. *Geoderma*, *274*, 54-67.

Chen, F., & Dudhia, J. (2001). Coupling an advanced land surface–hydrology model with the Penn State–NCAR MM5 modeling system. Part I: Model implementation and sensitivity. *Monthly Weather Review*, *129*(4), 569-585.

Chen, F., Mitchell, K., Schaake, J., Xue, Y., Pan, H. L., Koren, V., ... & Betts, A. (1996). Modeling of land surface evaporation by four schemes and comparison with FIFE observations. *J. of Geophysical Res.: Atmospheres*, *101*(D3), 7251-7268.

Chen, Y., Yang, K., Qin, J., Zhao, L., Tang, W., & Han, M. (2013). Evaluation of AMSR-E retrievals and GLDAS simulations against observations of a soil moisture network on the central Tibetan Plateau. *Journal of Geophysical Research: Atmospheres*, *118*(10), 4466-4475.

Chen, L., Li, Y., Chen, F., Barr, A., Barlage, M., & Wan, B. (2016). The incorporation of an organic soil layer in the Noah-MP land surface model and its evaluation over a boreal aspen forest. *Atmospheric Chemistry and Physics*, *16*(13), 8375-8387.

Clapp, R. B., & Hornberger, G. M. (1978). Empirical equations for some soil hydraulic properties. *Water resources research*, *14*(4), 601-604.

Cosby, B. J., Hornberger, G. M., Clapp, R. B., & Ginn, T. (1984). A statistical exploration of the relationships of soil moisture characteristics to the physical properties of soils. *Water Resources Research*, *20*(6), 682-690.

Cousin, I., Nicoullaud, B., & Coutadeur, C. (2003). Influence of rock fragments on the water retention and water percolation ina calcerous soil. *Catena*(53), 97-114.

Danalatos, N. G., Kosmas, C. S., Moustakas, N. C., & Yassoglou, N. (1995). Rock fragments IL Their impact on soil physical properties and biomass production under Mediterranean conditions. *Soil Use and Management*, *11*(3), 121-126.

Dickinson, R. E., M. Shaikh, R. Bryant, and L. Graumlich (1998), Interactive canopies for a climate model, *J. Clim.*, 11(11), 2823–2836.

Dirmeyer, P. A., (1995). Problems in initializing soil wetness. *Bull. Amer. Meteor. Soc.*, **76**, 2234–2240.

Dirmeyer, P. A., and J. Shukla, (1994). Albedo as a modulator of climate response to tropical deforestation. *J. Geophys. Res.*, **99**, 20 863–20 877.

Dirmeyer, P. A., Gao, X., Zhao, M., Guo, Z., Oki, T., & Hanasaki, N. (2006). GSWP-2: Multimodel analysis and implications for our perception of the land surface. *Bulletin of the American Meteorological Society*, *87*(10), 1381-1397.

Durner, W. (1994). Hydraulic conductivity estimation for soils with heterogeneous pore structure. *Water resources research*, *30*(2), 211-223.

Ek, M. B., K. E. Mitchell, Y. Lin, E. Rogers, P. Grunmann, V. Koren, G. Gayno, and J. D. Tarpley. (2003). Implementation of Noah land surface model advances in the National Centers for Environmental Prediction operational mesoscale Eta model, *J. Geophys. Res*., 108(D22), 8851, doi: 10.1029/2002JD003296.

Fellows, Aaron W.; Flerchinger, Gerald N.; Seyfried, Mark S.; and Lohse, Kathleen. (2017). *Data for Partitioned Carbon and Energy Fluxes Within the Reynolds Creek*

*Critical Zone Observatory*[Data set]. Retrieved from https://doi.org/10.18122/B2TD7V

Food and Agriculture Organization (FAO) (1991) *The digitised soil map of the World* (release 1.0). Report no. 67/1. Food and Agriculture Organization of the United Nations, Rome.

Garratt, J. R. (1994). Review: the atmospheric boundary layer. *Earth-Science Reviews*, *37*(1-2), 89-134.

Gao, Y., Li, K., Chen, F., Jiang, Y., & Lu, C. (2015). Assessing and improving Noah-MP land model simulations for the central Tibetan Plateau. Journal of Geophysical Research: Atmospheres, 120(18), 9258-9278.

Gayler, S., Ingwersen, J., Priesack, E., Wöhling, T., Wulfmeyer, V., & Streck, T. (2013). Assessing the relevance of subsurface processes for the simulation of evapotranspiration and soil moisture dynamics with CLM3. 5: comparison with field data and crop model simulations. *Environmental earth sciences*, *69*(2), 415-427.

Gayler, S., Wöhling, T., Grzeschik, M., Ingwersen, J., Wizemann, H. D., Warrach-Sagi, K., ... & Wulfmeyer, V. (2014). Incorporating dynamic root growth enhances the performance of Noah-MP at two contrasting winter wheat field sites. *Water Resources Research*, *50*(2), 1337-1356.

Goodrich, D. C., T. J. Schmugge, T. J. Jackson, C. L. Unkrich, T. O. Keefer, R. Parry, L. B. Bach, and S. A. Am, 1994: Runoff simulation sensitivity to remotely sensed initial soil water content. *Water Resour. Res.*, **30**, 1393–1405.

Heathman, G. C., M. Larose, M. H. Cosh, and R. Bindlish, (2009). Surface and profile soil moisture spatio-temporal analysis during an excessive rainfall period in the southern Great Plains, USA. Catena, 78, 159–169

Hengl, T., de Jesus, J. M., Heuvelink, G. B., Gonzalez, M. R., Kilibarda, M., Blagotić, A., ... & Guevara, M. A. (2017). SoilGrids250m: Global gridded soil information based on machine learning. *PLoS one*, *12*(2), e0169748.

Ke, Y., Leung, L. R., Huang, M., & Li, H. (2013). Enhancing the representation of subgrid land surface characteristics in land surface models. *Geoscientific Model Development*, *6*(5), 1609-1622.

Kemper, W. D., Nicks, A. D., & Corey, A. T. (1994). Accumulation of water in soils under gravel and sand mulches. *Soil Science Society of America Journal*, *58*(1), 56-63.

Koster, R. D., & Suarez, M. J. (1992). A comparative analysis of two land surface heterogeneity representations. *Journal of Climate*, *5*(12), 1379-1390.

Koster, R. D., Sud, Y. C., Guo, Z., Dirmeyer, P. A., Bonan, G., Oleson, K. W., ... & Kowalczyk, E. (2006). GLACE: the global land–atmosphere coupling experiment. Part I: overview. *Journal of Hydrometeorology*, *7*(4), 590-610.

Koster, R. D., Guo, Z., Yang, R., Dirmeyer, P. A., Mitchell, K., & Puma, M. J. (2009). On the nature of soil moisture in land surface models. *Journal of Climate*, *22*(16), 4322-4335.

Kumar, A., Chen, F., Barlage, M., Ek, M. B., & Niyogi, D. (2014). Assessing impacts of integrating MODIS vegetation data in the weather research and forecasting (WRF) model coupled to two different canopy-resistance approaches. *Journal of Applied Meteorology and Climatology*, *53*(6), 1362-1380.

Li, H., Wigmosta, M. S., Wu, H., Huang, M., Ke, Y., Coleman, A. M., & Leung, L. R. (2013). A physically based runoff routing model for land surface and earth system models. *Journal of Hydrometeorology*, *14*(3), 808-828.

Long, D., Longuevergne, L., & Scanlon, B. R. (2014). Uncertainty in evapotranspiration from land surface modeling, remote sensing, and GRACE satellites. *Water Resources Research*, *50*(2), 1131-1151.

Mahrt, L., & Ek, M. (1984). The influence of atmospheric stability on potential evaporation. *Journal of Climate and Applied Meteorology*, *23*(2), 222-234.

Monteith, J.L., 1973. Principles of Environmental Physics. Arnold, London, 241 pp.

Niu, G.-Y., Z.-L. Yang, R. E. Dickinson, and L. E. Gulden (2005), A simple TOPMODEL-based runoff parameterization (SIMTOP) for use in global climate models, *J. Geophys. Res.*, 110, D21106, doi:10.1029/2005JD006111.

Niu, G.-Y., Z.-L. Yang, R. E. Dickinson, L. E. Gulden, and H. Su (2007), Development of a simple groundwater model for use in climate models and evaluation with Gravity Recovery and Climate Experiment data, *J. Geophys. Res.*, 112, D07103, doi:10.1029/2006JD007522.

Niu, G. Y., Z. L. Yang, K. E. Mitchell, F. Chen, M. B. Ek, M. Barlage, A. Kumar, K. Manning, D. Niyogi, E. Rosero, M. Tewari, and Y. L. Xia. 2011. The community Noah land surface model with multiparameterization options (Noah-MP): 1. Model description and evaluation with local-scale measurements. *Journal of Geophysical Research-Atmospheres* **116**: D12109.

Novák, V., & Kňava, K. (2012). The influence of stoniness and canopy properties on soil water content distribution: simulation of water movement in forest stony soil. *European Journal of Forest Research*, *131*(6), 1727-1735.

Novák, V., & Šurda, P. (2010). The water retention of a granite rock fragments in High Tatras stony soils. *Journal of Hydrology and Hydromechanics*, *58*(3), 181-187.

Oleson, K., Lawrence, D., Bonan, G., Drewniak, B., Huang, M., Koven, C., ... & Swenson, S. (2013). Technical description of version 4.5 of the Community Land Model (CLM), 420 pp., doi: 10.5065.

Parajuli, K., Sadeghi, M., & Jones, S. B. (2017). A binary mixing model for characterizing stony-soil water retention. *Agricultural and Forest Meteorology*, *244*, 1-8.

Poltoradnev, M., Ingwersen, J., Imukova, K., Högy, P., Wizemann, H. D., & Streck, T. (2018). How well does Noah-MP simulate the regional mean and spatial variability of topsoil water content in two agricultural landscapes in southwest Germany?. *Journal of Hydrometeorology*, *19*(3), 555-573.

Patton, Nicholas R.; Lohse, Kathleen A.; Godsey, Sarah E.; Seyfried, Mark S.; and Crosby, Benjamin T. (2017). *Dataset for Predicting Soil Thickness on Soil Mantled Hillslopes* [Data set]. Retrieved from https://doi.org/10.18122/B2PM69

Penman, H.L., 1953. The physical basis of irrigation control. 13th Int. Hort. Congr., Vol. 2, pp. 913-923.

Raats, P. A., & Knight, J. (2018). The contributions of Lewis Fry Richardson to drainage theory, soil physics, and the soil-plant-atmosphere continuum. *Frontiers in Environmental Science*, *6*, 13.

Ryu, S. R., Chen, J., Noormets, A., Bresee, M. K., & Ollinger, S. V. (2008). Comparisons between PnET-Day and eddy covariance based gross ecosystem production in two Northern Wisconsin forests. *Agricultural and forest meteorology*, *148*(2), 247-256.

Schaap, M.G., F.J. Leij, and M. Th. van Genuchten. 2001. Rosetta: a computer program for estimating soil hydraulic parameters with hierarchical pedotransfer functions. *Journal of Hydrology*. 251:163-176.

Schaap, M.G. and W. Bouten. 1996. Modeling water retention curves of sandy soils using neural networks. *Water Resour. Res*. 32:3033-3040.

Schaap, M.G., Leij F.J. and van Genuchten M.Th. 1998. Neural network analysis for hierarchical prediction of soil water retention and saturated hydraulic conductivity. *Soil Sci. Soc. Am. J.* 62:847-855.

Senay, G. B., Leake, S., Nagler, P. L., Artan, G., Dickinson, J., & Glenn, J. T. (2011). Estimating basin scale evapotranspiration (ET) by water balance and remote sensing methods. *Hydrological Processes, 25*, 4037-4049.

Sheffield, J., Wood, E. F., & Arriola, F. M. (2010). Long-Term Regional Estimates of Evapotranspiration for Mexico Based on Downscaled ISCCP Data. *Journal of Hydrometeorology, 11*, 253-275.

Shrestha, S., Khatiwada, M., Babel, M. S., & Parajuli, K. (2014). Impact of climate change on river flow and hydropower production in Kulekhani hydropower project of Nepal. *Environmental Processes*, *1*(3), 231-250.

Šimůnek, J., Van Genuchten, M. T., & Šejna, M. (2016). Recent developments and applications of the HYDRUS computer software packages. *Vadose Zone Journal*, *15*(7).

van Genuchten, M. T. (1980). A closed-form equation for predicting the hydraulic conductivity of unsaturated soils. *Soil Science Society of America Journal*, 44, 892-898.

Xia, Y., and Coauthors, 2014: Evaluation of multi-model simulated soil moisture in NLDAS-2. *J. Hydrol*., **512**, 107–125

Xue, B.-L., and Coauthors, 2013: Modeling the land surface water and energy cycles of a mesoscale watershed in the central Tibetan Plateau during summer with a distributed hydrological model. *J. Geophys. Res. Atmos*., **118**, 8857–8868

Yang, Z.-L., and G.-Y. Niu (2003), The versatile integrator of surface and atmosphere processes: Part 1. Model description, *Global Planet. Change,* 38(1–2), 175–189, doi:10.1016/S0921-8181(03)00028-6.

Yang, K., Koike, T., Ye, B., & Bastidas, L. (2005). Inverse analysis of the role of soil vertical heterogeneity in controlling surface soil state and energy partition. *Journal of Geophysical Research: Atmospheres*, *110*(D8).

Yang, Z. L., G. Y. Niu, K. E. Mitchell, F. Chen, M. B. Ek, M. Barlage, L. Longuevergne, K. Manning, D. Niyogi, M. Tewari, and Y. L. Xia. 2011. The community Noah land surface model with multiparameterization options (Noah-MP): 2. Evaluation over global river basins. *Journal of Geophysical Research-Atmospheres* **116**: D12110.

Zheng, D., van der Velde, R., Su, Z., Wang, X., Wen, J., Booij, M. J., ... & Chen, Y. (2015). Augmentations to the Noah model physics for application to the Yellow River source area. Part I: Soil water flow. *Journal of hydrometeorology*, *16*(6), 2659-2676.

Zheng, D., R. van der Velde, Z. Su, X. Wang, J. Wen, M. J. Booij, A. Y. Hoekstra, and Y. Chen. (2015a). Augmentations to the Noah model physics for application to the Yellow River source area. Part II: Turbulent heat fluxes and soil heat

transport. *J. Hydrometeor.*, **16**, 2677–2694, doi:https://doi.org/10.1175/JHM-D-14-0199.1.

Zheng, D., Van Der Velde, R., Su, Z., Wen, J., & Wang, X. (2017). Assessment of Noah land surface model with various runoff parameterizations over a Tibetan river. *Journal of Geophysical Research: Atmospheres*, *122*(3), 1488-1504.

**Fig. 4.1.** Distribution of stone content along the depth visible from the soil pit dug during the installation of sensors at low sage station of Reynolds creek watershed.

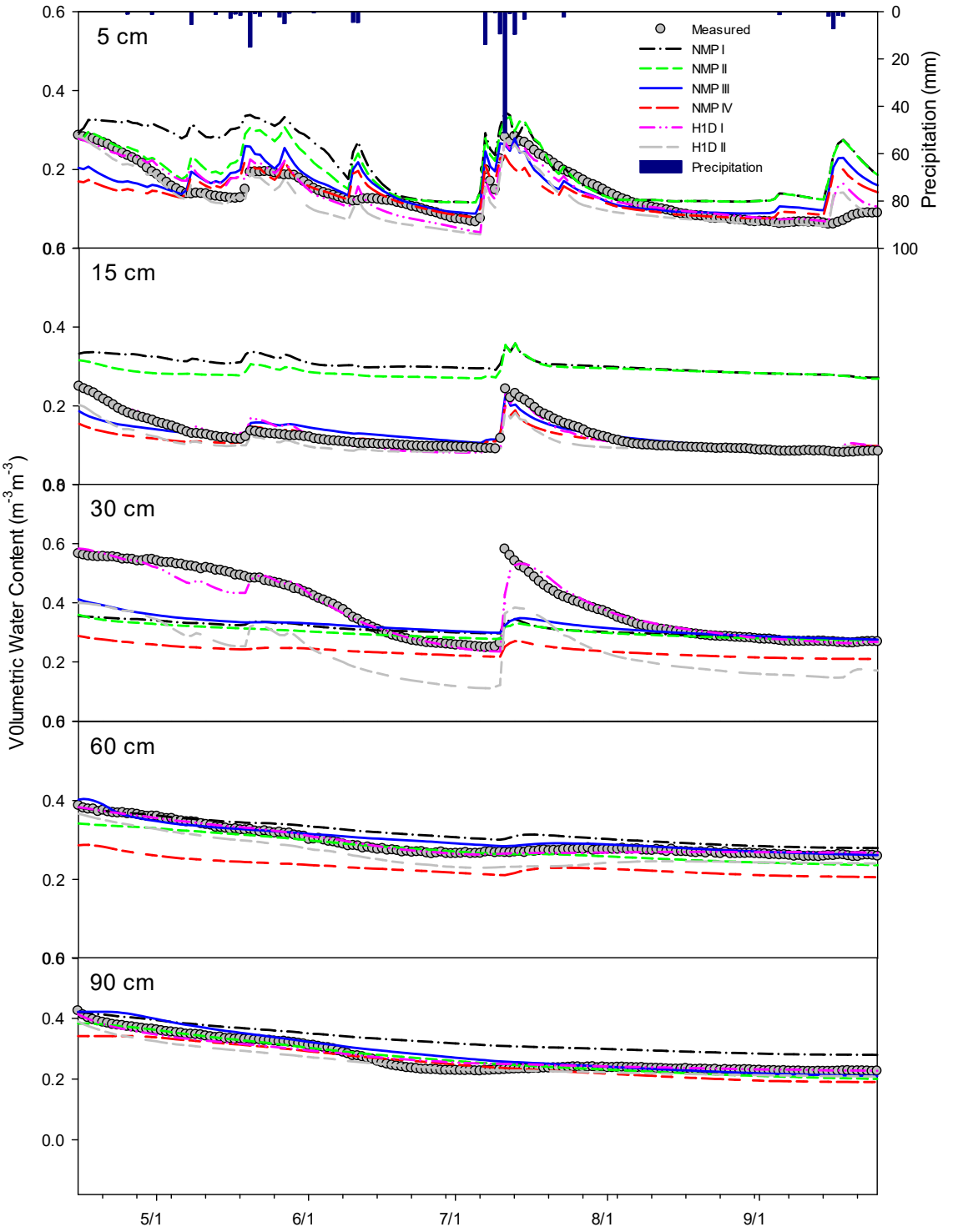


**Fig. 4.2.** Comparison of the daily average of Hydraprobe measured soil moisture and simulations produced by four Noah-MP (NMP I, NMP II, NMP III, NMP IV) and two HYDRUS-1D (H1D I, H1D II) simulations as described in Table 4.2, at depths; 5, 15, 30, 60 and 90 cm along with observed daily precipitation from 15 April to 28 September 2015.

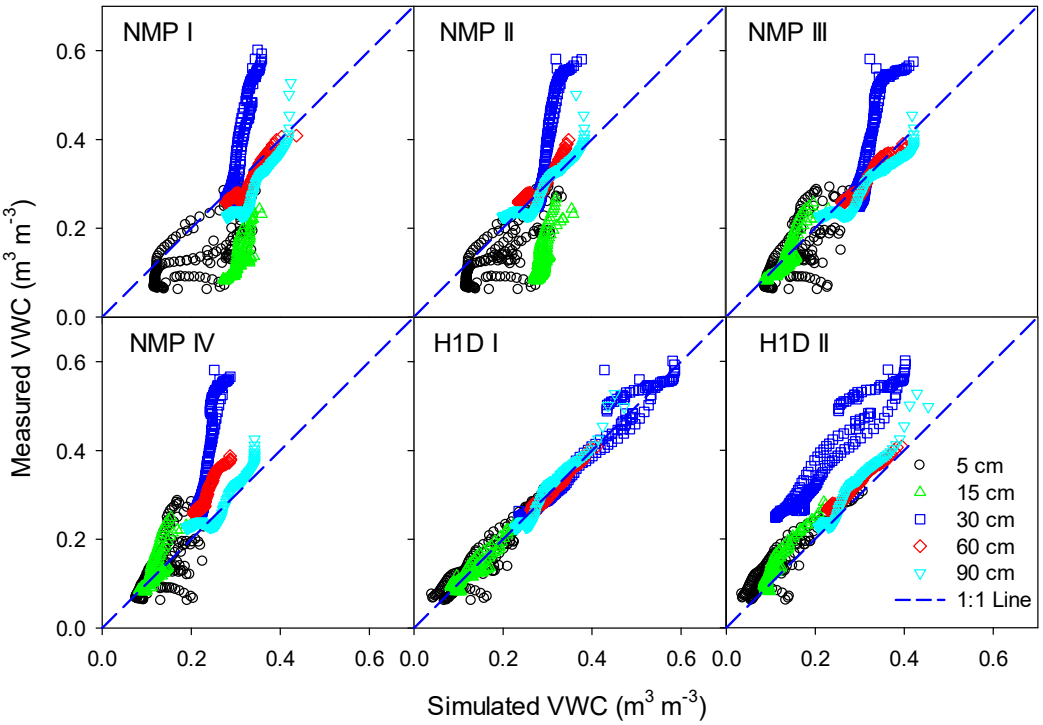


**Fig. 4.3**. Scatter plots between Hydraprobe measured and simulated soil moisture at 5, 15, 30, 60 and 90 cm depth. Four different Noah-MP land surface models were carried out along with two HYDRUS-1D numerical model simulations as described in Table 4.2.

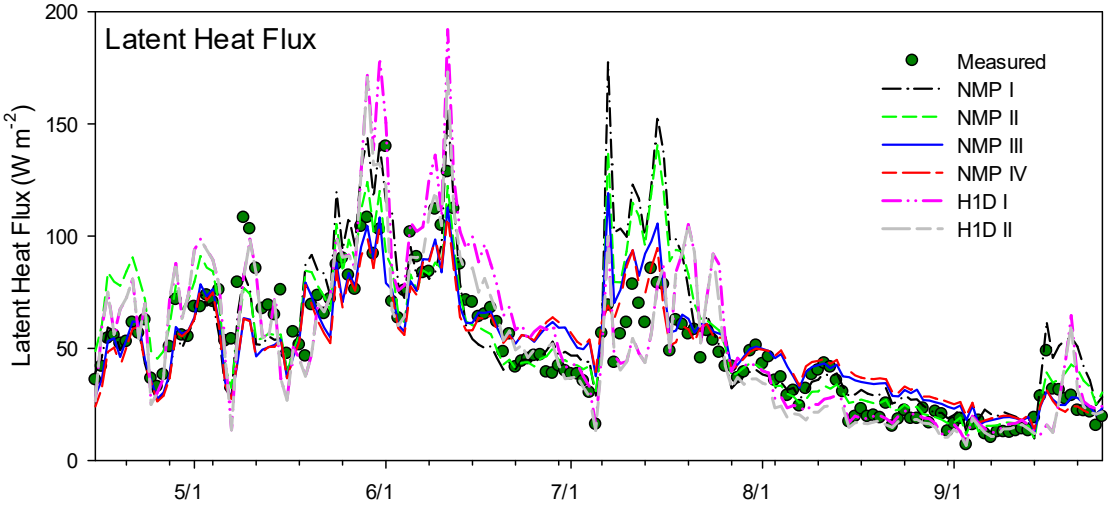


**Fig. 4.4.** Time series of the eddy covariance measured latent heat flux and estimated by four Noah-MP and two HYDRUS-1D simulations as mentioned in Table 4.2.

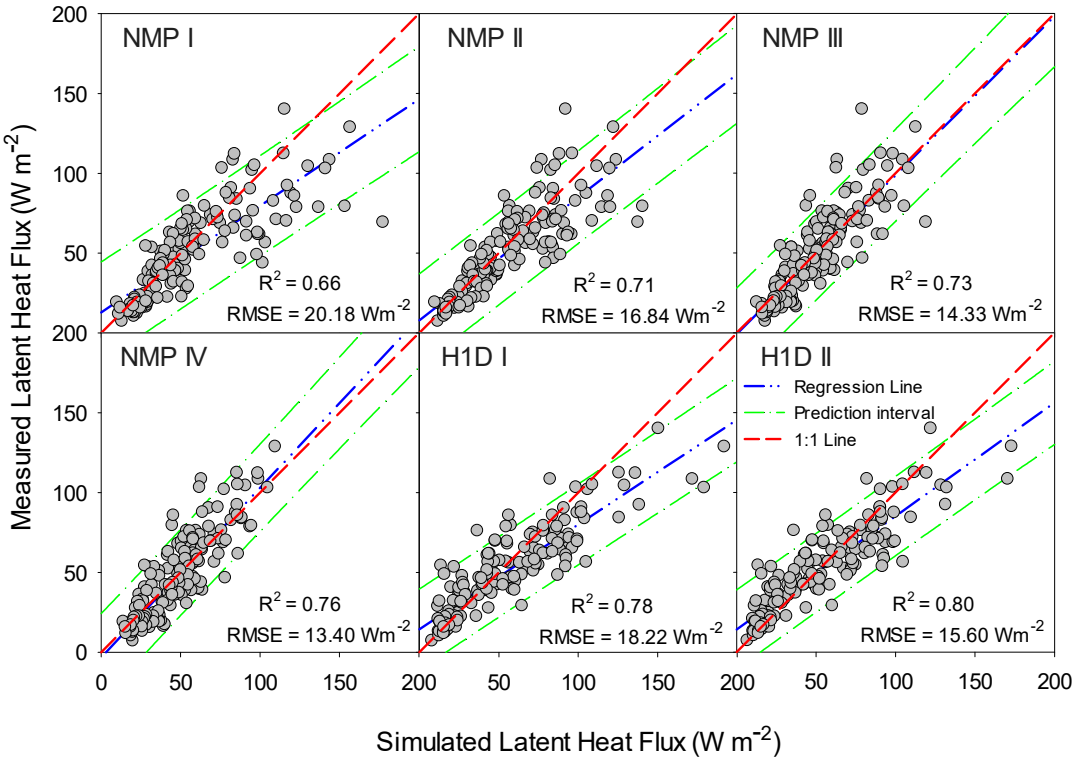


**Fig. 4.5.** Scatter plots between eddy covariance measured latent heat flux and estimated by four Noah-MP and two HYDRUS-1D simulations (Table 4.2). Regression lines and prediction intervals with 95% confidence are also shown. Root mean square error (RMSE) and coefficient of determination ($R^2$) computed between measured and simulated latent heat flux are reported as well.

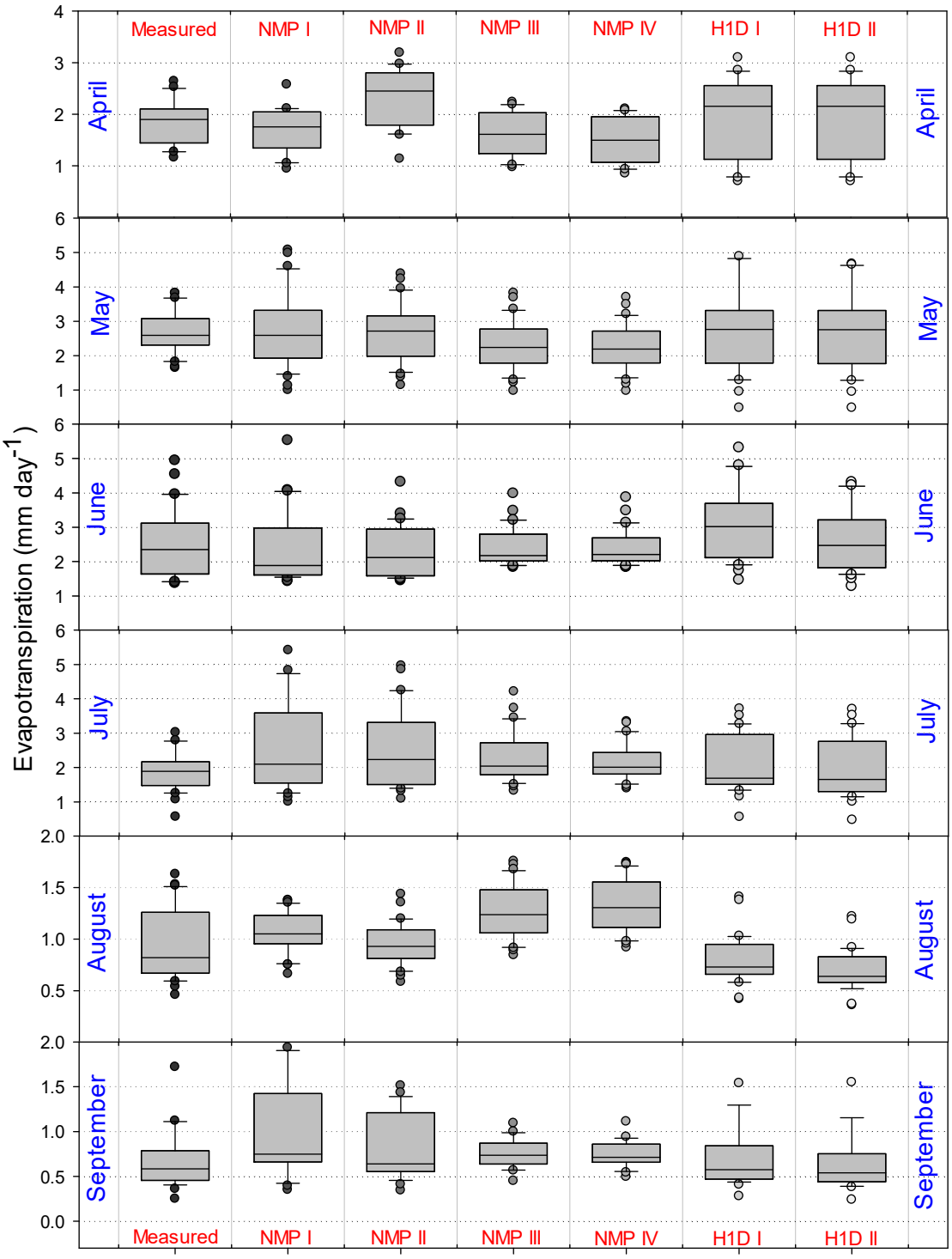


**Fig. 4.6.** Box plots showing daily evapotranspiration for each month during the simulation period (15 Apr – 28 Sep 2018) for the four Noah-MP and two HYDRUS-1D simulations (Table 4.2), along with eddy covariance system measurements at the lower sage station.

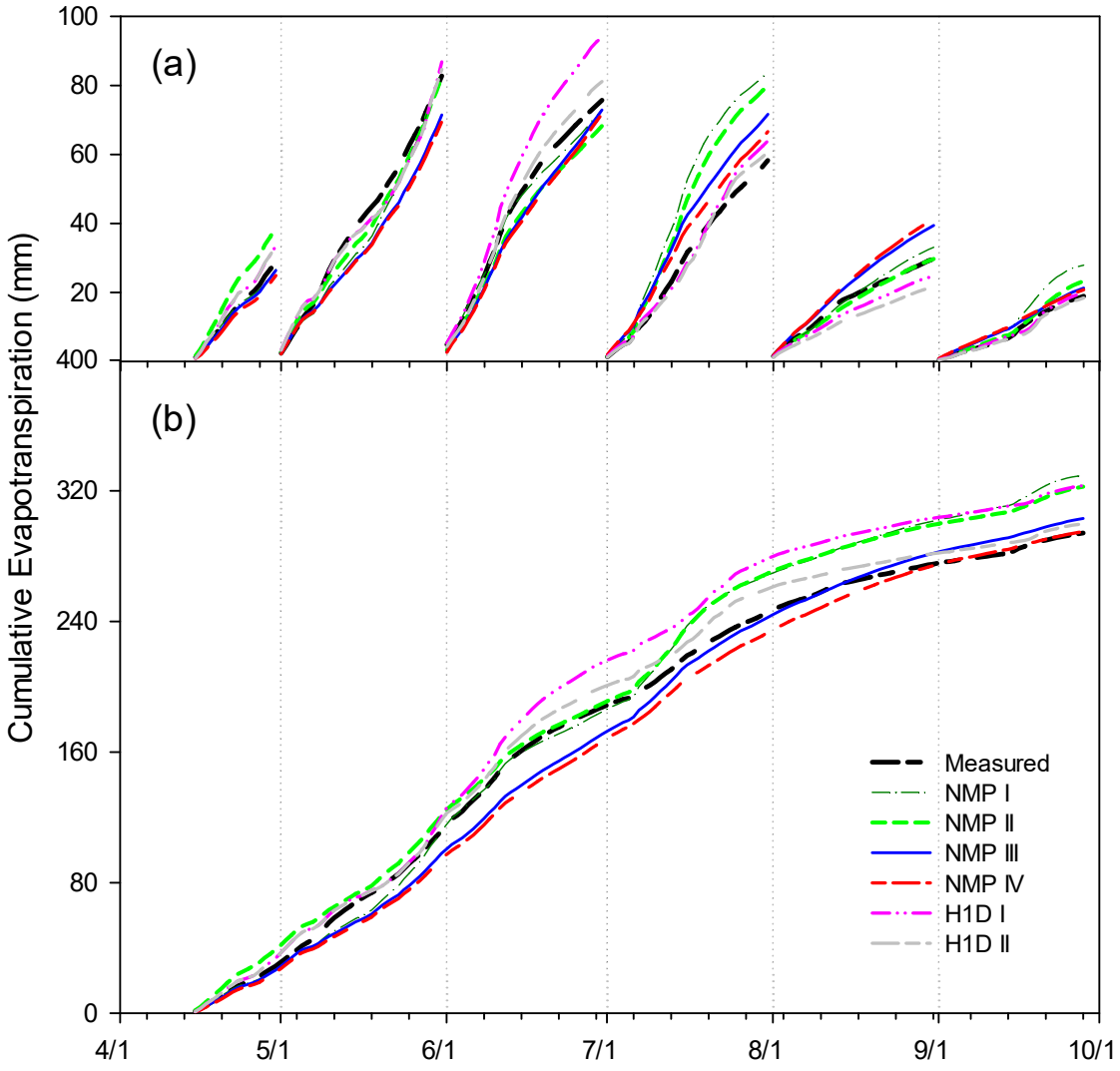


**Fig. 4.7.** Cumulative (a) monthly and (b) seasonal evapotranspiration measured by eddy covariance compared with the four Noah-MP two HYDRUS-1D simulations (Table 4.2) for the simulation period (15 Apr – 28 Sep 2018).

**Table 4.1.** Soil texture descriptions within the soil profile at the low sage site at Reynolds Creek Watershed. Soil bulk density listed is for the fine soil fraction without stone.

| Depth (cm) | Sand (%) | Silt (%) | Clay (%) | USDA Textural Class | Soil Bulk Density ($g/cm^3$) | Volumetric Stone Content ($m^3m^{-3}$) |
|---|---|---|---|---|---|---|
| 0-6 | 41 | 31 | 28 | Clay Loam | 0.848 | 0.27 |
| 6-20 | 25 | 34 | 41 | Clay | 1.173 | 0.17 |
| 20-31 | 23 | 32 | 45 | Clay | 0.813 | 0.38 |
| 31-80 | 54 | 5 | 41 | Sandy Clay | 1.355 | 0.39 |
| 80-135 | 53 | 23 | 24 | Sandy Clay Loam | 1.433 | 0.29 |

**Table 4.2.** Summary of the numerical experiments performed in this study.

| Numerical Experiment | Model | No. of Soil Materials | Parametrization Method | Stone Inclusion |
|---|---|---|---|---|
| NMP I | Noah-MP | 1 | Lookup table | No |
| NMP II | Noah-MP | 5 | Lookup table | No |
| NMP III | Noah-MP | 5 | Pedotransfer function | No |
| NMP IV | Noah-MP | 5 | Pedotransfer function | Yes |
| H1D I | HYDRUS-1D | 5 | Inverse Simulation | No |
| H1D II | HYDRUS-1D | 5 | Inverse Simulation | Yes |

**Table 4.3.** Root mean square error (RMSE) and coefficient of determination ($R^2$) computed between measured and simulated soil moisture at 5, 15, 30, 60 and 90 cm depth produced by four Noah-MP simulations (NMP I, NMP II, NMP III and NMP IV) and two HYDRUS-1D simulations (H1D I, H1D II) as described in Table 4.2.

| Measures | Depth (cm) | NMP I | NMP II | NMP III | NMP IV | H1D I | H1D II |
|---|---|---|---|---|---|---|---|
| RMSE ($m^3 m^{-3}$) | 5 | 0.09 | 0.06 | 0.05 | 0.05 | 0.03 | 0.03 |
| | 15 | 0.18 | 0.17 | 0.02 | 0.03 | 0.01 | 0.03 |
| | 30 | 0.11 | 0.12 | 0.10 | 0.17 | 0.02 | 0.15 |
| | 60 | 0.03 | 0.02 | 0.01 | 0.06 | 0.01 | 0.03 |
| | 90 | 0.06 | 0.02 | 0.02 | 0.03 | 0.01 | 0.02 |
| | **Mean** | **0.09** | **0.08** | **0.04** | **0.07** | **0.02** | **0.05** |
| $R^2$ | 5 | 0.51 | 0.59 | 0.45 | 0.43 | 0.81 | 0.82 |
| | 15 | 0.68 | 0.50 | 0.80 | 0.71 | 0.88 | 0.87 |
| | 30 | 0.88 | 0.89 | 0.84 | 0.89 | 0.95 | 0.90 |
| | 60 | 0.91 | 0.89 | 0.93 | 0.96 | 0.97 | 0.96 |
| | 90 | 0.93 | 0.91 | 0.92 | 0.89 | 0.95 | 0.96 |
| | **Mean** | **0.78** | **0.76** | **0.79** | **0.78** | **0.91** | **0.90** |

# CHAPTER 5

# SUMMARY, CONCLUSIONS AND RECOMMENDATIONS

This dissertation has quantified and accounted for the effect of stone content in montane soil ecosystems and evaluated its influence on estimation of actual evapotranspiration ($ET_A$) using one-dimensional numerical- and land surface-models. Chapters 2 through 4 presented the main scientific results of this dissertation. In this chapter, the important conclusions from these chapters are summarized with recommendations regarding the future directions and opportunities for research.

## 5.1. Summary

After introducing the dissertation topic in chapter 1, we determined the water retention curve (WRC) of soil, stone and stone-soil mixtures with varied volumetric stone content in chapter 2 to better understand the effect of stone content on soil hydraulic properties. The measured WRC for seven different stone types showed maximum and minimum saturated water contents of 0.55 $m^3$ $m^{-3}$ in pumice and 0.025 $m^3$ $m^{-3}$ in fine sandstone, respectively. Contrasting scenarios were studied considering a broad range of stone inclusions; (*i*) negligibly porous, (*ii*) significantly porous but less porous than the background soil, and (*iii*) more porous than the background soil. Our experimental data along with the numerical simulations demonstrated that stones can play an important role in the bulk stony-soil water retention characteristic. An averaging scheme based on individual water retention properties of stone fragments and of the soil matrix was introduced and tested using laboratory measurements with three distinct stone types embedded in a background soil matrix at various volumetric stone contents ($v$ = 0, 0.05,

0.1, 0.2, 0.3, 0.4 and 1). All WRC measurements demonstrated the extent to which the stone fragments contributed to water retention and water holding capacity of the stony soil. Stones exhibiting low porosity contribute less to water retention than the background soil matrix leading to a reduction in water retention with increasing volumetric stone content. However, the bulk stony soil water retention may increase significantly with increasing volume fraction of stones exhibiting high porosity such as with pumice. Hence, chapter 1 examines how stones present in soil, alter the effective hydraulic properties (particularly water holding capacity). A binary mixing model accounting for the effect of stone content on the resulting WRC for bulk stony soil was also introduced.

Chapter 3 described numerical model adjustments made for simulating $ET_A$ of stony soil in montane ecosystems, accounting for the water retention properties of soil stones. A numerical model (HYDRUS-1D) was employed to simulate $ET_A$ in natural settings in northern Utah and southern Idaho during the growing seasons of 2015 and 2016 based on meteorological and soil moisture measurements through a range of depths, adding information about volumetric stone content within the soil profile. The $ET_A$ was simulated under three different scenarios, considering soil with (i) no stones, (ii) highly porous stones, and (iii) negligibly porous stones. The simulation results showed significant overestimation of modeled $ET_A$ when neglecting stones, in comparison to $ET_A$ measured by eddy covariance. The modeled $ET_A$ assuming negligibly porous stones was much lower in all stations than estimates made considering highly porous stones due to the substantial decrease in soil water storage. The simulated root water uptake from stony soil was found to be sensitive to stone content, showing significant reductions in cumulative simulated $ET_A$ over the simulation period up to 30 percent of the total $ET_A$ computed without

accounting for the stone content. Assumptions of highly porous or negligibly porous stones in the soil, lead to reductions in simulated $ET_A$ of between 10% and 30%, respectively, when compared with the 'no stones' condition. The $ET_A$ was least affected when considering soil with highly porous stones, while the estimates were reduced significantly for stations with higher average stone content, when considering soil with negligibly porous stones.

Chapter 4, evaluated the performance of Noah-MP in simulating soil moisture and $ET_A$ by different numerical simulations. The numerical simulations were designed by representing the soil profile using five layers with; (i) single soil type and default parameter settings using different soil types for each layer, (ii) default soil parameters based on textural class, (iii) improved soil parameters from field observation and (iv) adjusted parameters accounting for stones. Additional simulations were performed using the HYDRUS-1D numerical model employing more detailed representation of soil hydraulic functions. These included; (i) neglecting the presence of stones and (ii) considering the effect of stone content. Results showed significant enhancement in the ability to simulate soil moisture as well as evapotranspiration with improved soil parameters in the Noah-MP LSM. Distinct bias in simulated soil moisture was observed while accounting for the presence of stone fragments. Accounting for stone content also improved the evapotranspiration estimates using Noah-MP as well as the HYDRUS-1D numerical model. Both models are dependent on parameter sets with combinations of alternative equations for different processes. The HYDRUS-1D model using more detailed soil parametrization was able to simulate soil moisture with greater accuracy, while significant biases were observed in simulated evapotranspiration as compared to the eddy covariance

measurements. Noah-MP on the other hand, effectively improved the simulation of evapotranspiration predicting the closest cumulative value for the simulation period when considering the soil stone content.

## 5.2. Conclusions

This dissertation examined the impact of stone content on soil hydraulic properties and facilitated incorporation of the developed concepts into the numerical and land surface models for estimation of $ET_A$ in montane ecosystems. Based on the research presented in chapters 2 – 4, the following conclusions are drawn:

i) Water retention curves estimated without considering stone water holding capacity may underestimate the water retention for stony soil with highly porous stones such as pumice and coarse sandstone.

ii) Stone hydraulic properties (i.e., porosity, pore-size distribution, etc.) must be accounted to better estimate stony soil hydraulic properties.

iii) Significant reductions in root water uptake might be expected due to the presence of stones with low porosity.

iv) The numerical simulation of $ET_A$ under different assumptions revealed the important role played by stones, common in many forest soils, in modulating water balance by affecting $ET_A$ in montane ecosystems.

v) The Noah-MP model informed with stone content information and using detailed soil properties, provided the best prediction of $ET_A$.

vi) Improvement in representation of soil properties along with stone content information can substantially improve the ability of land surface models to simulate soil water flow and $ET_A$.

### 5.3. Recommendations

As most forest soils are dominated by significant stone content, there is a need to expand studies on stony soils, emphasizing stone porosity and the fraction of stone content in order to better estimate the resulting stony soil hydraulic properties. Developing more accurate averaging schemes to estimate the WRC (e.g., under non-equilibrium condition) as well as predictive models for unsaturated hydraulic conductivity of stony soils should become an integral part of future research on numerical- and land surface-models.

Numerical models could be the best way to estimate $ET_A$ based on meteorological and soil moisture data where the advanced measurements (i.e., eddy covariance) are not available. More work is needed to address the spatial as well as vertical heterogeneity of soil including effects of stone content in stone-dominated soils common in montane ecosystems. We suggest it will become more important that soil surveys properly represent soil heterogeneity with better quantification of stone hydraulic properties. Further studies should also focus on investigating the effect of stone content on soil moisture sensors resulting in improvement in sensor placement and measurement approaches for stony soils. Soil map information should also take advantage of the latest databases to better account for variations in soil texture and stone content to improve land surface model simulations of $ET_A$ at regional scales. Higher resolution soil information and detailed sub-surface

processes are recommended for better simulations of soil moisture as well as boundary fluxes which could potentially improve studies focusing on land atmosphere interactions.

# APPENDICES

(Coauthors' approval letters)

Kshitij Parajuli
Utah State University
Civil and Environmental Engineering
4110 Old Main Hill
Logan, UT 84322-4110

07-20-2018

Gerald N Flerchinger
Research Hydraulic Engineer
USDA-ARS
Boise, Idaho
gerald.flerchinger@ars.usda.gov

Dear Dr. Flerchinger,

I am in the process of preparing my dissertation in the civil and environmental engineering department at Utah State University. I hope to complete my degree program in August 2018.

I am requesting your permission to include the attached paper of which you are coauthor as a chapter in my dissertation. I will include acknowledgments to your contribution as indicated. Please advise me of any changes you require.

Please indicate your approval of this request by signing in the space provided, attaching any other form or instruction necessary to confirm permission. If you have any questions, please contact me. I hope you will be able to reply immediately.

Thank you for your cooperation.

Yours Sincerely

Kshitij Parajuli

---

I hereby give permission to Kshitij Parajuli to use and reprint all of the material I have contributed to chapter 3 and chapter 4 of this dissertation.

Gerald N Flerchinger

Kshitij Parajuli
Utah State University
Civil and Environmental Engineering
4110 Old Main Hill
Logan, UT 84322-4110

07-20-2018

Morteza Sadeghi
Research Assistant Professor
Utah State University
Logan, Utah
morteza.sadeghi@usu.edu

Dear Dr. Sadeghi,

I am in the process of preparing my dissertation in the civil and environmental engineering department at Utah State University. I hope to complete my degree program in August 2018.

I am requesting your permission to include the attached paper of which you are coauthor as a chapter in my dissertation. I will include acknowledgments to your contribution as indicated. Please advise me of any changes you require.

Please indicate your approval of this request by signing in the space provided, attaching any other form or instruction necessary to confirm permission. If you have any questions, please contact me. I hope you will be able to reply immediately.

Thank you for your cooperation.

Yours Sincerely

Kshitij Parajuli

---

I hereby give permission to Kshitij Parajuli to use and reprint all of the material I have contributed to chapter 2 and chapter 4 of this dissertation.

Morteza Sadeghi

Kshitij Parajuli
Utah State University
Civil and Environmental Engineering
4110 Old Main Hill
Logan, UT 84322-4110

07-20-2018

Lin Zhao
Northwest Institute of Eco-Environment and Resources
Chinese Academy of Sciences
Lanzhou, Gansu, China
zhaolin_110@lzb.ac

Dear Dr. Zhao,

I am in the process of preparing my dissertation in the civil and environmental engineering department at Utah State University. I hope to complete my degree program in August 2018.

I am requesting your permission to include the attached paper of which you are coauthor as a chapter in my dissertation. I will include acknowledgments to your contribution as indicated. Please advise me of any changes you require.

Please indicate your approval of this request by signing in the space provided, attaching any other form or instruction necessary to confirm permission. If you have any questions, please contact me. I hope you will be able to reply immediately.

Thank you for your cooperation.

Yours Sincerely

Kshitij Parajuli

---

I hereby give permission to Kshitij Parajuli to use and reprint all of the material I have contributed to chapter 4 of this dissertation.

_____

Lin Zhao

Kshitij Parajuli
Utah State University
Civil and Environmental Engineering
4110 Old Main Hill
Logan, UT 84322-4110

07-20-2018

Mark S Seyfried
Soil Scientist
USDA-ARS
Boise, Idaho
mark.seyfried@ars.usda.gov

Dear Dr. Seyfried,

I am in the process of preparing my dissertation in the civil and environmental engineering department at Utah State University. I hope to complete my degree program in August 2018.

I am requesting your permission to include the attached paper of which you are coauthor as a chapter in my dissertation. I will include acknowledgments to your contribution as indicated. Please advise me of any changes you require.

Please indicate your approval of this request by signing in the space provided, attaching any other form or instruction necessary to confirm permission. If you have any questions, please contact me. I hope you will be able to reply immediately.

Thank you for your cooperation.

Yours Sincerely

Kshitij Parajuli

---

I hereby give permission to Kshitij Parajuli to use and reprint all of the material I have contributed to chapter 3 of this dissertation.

_____

Mark S Seyfried

ELSEVIER

Dear Kshitij Parajuli

We hereby grant you permission to reproduce the publication, "Parajuli K., Sadeghi. M., Jones S. B. (2017). A Binary Mixing Model for Characterizing Stony-Soil Water Retention. *Agricultural and Forest Meteorology*, 244, pp 1-8", at no charge **in your thesis, in print and on Digitalcommon** and subject to the following conditions:

1. If any part of the material to be used (for example, figures) has appeared in our publication with credit or acknowledgement to another source, permission must also be sought from that source. If such permission is not obtained then that material may not be included in your publication/copies.

2. Suitable acknowledgment to the source must be made, either as a footnote or in a reference list at the end of your publication, as follows:

   "This article was published in Publication title, Vol number, Author(s), Title of article, Page Nos, Copyright Elsevier (or appropriate Society name) (Year)."

3. Your thesis may be submitted to your institution in either print or electronic form.

4. Reproduction of this material is confined to the purpose for which permission is hereby given.

5. This permission is granted for non-exclusive world **English** rights only. For other languages please reapply separately for each one required. Permission excludes use in an electronic form other than as specified above. Should you have a specific electronic project in mind please reapply for permission.

6. This includes permission for UMI to supply single copies, on demand, of the complete thesis. Should your thesis be published commercially, please reapply for permission.

Yours sincerely

Jennifer Jones
Permissions Specialist
J.Jones@elsevier.com

CURRICULUM VITAE

**Kshitij (K) Parajuli, Ph.D.**
Civil and Environmental Engineering
Utah State University
parajuli@usu.edu
https://www.linkedin.com/in/kshparajuli/

## EDUCATION

**Ph. D.,** *Utah State University*,
Civil and Environmental Engineering USA (2014 - 2018)

**M. Eng.,** *Asian Institute of Technology*,
Water Engineering and Management Thailand (2011 - 2013)

**B. Eng.,** *Kantipur Eng. College*, *Tribhuvan University,*
Civil Engineering Nepal (2004 - 2009)

## PROFESSIONAL EXPERIENCE

**Research Assistant**, **Aug 2014 - Jul 2018**
Utah State University, Logan, UT, USA

**Research Associate**, **Jun 2013 - May 2014**
Asian Institute of Technology, Thailand

**Visiting Scientist**, **Oct 2012 - Dec 2012**
APEC Climate Center (APCC), Busan, South Korea

**Civil Engineer** (Level-7) **Jun 2011 - Dec 2011**
Nepal Electricity Authority, Kathmandu, Nepal

**Civil Engineer** (Gazzeted, Class III), **Dec 2009 - Jul 2011**
Ministry of Peace and Reconstruction, Government of Nepal

**Civil Engineer**, **Jun 2009 - Dec 2009**
Mailun Khola Hydropower Company (Pvt.) Ltd. Kathmandu, Nepal

## TEACHING AND MENTORING EXPERIENCE

1. **Teaching Assistant**, Utah State University, Faculty: *Scott B. Jones*; Course: Environmental Soil Physics - PSC 5670-6670 (Fall 2016)
2. **Research Mentor**, iUTAH Undergraduate Research Fellows (iFellows), Utah State University. Faculty mentor: *Scott B. Jones*; Student/Institute: *Shanae Tate/Brigham Young University*; Research Title: *The effects of elevation on evapotranspiration*. (May – July 2016)
3. **Research Mentor,** iUTAH Undergraduate Research Fellows (iFellows), Utah State University. Faculty mentor: *Scott B. Jones*; Student/Institute: *Joseph Ipson/Snow College*; Research Title: *Improving evapotranspiration estimates using soil heat flux*. (May – July 2015)

## HONORS, AWARDS, FELLOWSHIPS

| | |
|---|---|
| Outstanding Oral and Poster Presentation, *SSSA Annual Meeting* | 2017 |
| Robert Luxmoore Student Travel Award, *Soil Science Society of America* (SSSA) | 2017 |
| Dissertation Fellowship, *Utah State University* | 2017-18 |
| Graduate Student Leadership Conference, *SSSA* | 2016 |
| Outstanding Oral and Poster Presentation, *SSSA Annual Meeting* | 2016 |
| Outstanding Paper, J. Paul Riley Paper Competition, *AWRA Utah Section* | 2015 |
| Outstanding Paper, *EWRI World Env. & Water Resources Congress* | 2015 |
| Doctoral Fellowship, *iUTAH-EPSCOR, Utah State University* | 2014-17 |
| [Scholarship] CLIM-RUN School, *International Center for Theoretical Physics* | 2013 |
| [Scholarship] Summer School on Coastal Hazards, *Kiel University* | 2013 |
| Nepal Bidhya Bhusan Class ´B´ Gold Medal, *Government of Nepal* | 2013 |
| Hodaka Prize for Outstanding Student, *Asian Institute of Technology (AIT)* | 2013 |
| [Travel scholarship] Exceed Expert Seminar, *Exceed Excellence Center* | 2013 |
| NMFA Thesis Grant, *Asian Institute of Technology* | 2013 |
| [Scholarship] Young Scientist Support Program , *APEC Climate Center* | 2012 |
| Master's Fellowship, *Norwegian Ministry of Foreign Affairs (NMFA) - AIT* | 2011-13 |
| Merit Scholarship, *Kantipur Engineering College* | 2007, 09 |

## PUBLICATIONS

### Scientific Journals (Refereed)

1. **Parajuli, K.,** L. Zhao, S. B. Jones, D. G. Tarboton, M. Sadeghi, L. E. Hipps, A. Torres-Rua, G. N. Flerchinger (2018). Evaluating Noah-MP simulation of soil-moisture, -temperature and surface energy fluxes under different soil parameterization (Manuscript under preparation for *Journal of Hydrometeorology*)
2. **Parajuli, K.,** S. B. Jones, D. G. Tarboton, G. N. Flerchinger, L. E. Hipps, L. N. Allen, M. S. Seyfried (2018). Estimating actual evapotranspiration from stony-soil moisture dynamics in montane ecosystems. *Agricultural and Forest Meteorology,* (Under Review: AGRFORMET-D-18-00585)
3. **Parajuli K.**, Sadeghi. M., Jones S. B. (2017). A Binary Mixing Model for Characterizing Stony-Soil Water Retention. *Agricultural and Forest Meteorology,* 244, pp 1-8
4. Shrestha, S., **Parajuli. K**., Babel. M. S., Dhakal. S., (2015). Water-energy-carbon nexus: A case study of Bangkok, *Water Science and Technology: Water Supply*, 15(5), pp 889-897
5. Shrestha. S., Khatiwada. M., Babel. M. S., **Parajuli. K.**, (2014). Impact of Climate Change on River Flow and Hydropower Production in Kulekhani Hydropower Project of Nepal. *Environmental Processes*. 1 (3), pp 231-250.
6. **Parajuli. K**., Kang. K., Shrestha. S. (2014). Application of Statistical Downscaling in GCMs at Constructing the Map of Precipitation in the Mekong River Basin, *Russian Meteorology and Hydrology*, 39 (4), pp 271-282.

### Conference Proceedings (Refereed)

7. **Parajuli. K.,** (2015). Spatial Analysis of Actual Evapotranspiration Estimates from the iUTAH Climate Station Network. In Karvazy, K., & Webster, V. L. (Eds.), *World Environmental and Water Resources Congress 2015: Floods, Droughts, and Ecosystems,* Paper presented at World Environmental and Water Resources Congress, Austin, TX, (pp. 2252-2260). ASCE-EWRI. (*Awarded 2nd place in graduate student technical paper competition)*

**Thesis & Reports**

8. **Parajuli. K.** (2018). *Advancing methods to quantify actual evapotranspiration in stony soil ecosystems,* Ph.D. Dissertation, Utah State University, Utah, USA.
9. **Parajuli. K.** (2013). *Development and application of an index to quantify water, energy and carbon nexus*. Master's Thesis, Asian Institute of Technology, Thailand; Thesis ID WM 13-10.
10. **Parajuli, K.,** Kang, K., (2012). Downscaling of GCM and Development of Climate Map for Future Prediction of Precipitation in Mekong Region. *APEC Climate Center: YSSP 2012 final report*, Busan, South Korea: APEC Climate Center, pp 229-256, ISBN 978-89-97333-51-6.
11. **Parajuli. K.,** Adhikari. R., Khatiwada. M., Maharjan. R., Pokhrel. P. (2009). *Prefeasibility study of Upper Khudi Hydropower Project, 10 MW*, B. Eng. Major project report, Kantipur Engineering College, Lalitpur.

**Abstracts of Presentations**

12. **Parajuli K.**, Scott B. Jones, David G. Tarboton, Gerald Flerchinger, Lawrence E. Hipps, L. Niel Allen, Mark S. Seyfried. (2018) Effect of stone content on soil moisture dynamics and evapotranspiration, *Spring Runoff Conference*, Utah State University, Logan, UT, 27 March 2018.
13. **Parajuli K.**, Scott B. Jones, David G. Tarboton, Lin Zhao, Gerald Flerchinger. 2017. Simulating Stony Soil Impact on Evapotranspiration. *ASA-CSSA-SSSA Annual Meeting*. Tampa, FL, Oct. 23-26, 2017(*Awarded 4$^{th}$ place, Soil physics and hydrology division*).
14. Jones S. B., **K. Parajuli**, R. Zhou, W.Sheng, M. Sadeghi, T. E. Ochsner, J. Šimůnek. (2017). A Soil Moisture Monitoring and Forecast Network for Improved Water Resource Management and Risk Prediction, Presented at the *ASA-CSSA-SSSA Annual Meeting*, Tampa, FL, 22-26 October 2017.
15. **Parajuli K.**, Sadeghi. M., Jones S. B. (2016). Stone content influence on soil water retention, Presented at the *Soil Science Society of America Annual Meeting*, Phoenix, AZ, 6-9 November 2016 (*Awarded 3$^{rd}$ place, Soil physics and hydrology division*).

16. Tate. S., **Parajuli. K.** Jones. S.B. (2016). The effects of elevation on evapotranspiration. *iFellow Symposium,* University of Utah, Salt Lake City, UT, USA, 15 July 2016.
17. **Parajuli K.**, Sadeghi. M., Jones S. B. (2016). Measuring and Modeling the Influence of Rock Content on Soil Hydraulic Properties, *Student Research Symposium*, Utah State University, Logan, UT, 14 April 2016.
18. **Parajuli K.**, Sadeghi. M., Jones S. B. (2016). Influence of Stone Content in Soil Water Retention, *Spring Runoff Conference*, Utah State University, Logan, UT, 5 – 6 April 2016.
19. **Parajuli K.**, Sadeghi. M., Jones S. B. (2015). Rock Content Influence on Soil Hydraulic Properties, *AGU Fall Meeting*, San Francisco, CA, 14-18 December 2015.
20. **Parajuli. K.,** Jones S. B., Hipps. L. E. (2015). Numerical Modeling of Evapotranspiration from Montane Vegetation with Verification from Actual Surface Energy Balance Measurements, *SSSA Annual Meeting*, Minneapolis, MN. Nov 15-18, 2015.
21. Ipson. J., **Parajuli. K.**, Jones. S.B. (2015). Improving Evapotranspiration Estimates Using Soil Heat Flux. *iFellow Symposium,* University of Utah, Salt Lake City, UT, USA, 29 July 2015.
22. **Parajuli. K.** (2015). Estimating Evapotranspiration in iUTAH watersheds, *iUTAH Summer Symposium and All-Hands Meeting*. Midway, UT, 17 July 2015.
23. **Parajuli. K.,** (2015), Estimating Actual Evapotranspiration in Logan River Watershed, *Annual J. Paul Riley AWRA-Utah Section Student Conference,* Brigham Young University; Salt Lake Center, SLC, Utah. 13 April 2015 (*Awarded as top 5 paper in PhD category*).
24. **Parajuli. K.,** Jones S. B. (2015). Spatial Analysis of Actual Evapotranspiration Estimates from the iUTAH Climate Station Network, *Student Research Symposium*, Research Week 2015, Utah State University, Logan, Utah, USA, 6 – 10 April 2015.
25. Khatiwada M., Shrestha S., Babel M. S., **Parajuli K.** (2014). Impact of climate change on hydropower production potential in Kulekhani Hydropower, Nepal. *Expert*

*workshop on Managing Water Resources under Climate Uncertainty: Opportunities and Challenges*, Bangkok, Thailand, 17-18 October 2013.

26. **Parajuli. K.** (2013). Water Issues in Megacities: Challenges and Solutions, "EXCEED, Expert Seminar on Water Issues in Megacities" Ho Chi Minh City, Vietnam, 3-10 March 2013.
27. **Parajuli. K.** (2013). Water Supply and sanitation issues in Nepal, *Knowledge sharing workshop on Integrated River Basin Management at Asian Monsoon Region*, Asian Institute of Technology, Thailand, 5-6 January 2013.
28. **Parajuli. K.,** Kang. K., Shrestha. S. (2012). Downscaling of GCM and Development of Climate Map for Future Prediction of Climatic variables in Mekong Region, *Young Scientist Support program,* APEC Climate Center, Busan, S. Korea; 26 December 2012.
29. **Parajuli. K.** (2012). *Statistical downscaling of GCMs using SDSM*, Guest lecture presented to APCC researchers, APEC Climate Center, Busan, S. Korea; November, 2012.

**PROFESSIONAL TRAININGS**

1. Short Course on Thermo-TDR Sensors, *North Carolina State University*, Raleigh, NC, 7-8 June 2018.
2. Graduate Student Leadership Conference, *Soil Science Society of America*, Phoenix, AZ, 5-6 November, 2016.
3. Science communications workshop, *Alan Alda Center*, Logan, UT. 3 - 4 October, 2016.
4. Radiation Safety Training, *Utah State University,* Logan, UT. 25 May – 1 June, 2016.
5. NCL workshop, *National Center for Atmospheric Research (NCAR)*, Boulder, CO, 9-12 June, 2015.
6. Proposal Writing Training, *Utah State University*, Logan, UT. 3 February, 2015.
7. ASEAN-EU Science, Technology and Innovation Days, *SEA-EU-NET II*, Thailand, 21 – 23 January, 2014.
8. CLIM-RUN School, Building two-way communication: A week of Climate Services, *International Centre for Theoretical Physics*, Trieste, Italy, 2-6 December, 2013.

9. Summer School on Coastal Hazards, *"The Future Ocean", University of Kiel*, Germany 16-20 September, 2013.
10. Induction Training for newly recruited Permanent Engineers, *Nepal Electricity Authority,* Kharipati, Bhaktapur, 17-18 July, 2011.
11. A Training on Roadside Bio Engineering for Engineers and Environmentalists, *Geo-environment and Social Unit (GESU) and Department of Road,* Kathmandu, Nepal, 20 - 26 May, 2011.
12. AutoCAD training, *ARENA Multimedia*, Nepal, 1-31 January, 2009.

## SKILLS

| | |
|---|---|
| **Modeling tools** | Hydrus-1D/2D/3D, HEC-HMS, HEC-RESSIM, SDSM, CROPWAT, Qual2K, MODFLOW, Noah-MP |
| **Software** | AutoCAD, ArcGIS, ERDAS |
| **Programming** | MATLAB, Python, GrADS, NCL, R |
| **Field and Lab** | Experienced in working in laboratory and remote field locations, conducting instrumentation and measurement. |

## PROFESSIONAL AFFILIATION & MEMBERSHIP

1. Nepal Engineering Council, Class A., Civil Engineer (2009)
2. Soil Science Society of America (SSSA), Member since 2015
3. American Society of Civil Engineers (ASCE), Member since 2015
4. American Geophysical Union (AGU), Member since 2015

## PROFESSIONAL ACTIVITIES

**Manuscript Review**

i. Journal of Cleaner Production

**Session Chair**

i. Water Resources Planning and Management, iUTAH all hands meeting, Utah State University, Logan, UT. 14 July 2017.

**Poster Review Panel**

ii. iUTAH all hands meeting, Utah State University, Logan UT, 14 July 2017

iii. iFellow Symposium, University of Utah, Salt Lake City, UT, 15 July 2016.

iv. iUTAH Summer Symposium and All-Hands Meeting. Midway, UT, 17 July 2015.

## SOCIAL ACTIVITY AND PART TIME INVOLVEMENT

1. **Treasurer**: Executive committee of Utah State University – Nepali Student Association (USUNSA), (March 2015 – August 2016)
2. **Webmaster** : USUNSA Website (www.usunsa.org), (March 2015 – August 2016)
3. **President:** Asian Institute of Technology- Nepalese Society (AIT-NS), (April – September 2012)
4. **Member of Executive Committee**: Nepal Engineers Association- Bangkok Centre (NEA-BC), (March 2012 – February 2013)
5. **Volunteer**: CWIN- Nepal, a leading child right organization. Involved in creating the case studies of risk background children and teaching (April- June 2002)

## REFERENCES

**Scott B. Jones, Ph. D.**
Professor
Department of Plants, Soils and Climate
4820 Old Main Hill
Utah State University
Logan, UT 84322-4820
+1 (435) 797 2175
scott.jones@usu.edu

**David G. Tarboton, Sc. D.**
Professor
Civil and Environmental Engineering
4110 Old Main Hill
Utah State University
Logan, UT 84322-4110
+1 (435) 797 3172
dtarb@usu.edu

**Lawrence E. Hipps, Ph. D.**
Professor
Department of Plants, Soils and Climate
4820 Old Main Hill
Utah State University
Logan, UT 84322-4820
+1 (435) 797 2009
lawrence.hipps@usu.edu